2013 Residential Alternative Calculation Method

Algorithms

November 15, 2012

DRAFT

For instructions on how to submit written comments about this document to the California Energy Commission, please see the Notice of Staff Workshop:

www.energy.ca.gov/title24/2013standards/implementation/documents/2012-11-20_workshop/2012-11-20_workshop_notice_res_acm_manual.pdf

Contents

Figures

Appendix Figures

Tables

Introduction

[To be written]

1 California Simulation Engine (CSE)

1.1 OVERVIEW

The building modeled can have multiple conditioned and unconditioned zones. Each conditioned zone has an air handler associated with it, and each air handler can have supply and/or return ducts in an unconditioned zone (nominally the attic), and in the conditioned zone itself. Air handlers can operate independently in either a heating, cooling, or off mode. See Figure 1.

Every time step (nominally two minutes), the zone model updates the heat transfers to and from the zones and the zone mass temperatures. Each zone's conditions are updated in succession and independently, based on the conditions in the adjacent zones in the last time step.

The conditioned zone thermostat algorithms determine whether an air handler should be in a heating or cooling mode, or floating, and if heating or cooling, the magnitude of the load that must be met by the air handler to keep the conditioned zone at its current setpoint. If the setpoints cannot be satisfied, the conditioned zone floats with heating, cooling, or ventilation, at full capacity. In the off mode case the zones are modeled during the time step without duct or air handler effects.

Figure 1: Schematic of Zones and Air Handler Systems

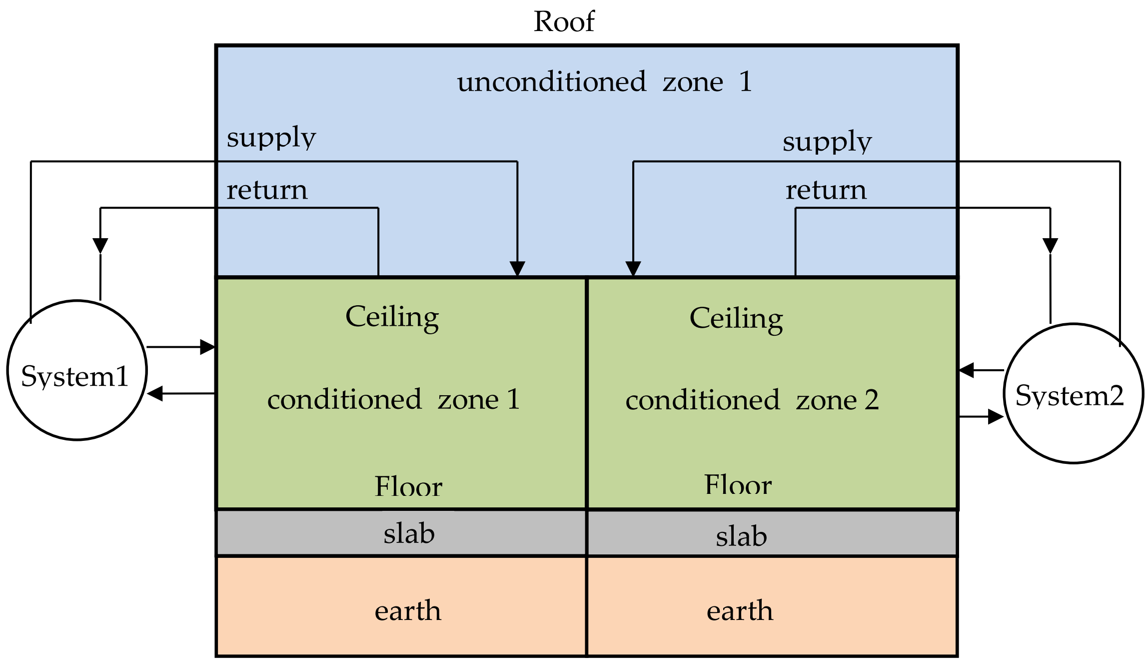

Although shown partly outside of the envelope, all ducts are assumed to be in either the conditioned or unconditioned zones only.

The duct system model determines duct losses, their effect on the conditions of the unconditioned and conditioned zones, and their effect on the heating or cooling delivery of the air handler system.

The duct system model allows unequal return and supply duct areas, with optional insulation thicknesses. The ducts can have unequal supply and return leakages, and the influence of unbalanced duct leakage on the unconditioned and conditioned zones infiltration and ventilation is taken into account. Every time step it updates the air handler and duct system heat transfers, and HVAC energy inputs, outputs, and efficiency.

For each window, the ASHWAT window algorithm calculates the window instantaneous shortwave, longwave, and convective heat transfers to the zones.

The AIRNET infiltration and ventilation algorithm calculates the instantaneous air flow throughout the building based on the air temperatures in the zones, and on the outside wind and air temperature. AIRNET also handles fan induced flows.

In the update processes, a zones mass-node temperatures are updated using a forward-difference (Euler) finite difference solution, whereby the temperatures are updated using the driving conditions from the last time step. For accuracy, this forward-difference approach necessitates a small time-step.

The small time-step facilitates the *no-iterations* approach we have used to model many of the interactions between the zones, and allows the zones to be updated independently.

For example, when the zone energy balance is performed for the conditioned zone, if ventilation is called for, the ventilation capacity, which depends on the zone temperatures (as well as maximum possible ventilation openings and fan flows), is determined from the instantaneous balance done by AIRNET. To avoid iteration, the ventilation flows, and the accompanying heat transfers are based on the most recently available zone temperatures.

To avoid iteration, a similar use of the last time-step data is necessary is dealing with inter-zone wall heat transfer. For example, heat transfer through the ceiling depends on the conditions in both zones, but these conditions are not known simultaneously. Thus, ceiling masses are treated as belonging to the attic zone, and updated at the same time as other attic masses, partly based on the heat transfer from the conditioned zone to the ceiling from the last time step. In turn, when the conditioned zone is updated it determines the ceiling heat transfer based on the ceiling temperature determined two-minutes ago when the attic balance was done.

Similarly, when the conditioned zone energy balance is performed, if for example heating is called for, then the output capacity of the heating system needs to be known, which requires knowing the duct system efficiency. But the efficiency is only known after the air handler simulation is run. To avoid iteration between the conditioned zone and attic zones, the most recent duct efficiency is used to determine the capacity in the conditioned zones thermostat calculations. When the attic simulation is next performed, if the conditioned zone was last running at capacity, and if the efficiency now calculated turns out to be higher than was assumed by the thermostat calculations, then the load will have exceeded the limiting capacity by a small amount depending on the assumed vs. actual efficiency. In cases like this, to avoid iteration, the limiting capacity is allowed to exceed the actual limit by a small amount, so that the correct energy demand is determined for the conditioned zone load allowed.

1.1.1 Schematic of Zone Thermal Network

Figure 2 shows a schematic of the zone model network. It models a single zone whose envelope consists of any number of walls, ceilings, floors, slabs, and windows, and can be adjacent to other conditioned or unconditioned zones. The envelope constructions can be made of any number of layers of different materials of arbitrary thermal conductivity and heat capacity. Each layer is modeled with one or more "T" networks in series. Each T has the layer heat capacitance, cap_{ij}, centered between by two thermal conductances, where the first subscript corresponds to the wall construction number and the second to the layer number. Framed constructions are treated as two separate surface areas, the surface area of the part between framing, and the surface area of the part containing the framing itself; the heat flow is assumed to follow independent and parallel paths through these two surfaces.

Figure 2: Schematic of Simulation Network

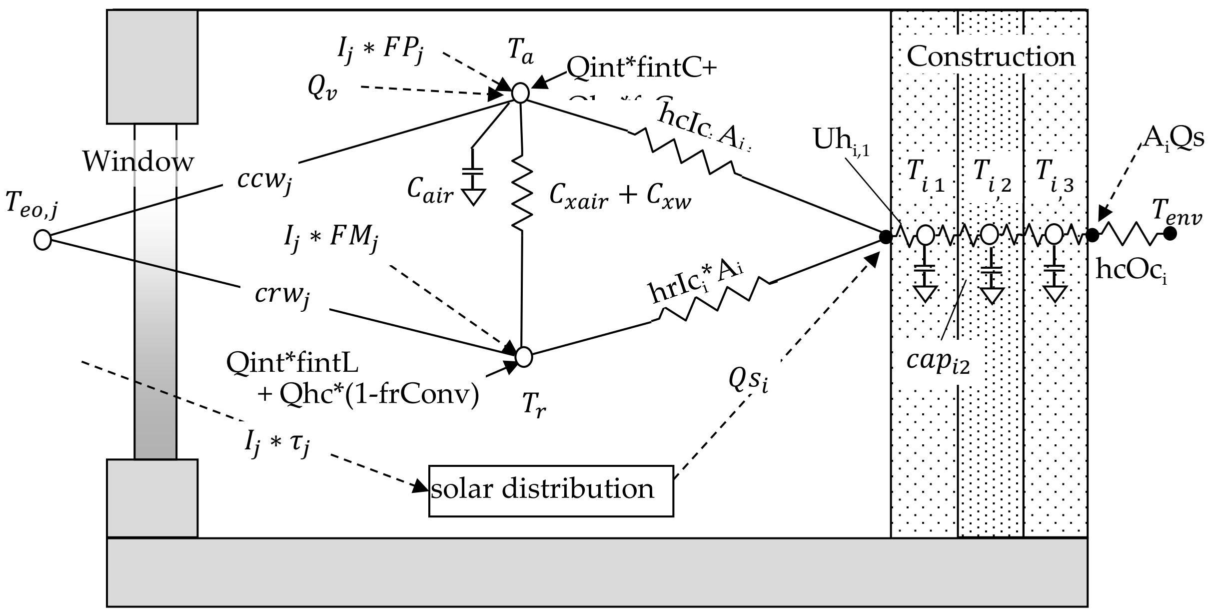

The room air, represented by the mass node Ta, is assumed to be well-mixed and have heat capacitance C_{air} (Btu/F). The air is shown in Figure 2 to interact with all of the building interior construction surfaces via convection coefficients $hcIc_i$ for surface i. The overall conductance through the window between T_a and an effective outdoor temperature T_{eo} is ccw_j for window surface j. The conductances ccw_j and the corresponding radiant value crw_j are outputs of the ASHWAT windows algorithm applied to window j each time step.

A mean radiant temperature node, T_r, acts as a clearinghouse for radiant exchange between surfaces. With conductances similar to those of the air node: $hrIc_i$ and crw_j.

Depending on the size of the zone and the humidity of the air, the air is assumed to absorb a fraction of the long-wave radiation and is represented by the conductance C_{Xair}.

The internal gains, $Qint$, can be specified in the input as partly convective (fraction $fintC$), partly long wave ($fintLW$), and partly shortwave (fintSW). The heating or cooling heat transfers are shown as Qhc (+ for heating, - for cooling). If Qhc is heating, a fraction ($frConv$) can be convective with the rest long-wave. The convective parts of $Qint$ and Qhc are shown as added to the air node. The long wave fraction of Qint and Qhc are shown added to the T_r node.

Additional outputs of the ASHWAT algorithm are FP_j the fraction of insolation I_j incident on window j that ultimately arrives at the air node via convection, and FM_j, the fraction that arrives at the radiant node as long-wave radiation.

The term Qs_i is the the total solar radiation absorbed by each construction surface i, as determined by the solar distribution algorithm. The short wave part of the internal gains, Qint $*$

fintSW, is distributed diffusely, with the same diffuse targeting as the diffusely distributed solar gains.

Solar gains absorbed at the outside surface of constructions are represented by Qs_o in Figure 2.

The slab is connected to the Ta and Tr in a similar fashion as the wall surfaces, although the slab/earth layering procedure is different than for walls.

1.1.2 Schematic of Reduced Thermal Network

Before a zone energy balance is formulated it is convenient to dissolve all the massless nodes from the network of Figure 2 (represented by the black dots), except for the mean radiant temperature node Tr. Figure 3 shows the resulting reduced network. A massless node is eliminated by first removing the short-wave gains from the node by using the current splitting principle (based on superposition), to put their equivalent gains directly onto adjacent mass nodes and other nodes that have fixed temperatures during a time step. Then the massless node can be dissolved by using Y-Δ transformations of the circuit.

Figure 3: Network after Dissolving Massless Nodes

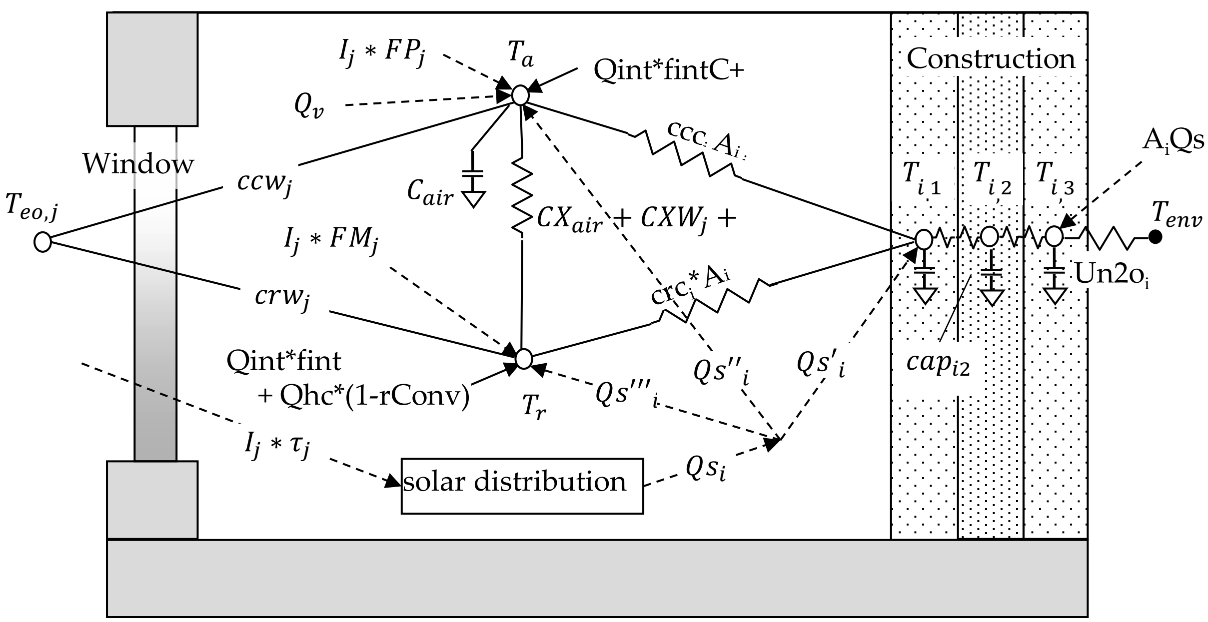

For example, to eliminate the massless surface node of layered mass in Figure 2, the gain Qs_i absorbed by the surface node is split into three parts: Qs_i' to the $T_{i,1}$ node, Qs_i'' to the Ta node and Qs_i''' to the Tr node. For example, by current splitting,

$$Qs_i' = Qs_i \frac{Uh_{i,1}}{hcIc_i + hrIc_i + Uh_{i,1}}$$

Equation 1

A Y-Δ transformation of the remaining Y circuit gives the ccc_i and crc_i conductances, as well as an additional cross conductance CXC_i that is added to CXair. For example,

$$ccc_i = \frac{hcIc_i * Uh_{i,1}}{hcIc_i + hrIc_i + Uh_{i,1}}$$

Equation 2

1.1.3 Zone Balance Calculation Sequence

The temperatures in the zone are determined using a thermal balance method. The following procedure is followed each time step.

At the start of the simulation, say time t, assume all temps $Ta(t), Tr(t), T_{i,1}(t), T_{i,2}(t)$, etc. are known along with all the solar gains, internal gains, etc.

(1) First, the layered mass temperatures are updated using the explicit Euler routine (see Section 1.2), giving $T_{i,1}(t + dt), T_{i,2}(t + dt)$, etc. The Euler method determines each of these mass temperatures assuming that all the boundary conditions (temperatures and heat sources) that cause the change in the mass temperatures, are conditions at time t. Thus the mass node temperatures can be in any order, independently of each other.

(2) Next, a steady-state instantaneous energy balance at the Ta and Tr nodes is made at time t+ dt. This balance involves the mass temperatures determined for time t + dt in Step-1, as well other heating or cooling sources at time t+ dt. The balance in this step involves querying the HVAC control algorithm which allows heating, cooling and ventilation (forced or natural) in response to scheduled setpoints. The idealized control system is assumed to keep the zone at exactly the scheduled setpoint unless Ta is in the deadband or if the HVAC capacity is exceeded, whereupon the system runs at maximum capacity, and Ta floats above or below the relevant setpoint. While the heating, cooling and forced ventilation system capacities are scheduled inputs, the natural ventilation capacity is dependent on the current zone and environment conditions.

Thus, the energy balance at the Ta and Tr nodes returns either the heating, the cooling or the ventilation required to meet the setpoint, or else returns the floating Ta that results at the capacity limits or when Ta is in the deadband.

At this stage the conditions have been predicted for the end of the time step, and steps 1 and 2 and repeated. The various boundary conditions and temperature or air flow sensitive coefficients can be recalculated as necessary each time step at the beginning of step (1), giving complete flexibility to handle temperature sensitive heat transfer and control changes at a time step level.

Note that step (2) treats the energy balance on Ta as a steady state balance, despite the fact that air mass makes it a transient problem. However, as shown in Section 1.3.1, if the air mass temperature is updated using an implicit-difference method, the effect of the air mass can be duplicated by employing a resistance, *Δt/Cair*, between the Ta node and a fictitious node set at the beginning of the time-step air temperature TaL = Ta(t), and shown as such in Figure 3.

<u>The overall CSE Calculation Sequence is summarized below:</u>

Hour

Determine and distribute internal gains.

Sub-hour

Determine solar gain on surfaces.

Determine surface heat transfer coefficients.

Update mass layer temperatures.

Find AirNet mass flows for non-venting situation (building leakage + last step HVAC air flows).

Find floating air temp in all zones / determine if vent possibly useful for any zone.

If vent useful

- find AirNet mass flows for full venting
- find largest vent fraction that does not sub-cool any zone; this fraction is then used for all zones.
- if largest vent fraction > 0, update all floating zone temperatures assuming that vent fraction

Determine HVAC requirements for all zones by comparing floating temp to setpoints (if any)

- System heating / cooling mode is determined by need of 1st zone that requires conditioning
- For each zone, system indicates state (t and w) of air that could be delivered at register (includes duct loss effects). Zone then requests air flow rate required to hold set-point temperature

Determine HVAC air flow to zones (may be less than requested); determine zone final zone air temperatures.

Determine system run fraction and thus fuel requirements.

Determine zone humidity ratio for each zone.

Calculate comfort metrics for each zone.

1.2 UPDATING LAYERED MASS TEMPERATURES

The heat transfer through the layered constructions is assumed to be one dimensional. The heat conduction equation ($\frac{\partial^2 T^2}{\partial x^2} = \frac{1}{\alpha}\frac{\partial T}{\partial t}$) is solved by using finite differences (Δt and Δx) to approximate the differential increments in time and distance; α is the thermal diffusivity. The smaller the finite increments, the more accurate the solution. The homogeneous layers are divided into lumps Δx thick, and the lumps are represented by the two-conductance/one-capacitance "T" circuits shown for each layer in Figure 2. Frequently the actual layer thicknesses as sufficiently thin that Δx can be taken as the layer thickness. However, at times the actual layer of homogeneous material must be divided into smaller thicknesses. See Section 1.4–Discretization Errors for the criterion used to determine Δx and Δt.

The temperatures of the mass nodes are updated every time step using the Euler explicit numerical integration method (see Press et al), whereby the change in temperature of the mass during the time step is based only on the boundary conditions at the beginning of the time step. The boundary conditions are the temperatures of the surrounding nodes and other heat flow sources.

To update $T_{i,1}$ in Figure 3, for example, if the rate of heat transfer into $T_{i,1}$ is equated to its rate of change in internal energy, resulting in the differential equation for mass temperature $T_{i,1}$:

$$\frac{dT_{i,1}}{dt} = \frac{Tss_{i,1} - T_{i,1}}{\tau}$$

Equation 3

where $T_{i,1}$ is the surface layer mass temperature, and $Tss_{i,1}$ is the temperature $T_{i,1}$ would have if steady state were reached:

$$Tss_{i,1} = \frac{ccc_{i,1}Ta + crc_{i,1}Tr + Ubn_{i,1}T_{i,2} + Qs_i{}'}{ccc_{i,1} + crc_{i,1} + Ubn_{i,1}}$$

Equation 4

$Qs_i{}'$ is given by Equation 1, $ccc_{i,1}$ by Equation 2, $T_{i,2}$ is the temperature of mass node 2, and τ is the time constant of mass node 1 given by:

$$\tau = \frac{cap_{i,1}}{ccc_{i,1} + crc_{i,1} + Ubn_{i,1}}$$

Equation 5

The heat capacity of layer-1 is $cap_{i,1}$ (Btu/ft^2-F). $Ubn_{i,1}$ is the conductance between nodes 1 and 2, given by:

$$Ubn_{i,1} = \frac{1}{\frac{1}{Uh_{i,1}} + \frac{1}{Uh_{i,2}}}$$

Equation 6

To integrate of Equation 3 over a time step, the Euler procedure assumes that the right hand side of the equation remains constant over the time step at its value at the beginning of the time step. In this case the mass temperature at the end of the time step becomes:

$$T_{i,1}(t + \Delta t) = T_{i,1}(t)\left(1 - \frac{\Delta t}{\tau}\right) + Tss\left(\frac{\Delta t}{\tau}\right)$$

Equation 7

If the capacitance of any layer is zero (a convecting air layer for example) its updated temperature is set equal to Tss. That is, the temperature at the central node is determined by a steady state energy balance.

All of the mass nodes are updated in an analogous fashion each time step. The order in which the masses are updated is irrelevant because they are updated based only on the values of variables at the beginning of the time step, not on the values that may have been updated since.

1.3 ZONE ENERGY BALANCE

1.3.1 Implicit Update of Air Temperature

Similar to the energy balance on the construction mass nodes, an energy balance on the air node gives the differential equation:

$$\frac{dT_a}{dt} + \frac{T_a}{\tau_a} = \frac{Tss}{\tau_a}$$

Equation 8

where Tss, the asymptotic steady state temperature of Ta, includes all the sources connected to Ta. For simplicity, if the zone only contained the one construction (*i* = 1) and one window (*j*=1), like in Figure 3, then from a steady state energy balance Tss is given by:

$$T_{ss} = [T_{out}\left(U_{inf} + U_v\right) + ccw_1 Awin_1 T_{out} + ccc_1 Acon_1 T_{1,1} + Acon_1 Qs_1'' + Awin_1 Qsw_1''$$
$$+ Qint * fintC + Qhc * frConv + CX * Tr]/Usum$$

Equation 9

where

$$CX = CXair + CXW_1 + CXC_1$$

Equation 10

$$Usum = U_{inf} + U_v + ccw_1 Awin_1 + ccc_1 Acon_1 + CX$$

Equation 11

and the air time constant is:

$$\tau_a = \frac{Cair}{Usum}$$

Equation 12

Equation 8 is solved using an full implicit (or backward time) difference, similar to the Euler explicit method except here the right hand side of the equation remains constant over the time step at its value at the end of the time step, not its value at the beginning as in the Euler method. Thus, Equation 8 then becomes:

$$T_a(t + \Delta t) = \frac{\frac{T_a(t)\tau_a}{\Delta T} + Tss(t + \Delta t)}{\frac{\tau_a}{\Delta t} + 1}$$

Equation 13

Where the times t and $t+\Delta t$ in parenthesis indicate the terms are evaluated at the beginning and end of the time step, respectively. Substituting Equation 12 for τ_a, Equation 13 can be put in the convenient form:

$$T_a(t+\Delta t) = \frac{\frac{T_a(t)Cair}{\Delta T} + Usum * Tss(t+\Delta t)}{\frac{Cair}{\Delta t} + Usum}$$

Equation 14

As this equation shows, with the implicit difference the effect of the air mass can be thought of as a resistance, $\Delta t/Cair$, between the Ta node and a fictitious node set at the air temperature at the value it was at the beginning of the time step, $TaL = Ta(t)$. This alternative is known as an 'associated discrete circuit'. Leaving out the explicit time references, Equation 14 can be written:

$$Ta = \frac{\frac{TaL * Cair}{\Delta T} + Usum * Tss}{\frac{Cair}{\Delta t} + Usum}$$

Equation 15

where Ta and Tss are evaluated at the end of the time step, and TaL stands for $T_a(t)$ at the beginning of the time step. Note that Equation 15 still contains the variable Tr (hidden in Tss) which is unknown. Tr can be eliminated by making an energy balance on the Tr node and substituting the expression for Tr into Equation 15. This is done for the complete set of equations that follow.

1.3.2 Zone Balance Equations

The complete set of zone energy balance equations for multiple windows and constructions are given below. Terms containing Qv and Qhc are kept separate so that the resulting equations can be solved for Qv or Qhc when Ta is fixed at a setpoint.

1.3.2.1 Air Node Balance

The energy balance equation on the Ta node, comparable to Equation 15 above is:

$$Ta = \frac{Qv + Qhc \cdot frConv + Nair + CX \cdot Tr}{Dair + CX}$$

Equation 16

The Equation 16 form, using Q_v, is used when heat is transferred to a conditioned zone with ventilation or infiltration air. When heat is transferred to an unconditioned zone due to ventilation or infiltration, Q_v is replaced by the essentially equivalent form given by Equation 17, wherein Q_v is replaced by $Q_v = mC_p\Delta T$ such that $mdot * c_p * T$ is added to the numerator and $mdot * c_p$ is added to the denominator. This was implemented to eliminate oscillations in Ta.

$$Ta = \frac{ST + Qhc \cdot frConv + Nair + CX \cdot Tr}{SB + Dair + CX}$$

Equation 17

where,

$$ST = \sum mdot * c_p * T,$$

Equation 18

where T is the temperature of the air in the zone supplying the infiltration or ventilation air.

$$SB = \sum mdot * c_p$$

Equation 19

$$CX = CXair + \sum^{con} Acon_i \cdot cxc_i + \sum^{win} Awin_i \cdot cxw_i$$

Equation 20

with the sum's for all constructions and all windows respectively.

$$Nair = TaL\left(\frac{Cair}{dt}\right) + Qint \cdot fintC + \sum^{con} Acon_i \cdot \left(ccc_i \cdot T_{i1} + \frac{Q_{si} \cdot hcIc_i}{hcIc_i + hrIc_i + Uh_{i1}}\right) + \sum^{win} \left[Awin_i\left(ccw_i \cdot Teo_i \ + I_j \cdot FP_j\right)\right]$$

Equation 21

$$Dair = \frac{Cair}{dt} + \sum^{con} Acon_i \cdot ccc_i + \sum^{win} Awin_i \cdot ccw_i$$

Equation 22

Qv is the heat transfer to the air node due to infiltration and forced or natural ventilation.

1.3.2.2 Radiant Node Balance

An energy balance on the Tr node gives Equation 23.

$$Tr = \frac{Qhc \cdot (1 - frConv) + N_{rad} + CX \cdot Ta}{Drad + CX}$$

Equation 23

where,

$$Nrad = Qint \cdot fintLW + \sum^{con} Acon_i \left[crc_i \cdot T_{i1} + Qsi_i \cdot \frac{hrIc_i}{hcIc_i + hrIc_i + Uh_{i1}} \right]$$
$$+ \sum^{win} Awin_i \left[crw_i \cdot Teo_i + I_j \cdot FM_j \right]$$

Equation 24

$$Drad = \sum^{con} Acon_i \cdot crc_i + \sum^{win} Awin_i \cdot crw_i$$

Equation 25

1.3.2.3 Simultaneous Solution of Ta and Tr Equations

Equation 16 and Equation 23 can be solved simultaneously to eliminate Tr and give Ta explicitly:

$$Ta = \frac{(Qv + Qhc \cdot frConv + Nair)(Drad + CX) + CX(Nrad + Qhc(1 - frConv)}{(Dair + Drad)CX + Dair \cdot Drad}$$

Equation 26

Similar to Equation 16 and Equation 17), the alternate form of Equation 26 is given by Equation 27.

$$Ta = \frac{(ST + Qhc \cdot frConv + Nair)(Drad + CX) + CX(Nrad + Qhc(1 - frConv)}{(SB + Dair + Drad)CX + (SB + Dair)\mathrm{D}rad}$$

Equation 27

Substituting Ta from Equation 26 into Equation 23 gives Tr.

1.3.2.4 Qhc and Qv Equations

When *Ta* is at either the heating or cooling setpoints, Equation 26 is solved to determine the required *Qhc*. In this case *Qv* is set *to QvInf.*

$$Qhc = \frac{Ta(Dair * Drad + CX(Dair + Drad)) - (Nair + Qv)(Drad + CX) - Nrad * CX)}{frConv * Drad + CX}$$

Equation 28

Similarly, when Ta is at the ventilation setpoint, Equation 26 can be solved for Qv to give:

$$Qv = \frac{(Dair * Drad + CX(Dair + Drad))Ta - CX(Nrad + Qhc(1 - frConv))}{Drad + CX} - (Qhc * frConv + Nair)$$

Equation 29

With Qhc = 0 this becomes:

$$\text{Qv} = \frac{(Dair * Drad + CX(Dair + Drad))Ta - Nair(Drad + CX) - CX * Nrad}{Drad + CX}$$

Equation 30

The zone balance is essentially an instantaneous balance, so all the temp inputs are simultaneous values from the end of the time step (with the exception of TaL; see Section 1.3.1). Although the balance is with contemporary temperatures, many of the heat flows in $Nair$ etc., are based on last time step conditions.

1.3.3 Thermostat Logic

At the end of each time step the program finds the floating temperature of the zone without HVAC ($Qhc = 0$) and with venting $\text{Qv} = \text{QvInf}$. This floating temperature found from Equation 26 is defined as TS1. Next, the venting capacity is determined (see Section 1.9.3.10, Heat Flow), and Equation 26 is solved for Ta at the full venting capacity. This Ta is defined as TS2.

TS1 will satisfy one of the four cases:

- TS1>TC
- TC > TS1 > TD
- TD > TS1 > TH
- TH > TS1

Similarly, TS2 will satisfy one of the four cases:

- TS2 > TC,
- TC > TS2 > TD
- TD > TS2 > TH
- TH > TS2

where TC, TD, and TH are the scheduled cooling, ventilation, and heating setpoints, with TC > TD > TH.

Based on the cases that TS1 and TS2 satisfy, nested logic statements determine the appropriate value of heating, cooling, venting, or floating .

For example, if TS1 and TS2 are both > TC, then Q_v is set $QvInf$ and Ta is set to TC, and Equation 28 is solved for the required cooling, Qhc. If Qhc is smaller than the cooling capacity at this time step then Qhc is taken as the current cooling rate and the zone balance is finished and the routine is exited. If Qhc is larger than the cooling capacity then Qhc is set to the cooling capacity, and Equation 26 is solved for Ta, floating above TC due to the limited cooling capacity. If Ta < TS2 then Ta and Qhc are correct and the zone balance routine is exited. If this Ta > TS2 then Ta is set equal to TS2, Qhc is set to zero, and Equation 29 is solved for the ventilation rate Qv, and the Zone Balance routine is complete.

Similar logic applies to all other logically possible combinations of the TS1 and TS2 cases above.

1.3.4 Limiting Capacities

The limiting capacity of the heating and cooling system is determined each time step by multiplying the scheduled nominal air handler input energy capacity by the duct system efficiency. To avoid iteration between the conditioned zone and unconditioned zone simulations, the duct system efficiency is taken from the last time-step's unconditioned zone simulation, or unity if the system mode (heating, cooling, venting, or floating) has changed.

1.4 DISCRETIZATION ERRORS

The temperatures predicted by Equation 7, which updates the layered mass temperatures, is subject to errors due to the finite lump size chosen to represent real wall homogeneous layers. It is also subject to errors due to the finite time step Δt. Similarly Equation 14 for updating the air mass temperature is subject to error due to the finite time step chosen.

Discretization errors can be made negligible by reducing the layer thicknesses and time step to very small values. However for practical run time minimization purposes it is useful to have large Δt and Δx layers, insofar as accuracy allows. The range of choices of Δt and Δx is narrowed if accurate results are only required for a limited range of frequencies of the driving boundary conditions. Only extremely thin lumped layers have the correct frequency response at high frequencies. To model environmental influences, 3 cycles/day (8-hr period sinusoid) is likely the highest frequency necessary to consider when determining the frequency response of buildings (Goldstein, Anderson and Subbarao). Higher frequencies may be desirable for accurately modeling things like control step changes. During the program development, accuracy was measured by analyzing the frequency response at 3 cycles/day.

The exact frequency response of a layered wall can be obtained using the matrix method (Section 3.7 of Carslaw & Jaeger) which gives the inside driving point admittance (from the inside air node), the outside driving point admittance, and the transfer admittance, for any frequency. The magnitude of the inside driving point admittance is the principle parameter used to assess algorithm accuracy.

At the frequency chosen, 3 cycles/day say, the exact driving point admittance of the real wall (with homogeneous layers) can be obtained from the matrix method. Similarly the exact driving point admittance of the lumped wall which the user has chosen to represent the real wall, can also be determined by the matrix method. Comparing these two results shows the accuracy of the lumping assumptions, independent of time step considerations.

The time discretization error associated with Equation 7 at the frequency chosen can be assessed by comparing the driving point admittance predicted by the CSE code, when the air node is driven with a sinusoidal temperature at the chosen frequency, to the theoretical admittance of the lumped wall. Note that this procedure measures the global discretization error, larger potentially than the per time-step error.

Using this procedure for typical lightweight residential construction, we have confirmed that the errors in the temperature predictions made by the CSE finite difference algorithms indeed tend toward zero as Δt and Δx are reduced toward zero.

1.4.1 Layer Thickness of a Homogeneous Material

The lumped layer thickness, Δx, should be is chosen thin enough that the single temperature of the lumped layer is a good measure of the average temperature over a width Δx of the sinusoidal temperature distribution in the material. That is, the temperature of the sinusoidal wave should not vary much over the layer width. This criterion is similar to that used by Chirlian (1973) to determine the appropriate lump sizes in electrical circuits.

The wave length of the temperature distribution in a particular material is given by

$$\lambda = 2\pi d_p$$

Equation 31

where d_p , the penetration depth, an intrinsic characteristic of the material, is given by

$$d_p = \sqrt{2\alpha/\omega}$$

Equation 32

where the angular frequency $\omega = 2\pi/period$, α is the thermal diffusivity of the layer material, and ω is the highest angular frequency of the environmental boundary conditions for which good frequency response is desired. As a general guideline it is suggested that the lumped layer thicknesses, Δx, be chosen to be thinner than the penetration depth for the layer. That is, select

$$\Delta x \lesssim d_p$$

Equation 33

Substituting Equation 32 into Equation 33 shows that the rule of Equation 33 limits the lump size Δx to about 16% of the wavelength:

$$\Delta x \lesssim dp = \lambda/2\pi = 0.16\lambda$$

Equation 34

The Equation 33 rule is more important for the modeling of layers on the inner side of the wall, where the layers are subjected to the higher frequency harmonics of inside driving conditions. Deeper into the wall the high frequency harmonics begin to be damped (by about a factor of $e^{-\frac{\Delta x}{d_p}}$), so accurate modeling is of less significance.

1.4.2 Choosing the Time Step

The time step used in the code is input by the user. For high accuracy Equation 7 and Equation 14 should be applied using a time step that is a small fraction of the smallest time constant of any layer.

$$\Delta t \ll \tau$$

Equation 35

Thin layers of a material have a smaller time constant τ than thick layers. The time constant of a layer scales as $\sim \beta^2$, where β is the a layers dimensionless thickness defined as $\beta = \Delta x/d_p$. Thus, if a layers dimensionless thickness is reduced by a factor of two, the time constant is reduced by a factor of four. Therefore the time to run an annual simulation can increase rapidly for small β's. Small tau layers have cv increased such that tau = dt.

Note that the Euler mass layer update algorithm of Equation 7becomes unstable when $\Delta t > \tau$. The predicted temperatures will oscillate with increasing amplitude each time step. The code outputs warnings whenever a mass node update is performed for which $\Delta t > \tau$.

Like the explicit Euler method, the implicit differencing used at the air node is most accurate for small time steps relative to the air's time constant (Equation 12). The implicit difference method is never unstable, and time steps larger than the air time constant give useful, if somewhat inaccurate predictions. The air balance could have been solved using an Euler difference, but since the air time constant is likely the smallest in the zone, it would dictate smaller time steps than is afforded using the implicit method

.

1.5 SURFACE HEAT TRANSFER COEFFICIENTS

The radiation coefficients for surfaces inside the conditioned zone are given in Section 1.6.1 where the long-wave radiant network model is discussed.

1.5.1 Local Wind Velocity Terrain and Height Correction

The wind velocity as a function of height at the house site is obtained from the meteorological station wind measurement by making adjustments for terrain and height differences between the meteorological station and the house site.

1.5.1.1 Sherman-Grimsrud method

This method uses Equation 36 which determines the wind velocity $V(z)$, in ft/sec, at any height z (ft) based on the wind velocity, V_{met} in ft/sec, measured at a location with a Class II terrain (see Table 1) and at a height of 10-meters (32.8 ft):

$$V(z) = SC * V_{met} * \alpha * \left(\frac{z}{32.8}\right)^{\gamma}$$

Equation 36

where,

α and γ are obtained from Table 1 for the terrain class at the building location.

SC = shielding coefficient from Table 2 for the building location.

$V(z)$ = wind velocity at height z at the building location (ft/sec).

V_{met} = wind velocity (ft/sec) measured at 10-meters height in a Class II location.

The terrain factor of Table 1 is a general factor describing the influence of the surroundings on a scale on the order of several miles. The shielding factor of Table 2 is a local factor describing the influence of the surroundings on a scale of a few hundred yards.

Table 1: Parameters for Standard Terrain Classifications

Class	γ	α	Description
I	0.10	1.30	ocean or other body of water with at least 5km of unrestricted expanse
II	0.15	1.00	flat terrain with some isolated obstacles(buildings or trees well separated)
III	0.20	0.85	rural areas with low buildings, trees, etc.
IV	0.25	0.67	urban, industrial, or forest areas
V	0.35	0.47	center of large city

Table 2: Local Shielding Parameters

Class	C'	SC	Description
I	0.324	1.00	no obstructions or local shielding
II	0.285	0.880	light local shielding with few obstructions
III	0.240	0.741	moderate local shielding, some obstructions within two house heights
IV	0.185	0.571	heavy shielding, obstructions around most of the perimeter
V	0.102	0.315	very heavy shielding, large obstructions surrounding the perimeter within two house heights.

1.5.1.2 Implementation

If it is assumed that the default value of the terrain classification at the building location is Class IV terrain of Table 1, and the default local shielding coefficient is SC= 0.571 of Class IV of Table 2, then the wind velocity at the building site at height ***z*** is given by:

$$\mathrm{V(z)} = \mathrm{SC} * \mathrm{V_{met}} * \alpha * \left(\frac{\mathrm{ze}}{32.8}\right)^{\gamma} = 0.571 * V_{met} * 0.67 * \left(\frac{z}{32.8}\right)^{0.25}$$

or,

$$V(z) = 0.16 * z^{0.25} * V_{met}$$

For example, for 1, 2, and 3 story buildings, of 9.8 ft (3-m), 19.7 ft (6-m), and 29.5 ft (9-m), respectively, then the local eave height wind velocities are:

$\mathrm{V(9.8)} = 0.16 * 9.8^{0.25} * V_{met}$ = 0.28 $\mathrm{V_{met}}$ for a 1-story building.

V(19.7) = 0.34 $\mathrm{V_{met}}$ for a 2-story building.

V(29.5) = 0.38 $\mathrm{V_{met}}$ for a 3-story building.

(References: Sherman & Grimsrud (1980), Deru & Burns (2003), Burch & Casey (2009), European Convention for Constructional Steelwork (1978).)

1.5.2 Convection Coefficient for the Inside and Outside Surfaces of the Zones

The schematic buildings in Figure 4 and Figure 5 show all of the possible interior heat transfer situations for which the convection heat transfer coefficients are determined. The figures symbolically show the nature of the heat transfer boundary layer, and the heat flow direction. The symbols used are explained at the end of this document. Similar schematics have not been done for the outside surfaces.

The equations are developed that give the heat transfer coefficient for each of the Figure 4 and Figure 5 situations, and for the building outside surfaces. The heat transfer coefficients depend on the surface tilt angle θ ($0 \leq \theta \leq 90$), the surface and air temperatures, and on whether the heat flow of the surface has an upward or downward facing component.

The results, which apply to both the UZ and CZ zones, can be summarized as follows:

1.5.2.1 Inside surfaces

For floors, and either vertical walls, or walls pulled-in-at-the-bottom:

If Tair > Tsurf use Equation 53. (heat flow down)

If Tair < Tsurf use Equation 52. (heat flow up)

For ceilings (horiz or tilted), and walls pulled-in-at-the-top:

If Tair > Tsurf use Equation 52. (heat flow up)

If Tair < Tsurf use Equation 53. (heat flow down)

1.5.2.2 Outside surfaces

For all vertical walls, and walls with moderate tilts use Equation 54.

For horizontal or tilted roof, use Equation 57.

Figure 4: Heat Flow Down Situations

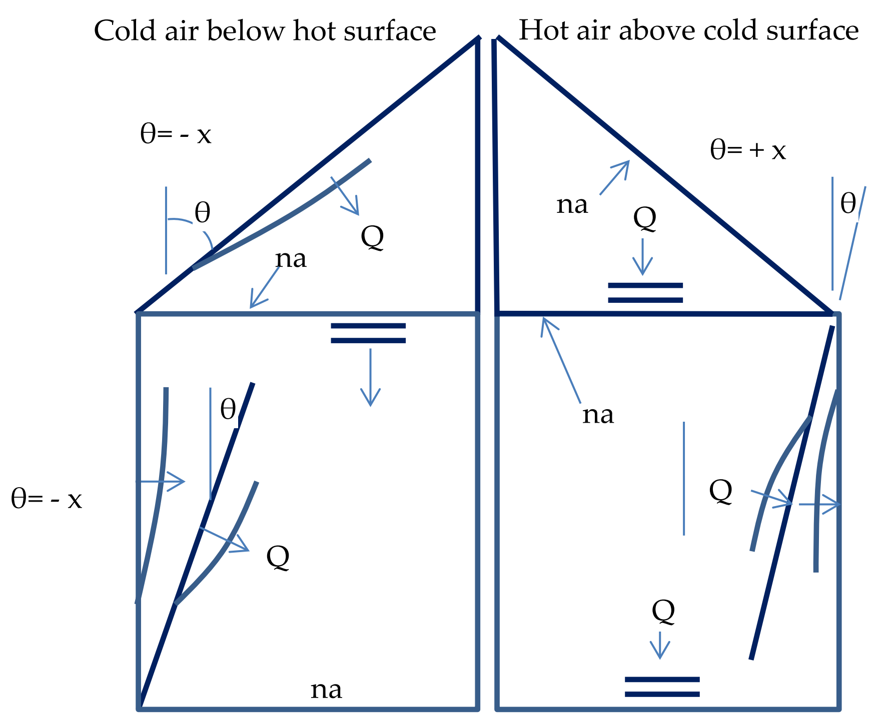

Figure 5: Heat Flow Up Situations

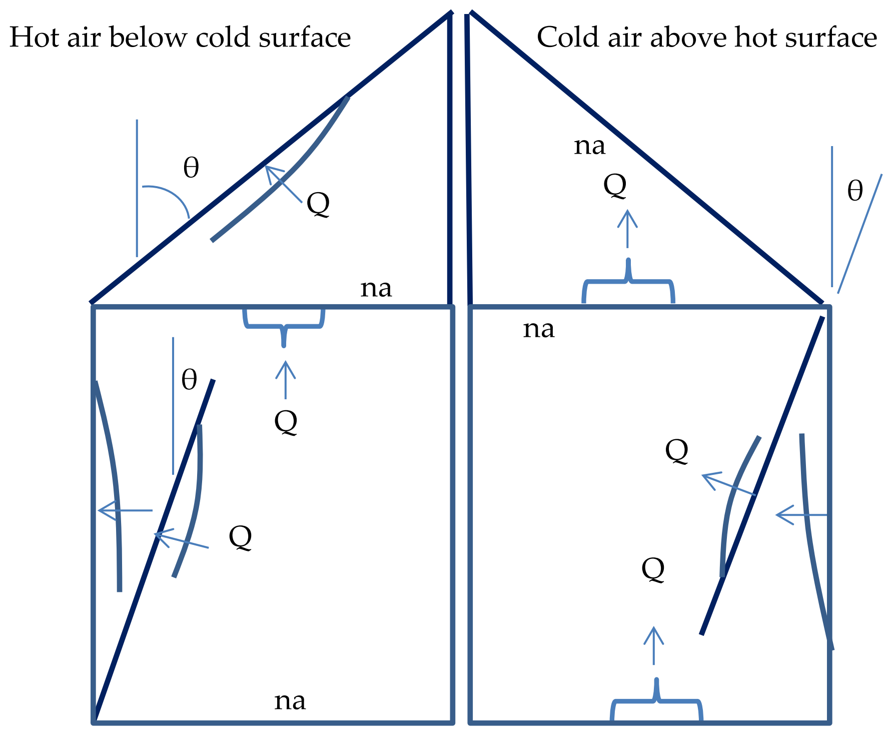

Explanation of Symbols

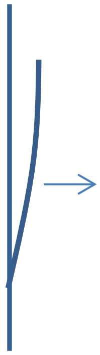

symbolizes the direction in which the boundary layer is thickening, and the direction of positive heat flow.

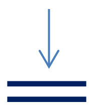

symbolizes the air is stratified next to the surface and the direction the heat flow would be if there is any--the Figs. 1 eqns give zero heat flow in this case.

na symbolizes the equations are n/a (not applicable) to the adjacent surface, because the surface doesn't have an an upward or downward facing component, as the case requires .

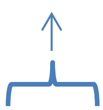

symbolizes plumes of air buoyantly leaving the adjacent surface, and the direction of heat flow, due to Rayleigh-Benard instability.

1.5.2.3 Natural convection equations

Equation 37, from Churchill and Chu (see Eq. 4.86, Mills (1992)), is used to determine the natural convection coefficients for tilted surfaces. The choice of this equation is partly informed by the work of Wallenten (2001), which compares the Churchill and Chu equation with other correlations and experimental data.

Equation 37 is for turbulent convection ($10^9 < \mathrm{Ra} < 10^{12}$), expected to be the dominant case in room heat transfer.

Equation 37 applies to either side of a tilted surface for angles ($0 \le \theta \le 88^o$) if the heat flow has a downward component, or the heat flow is horizontal.

Equation 37 also applies to either side of a tilted surface for angles $\theta < 60^o$ if the heat flow has an upward component, or the heat flow is horizontal.

$$Nu = 0.68 + 0.67(Ra \cdot \psi)^{0.25}(1 + 1.6 * 10^{-8} Ra \cdot \psi)^{\frac{1}{12}}$$

Equation 37

where,

Ra = the Rayleigh number.

Nu = the Nusselt number.

Pr = the Prandtl number.

$$\psi = \left[1 + \left(\frac{0.492}{Pr}\right)^{\frac{9}{16}}\right]^{-\frac{16}{9}}$$

Using $\psi = 0.349$ for $Pr = 0.72$, Equation 37 reduces to:

$$Nu = 0.68 + 0.515Ra^{0.25}(1 + 5.58 * 10^{-9}Ra)^{1/12}$$

Equation 38

For high Ra [$Ra \approx> 10^9$] , neglecting the additive terms "1" and "0.68" in Equation 37 gives:

$$Nu = 0.1057Ra^{1/3}$$

Equation 39

By the definition of the Nusselt number, the natural convection heat transfer coef, h_n is:

$$h_n \equiv Nu * \frac{k(air)}{L_{char}}$$

At 70F, $Ra = 1.66x10^6L^3|\Delta T|cos(\theta)$, and $k = 0.0148$, Equation 39 reduces to:

$$h_n = 0.185\left(|\Delta T|cos(\theta)\right)^{1/3}$$

Equation 40

Note that h_n is independent of characteristic length L_{char}.

Downward heat flow

According to Mill's(1992) Equation 37 doesn't apply to downward heat flow for $\theta > 88^o$. At 70 F, for a 20 ft characteristic length, the 0.68 term predicted by Equation 38 for $\theta = 90^o$ corresponds to $h_n = \frac{0.68k}{L} = 0.0005$; essentially zero. Although the downward heat flow is ideally stably stratified (three cases shown in Figure 4), most measurements and modeling practice indicate h may be larger than zero. We use the equation of Clear et al. for the minimum, for heat flow down:

$$Nu = 0.27Ra^{0.25}$$

Equation 41

Clear's equation reduces to:

$$h_n = 0.27(0.0148)\left(\frac{4}{L}\right)\left(1.642E6\Delta T\left(\frac{L}{4}\right)^3\right)^{0.25}$$

or

$$h_n = 0.202\left|\frac{\Delta T}{L_{char}}\right|^{\frac{1}{4}}$$

Equation 42

where, L_{char} is the wall characteristic length; see Equation 51 definitions.

Adding this h to Equation 40 gives:

$$h_{down} = MAX\left[0.185\left(|\Delta T|cos(\theta)\right)^{\frac{1}{3}}, 0.202\left|\frac{\Delta T}{L_{char}}\right|^{\frac{1}{4}}\right] \quad 0 \le \theta \le 90$$

Equation 43

The following simplification is made, where the exponent of the second term is changed to 1/3, so that $|\Delta T|^{1/3}$ can be factored out:

$$h_{down} = |\Delta T|^{1/3} MAX\left[0.185\left(cos(\theta)\right)^{\frac{1}{3}}, 0.202 L_{char}^{-\frac{1}{3}}\right] \quad 0 \le \theta \le 90$$

Equation 44

Changing the exponent means Equation 44 gives same answer as Equation 43 only when $\frac{\Delta T}{L_{char}} = 1$. But Equation 44 would have acceptable error for other $\frac{\Delta T}{L_{char}}$ ratios, and gives more or less the right dependence on ΔT. If in addition, one assumes a typical $L_{char} = 15$, say, then the minimum term becomes: $0.202 L_{char}^{-\frac{1}{3}} = 0.08$, giving the final reasonable form:

$$h_{down} = |\Delta T|^{1/3} MAX\left[0.185\left(cos(\theta)\right)^{\frac{1}{3}}, 0.08\right] \quad 0 \le \theta \le 90$$

Equation 45

Upward heat flow for $\theta \le 60^o$

For the inside & outside of walls where the heat flow has an upward (or horizontal heat flow at the limit $\theta = 0^o$), and the outside of roofs, Equation 40 applies:

$$h_n = 0.185\left(|\Delta T|cos(\theta)\right)^{1/3}$$

Upward heat flow for $\theta > 60^o$

To handle cases of upward heat flow for $\theta > 60^o$, h_{up} is found by interpolating between Equation 40, evaluated at $\theta = 60^o$, and Equation 47 at 90^o. Equation 46, for heat transfer from a horizontal surface ($\theta = 90$), is from Clear et al. (Eq. 11a). It is close to the much used McAdams equation suggested by both the Mills(1992) and Incropera-Dewitt textbooks.

$$Nu = 0.15Ra^{1/3}$$

Equation 46

At 70-F, Equation 46 reduces to

$$h_n \ = \ 0.26(\varDelta T)^{1/3}$$

Equation 47

Interpolating, for upward heat flow cases with $\theta \geq 60^o$:

$$h_{up} = 0.185\left(\varDelta T cos(60)\right)^{1/3} + \frac{\left(0.26(\varDelta T)^{1/3} - 0.185\left(\varDelta T cos(60)\right)^{1/3}\right)(\theta - 60)}{30}$$

which reduces to:

$$h_{up} = \ (0.00377 * \theta - 0.079)|\varDelta T|^{\frac{1}{3}} \qquad \text{for } 60^o \leq \theta \leq 90$$

Equation 48

where θ is in degrees.

1.5.2.4 Inside forced convection equation

Measured forced convection heat transfer coefficients are frequently correlated using an equation of the form

$$h_{ach} = h_{forcedIN} = C_{ach} * ACH^{0.8}$$

Equation 49

The RBH model (Barnaby et al. (2004) suggests using h_f = 0.88 Btu/hr-ft²F at ACH = 8. This gives $C_{ach} = \ 0.167$. Walton (1983) assumes h = 1.08 when the "air handler system is moving air through the zone." If this was at 8 ach, then this implies $C_{ach} = 0.205$.

1.5.2.5 Outside forced convection equation for all walls and all roofs

From Clear et al. (2001, Eq. (11a)),

$$Nu = W_f R_f 0.037 Re^{0.8} Pr^{1/3}$$

Equation 50

Clear et al. used the Reynolds number based on a free-stream wind velocity 26.2 ft (8 m) above the ground.

At 70F, Equation 50 reduces to:

$$h_V = k * \frac{Nu}{L} = 0.527 W_f R_f \frac{V^{0.8}}{L^{0.2}}$$

Equation 51

where for walls,

$L =$ wall $L_{char} = 4\frac{Wall\ Area}{Wall\ Perimeter}\left(= 4\frac{Height*Width}{2(Height+width)} \approx height\ of\ square\ wall = Z_{eave}\right)$

$V =$ wind velocity at eave height at building location, in ft/sec, $= 0.16 * Z_{\mathrm{eave}}^{0.25} * V_{met}$ from Section 1.5.1.2.

$V_{met} =$ freestream wind velocity, in ft/sec, 10 m (32.8 ft) above the ground at the meteorological station site.

$R_f =$ Table 3 value.

$W_f = 0.63$

The wind direction multiplier, W_f, is defined as the average h of all of the vertical walls, divided by the h of the windward wall, with this ratio averaged over all wind directions. We estimated W_f using the CFD and wind tunnel data of Blocken et al. (2009) for a cubical house. Blocken's Table 6 gives a windward surface convection coefficient of $\mathrm{h_c} \approx 4.7\mathrm{V}^{0.84}$ (SI units), averaged over wind direction. Blocken's Figure 9 gives $\overline{h_c} \approx 7.5$ averaged over all vertical surfaces, for wind speed $\mathrm{V_{met}} =$ 3-m/s. Thus, we estimate $\mathrm{W_f} = \frac{7.5}{4.7\mathrm{V}^{0.84}} = 0.63$.

and for roofs,

$\mathrm{L} =$ roof $\mathrm{L_{char}} = 4\frac{Roof\ Plan\ Area}{Roof\ Perimeter}\left(= 4\frac{Length*Width}{2(Length+width)} \approx \sqrt{Roof\ Area}\ \ for\ square\ roof \approx Z_{eave}\right)$

V = wind velocity 9.8 ft (3 m) above the eave height at building location, in ft/sec.

$= 0.16 * (\mathrm{Z_{eave}} + 9.8)^{0.25} * \mathrm{V_{met}}$

$W_f = 1$

$R_f =$ Table 3 value.

Walton (1983) assumed that the ASHRAE roughness factors of Table 3 apply to the convection coefficient correlations. The Clear et al. (2001) experiments tend to confirm the validity of these factors. Blocken et al. (2009) says, "The building facade has been assumed to be perfectly smooth. Earlier experimental studies have shown the importance of small-scale surface roughness on convective heat transfer. For example, Rowley et al. found that the forced convection coefficient for stucco was almost twice that for glass. Other studies showed the important influence of larger-scale surface roughness, such as the presence of mullions in glazed areas or architectural details on the facade, on the convection coefficient."

Table 3: Surface Roughness Parameter R_f (Walton 1981)

Roughness Index	Rf	Example
1 (very rough)	2.1	Stucco
2 (rough)	1.67	Brick
3 (medium rough)	1.52	Concrete
4 (Medium smooth)	1.13	Clear pine
5 (Smooth)	1.11	Smooth plaster
6 (Very Smooth)	1	Glass

1.5.2.6 Inside combined natural and forced convection

The combined convection coefficient is assumed to be the direct sum of the natural and forced convection coefficients:

For upward and horizontal heat flow:

$$h_{combined} = h_{up} + h_{ach}$$

Equation 52

where,

$h_{up} =$ Equation 40 or Equation 48 depending on whether θ is < or > 60°.

h_{ach} = Equation 49

For downward heat flow:

$$h_{combined} = h_{down} + h_{ach}$$

Equation 53

where,

h_{down} = Equation 45

h_{ach} = Equation 49

1.5.2.7 Outside combined natural and forced convection

The conclusion of Clear et al. (2001) is that the combined convection coefficient is best correlated by assuming it to be the sum of the natural and forced coefficients. For roofs, Clear et al. (2001) assumes that the natural and forced convection are additive, but that natural convection is suppressed by the factor η given by Equation 56 when forced convection is large ($\eta \rightarrow 0$ as the

Reynolds number becomes large). We also assume this attenuation of the natural convection applies to the outside of the walls.

For all vertical walls, and walls with moderate tilts:

$$h_{combined} = \eta h_n + h_V$$

Equation 54

where,

h_n = Equation 40

h_V = Equation 51

$\eta = \frac{1}{1+\frac{1}{\ln\left(1+\frac{0.06L|\Delta T|}{V^2}\right)}}$ (to avoid divide by zero, if V= 0, could set to V = 0.001)

where L & V are the same as used in Equation 51 for walls.

For roofs, Clear et al. (2001) assumes that the natural and forced convection are additive, but that natural convection is suppressed by the factor η when forced convection is large ($\eta \rightarrow 0$ as the Reynolds number becomes large). Clear gives η as:

$$\eta = \frac{1}{1+\frac{1}{\ln\left(1+\frac{Gr_L}{Re_L^2}\right)}}$$

Equation 55

At 70F, with $Gr = 2.28x10^6 L^3|\Delta T|$, $\mathrm{Re}^2 = (6140\mathrm{VL})^2$, and $\mathrm{L} = \mathrm{L}_{\mathrm{char}}$ for surface , Equation 55 reduces to:

$$\eta = \frac{1}{1+\frac{1}{\ln\left(1+\frac{0.06L|\Delta T|}{V^2}\right)}}$$

Equation 56

For roofs:

$$h_{combined} = \eta h_n + h_V$$

Equation 57

where,

$h_n =$ Equation 45 for downward heat flow.

$h_n =$ Equation 47 for upward heat flow.

$h_V =$ Equation 51 for upward or downward heat flow.

η is from Equation 56

L & V are the same as used in Equation 51 for roofs.

1.5.2.8 *Plots of equations*

In Figure 6, the left hand column of plots are of Equation 53, for the downward heat flow cases shown in Figure 4. The right hand side plots are of Equation 52, for upward heat flow cases of Figure 5. All of the plots assume $T_{film} = 70F$, and $L_{char} = Z_{eave} = 20$ ft.

Figure 6: Plots of Equations for Downward and Upward Heat Flow

DOWNWARD HEAT FLOW (Equation 53): *UPWARD HEAT FLOW (Equation 52):*

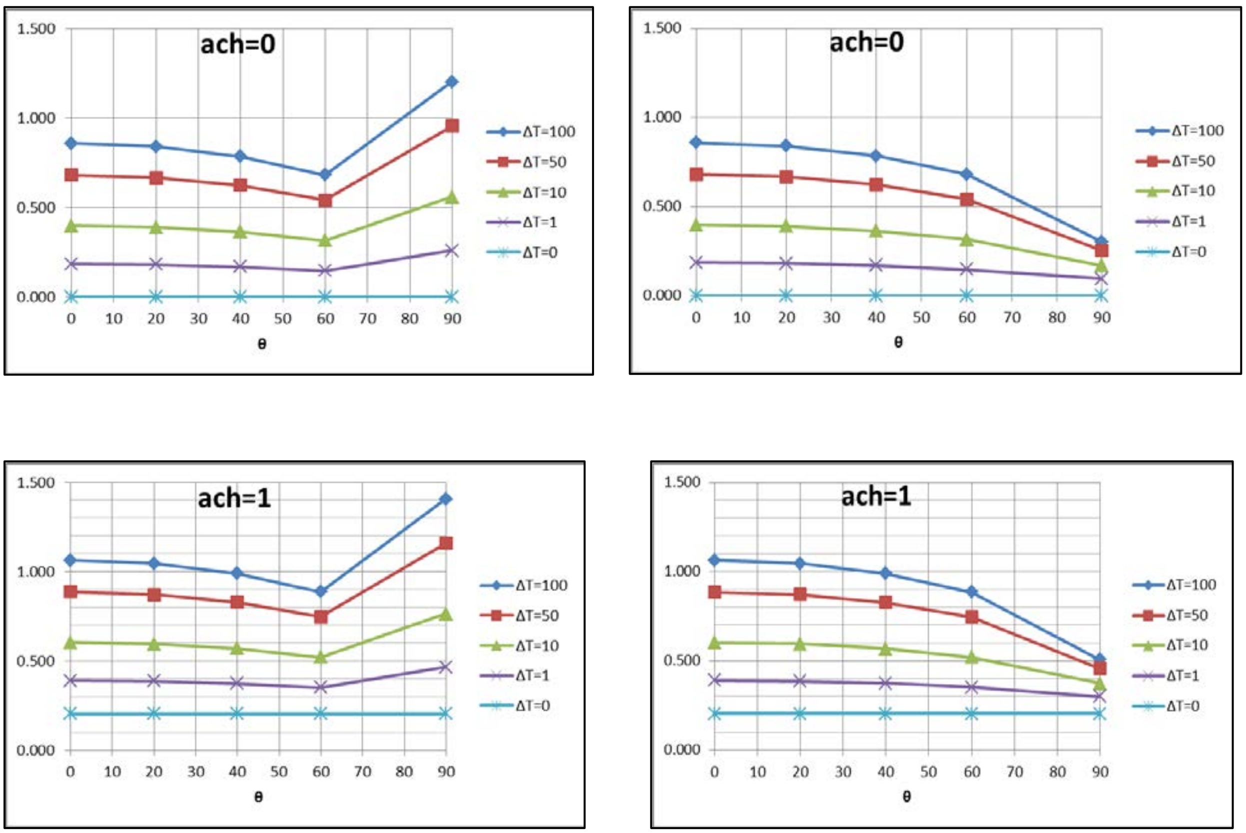

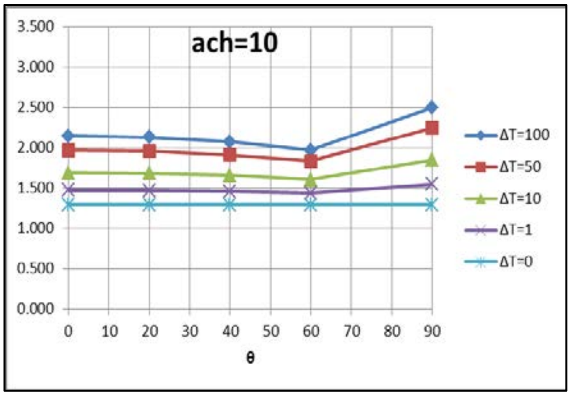

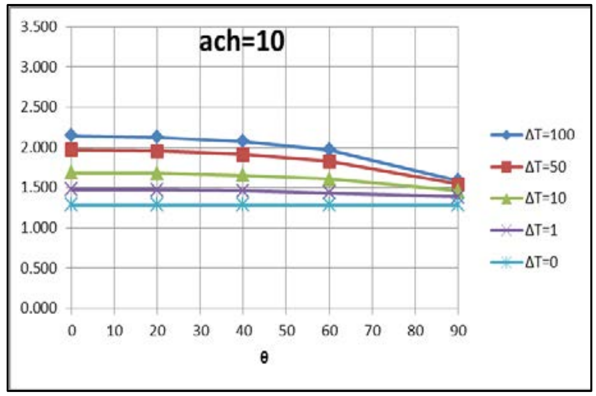

<u>OUTSIDE surface convection coefficient Plot for a horizontal roof:</u>

For $\Delta T = 50\ F$, $L_{char} = 20$ ft, $R_f = 1.67$:

Figure 7: Outside Convection Coefficients, Natural Up and Down, and Forced

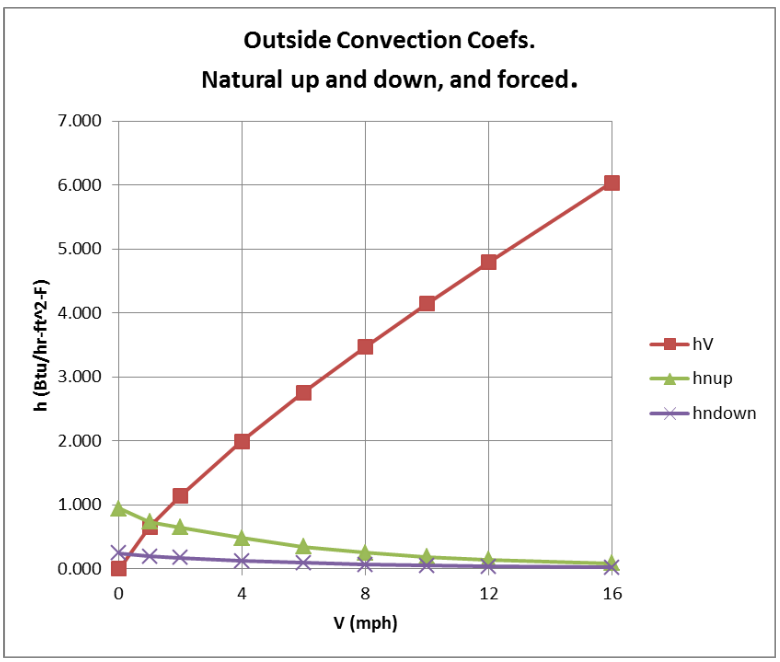

1.5.3 Outside Radiation Coefficients

1.5.3.1 Wall surfaces

The net long wave radiation heat exchange between the outside surface and the environment is dependent on surface temperature, the spatial relationship between the surface and the surroundings, and the properties of the surface. The relevant material properties of the surface, emissivity ε and absorptivity α, are complex functions of temperature, angle, and wavelength. However, it is generally assumed in building energy calculations that the surface emits or reflects diffusely and is gray and opaque ($\alpha = \varepsilon, \tau = 0, \rho = 1 - \varepsilon$).

The net radiant heat loss from a unit area of the outside of a construction surface to the outside environment is given by:

$$q_{rad} = \varepsilon\epsilon_g\sigma F_{gnd}(T_s^4 - T_g^4) + \varepsilon\sigma F_{sky}\beta\left(T_s^4 - T_{sky}^4\right) + \varepsilon\sigma F_{sky}(1-\beta)(T_s^4 - T_a^4)$$

Equation 58

where,

ε = surface emissivity.

ϵ_g = ground emissivity is assumed to be 1.

σ = Stephan-Boltzmann constant.

T_s = outside surface temperature.

T_a = outside dry bulb temperature.

T_g = ground surface temperature.

T_{sky} = effective temperature of sky.

F_{gnd} = view factor from surface to ground.

F_{sky} = view factor from surface to sky.

$\beta = \cos\left(\frac{\phi}{2}\right)$

The sky irradiance is taken as a β weighted average of that from T_{sky} and that from T_a.

1.5.3.2 Fsky, Fgnd, and β

Howell (1982, #C-8, p.94), gives the fraction of the radiation leaving the window surface and reaching the sky by:

$$F_{sky} = \frac{1 + \cos\phi}{2}$$

The fraction leaving the window incident on the ground is:

$$F_{gnd} = \frac{1 - \cos\phi}{2}$$

where, φ = surface tilt angle, the angle between ground upward normal and window outward normal (0° corresponds to a horizontal skylight, 90° to a vertical surface).

The parameter β accounts for the sky temperature's approach to the air temp near the horizon. β is the fraction of the sky effectively at Tsky; (1-β) is the fraction of the sky effectively at Ta. β is used by Walton (1983), and Energy Plus (2009), but appears to have little theoretical or experimental basis.

Walton (1983) give β as:

$$\beta = \cos\left(\frac{\phi}{2}\right)$$

Since $\cos\left(\frac{\varphi}{2}\right) = \sqrt{\frac{1+\cos\varphi}{2}}$, it is noted that $F_{sky} = \beta^2$, and $F_{sky}\beta = \beta^3$.

1.5.3.3 Net radiant heat loss from a unit area

Equation 58 can be written as

$$q_{rad} = h_{rg}(T_s - T_g) + h_{rsky}(T_s - T_{sky}) + h_{rair}(T_s - T_a)$$

Equation 59

where,

$$h_{rg} = \varepsilon\sigma F_{gnd}(T_s^2 + T_g^2)(T_s + T_g)$$

$$h_{rsky} = \epsilon\sigma\, F_{sky}\beta(T_s^2 + T_{sky}^2)(T_s + T_{sky})$$

$$h_{rair} = \varepsilon\sigma\, F_{sky}(1-\beta)(T_s^2 + T_a^2)(T_s + T_a).$$

T_g is assumed to be equal to Ta, so Equation 59 becomes

$$q_{rad} = h_{rsky}(T_s - T_{sky}) + h_{ra}(T_s - T_a)$$

Equation 60

where,

$$h_{rsky} = \epsilon\sigma\, F_{sky}\beta\,(T_s^2 + T_{sky}^2)(T_s + T_{sky})$$

Equation 61

$$h_{rair} = \varepsilon\sigma\,\left(F_{sky}(1-\beta) + F_{gnd}\right)(T_s^2 + T_a^2)(T_s + T_a)$$

Equation 62

For a vertical surface, $F_{sky}\beta = 0.354$, and $F_{sky}(1-\beta) + F_{gnd} = 0.646$, so

$$h_{rsky} = 0.354\epsilon_s\sigma\,(T_s^2 + T_{sky}^2)(T_s + T_{sky}) \approx 4(0.354)\varepsilon_s\sigma\bar{T}^3$$

$$h_{rair} = (0.146 + 0.5)\varepsilon_s\sigma(T_s^2 + T_a^2)(T_s + T_a) \approx 4(0.646)\varepsilon_s\sigma\bar{T}^3$$

1.5.3.4 Total effective conductance and outside effective temperature, Tenv, for walls

Adding the exterior convection coefficient, *hco*, of Equation 40 to Equation 60 gives the total net heat transfer from the outside surface :

$$q_{rad+conv} = h_{rsky}(T_s - T_{sky}) + (h_{rair} + h_{co})(T_s - T_a)$$

Equation 63

This can be written as,

$$q_{rad+conv} = h_o(T_s - T_{env})$$

Equation 64

where h_o is the effective exterior conductance to the conductance weighted average temperature, T_{env}.

$$h_o = h_{rsky} + h_{rair} + h_{co}$$

Equation 65

$$T_{env} = \frac{h_{rsky}T_{sky} + (h_{rair} + h_{co})T_a}{h_{rsky} + h_{rair} + h_{co}}$$

Equation 66

1.5.3.5 Outside window surfaces

The ASHWAT window algorithm of Section 1.7 utilizes the irradiation intercepted by the window. From Equation 58 this can be deduced to be:

$$G = F_{gnd}\sigma T_{gnd}^4 + F_{sky}\beta\sigma T_{sky}^4 + F_{sky}(1-\beta)\sigma T_{air}^4$$

Equation 67

1.5.4 Sky Temperature

It is possible to approximate the long wave radiation emission from the sky as a fraction of blackbody radiation corresponding to the temperature of the air near the ground. The sky emittance ε_{sky} is defined such that the sky irradiation on a horizontal surface is $\sigma\varepsilon_{sky}T_a^4$.

The effective temperature of the sky is obtained by equating the blackbody emissive power of the sky at T_{sky}, to the sky irradiation:

$$\sigma\, T_{sky}^4 = \sigma\varepsilon_{sky}T_a^4$$

or,

$$T_{sky} = \varepsilon_{sky}^{0.25}T_a,$$

Equation 68

where T_{sky} and T_a are in degrees Rankine.

The value of ε_{sky} depends on the dewpoint temperature, cloud cover, and cloud height data. Martin and Berdahl (1984) give the ε_{sky} for clear skies as ε_o:

$$\varepsilon_o = 0.711 + 0.56\frac{T_{dew}}{100} + 0.73\left(\frac{T_{dew}}{100}\right)^2 + 0.013\cos\left(\pi\frac{hr}{12}\right) + 0.00012\,(P_{atm} - 1000)$$

Equation 69

where,

T_{dew} = the dewpoint temperature in Celsius.

hr = hour of day (1 to 24).

P_{atm} = atmospheric pressure in millibars.

1.5.4.1 Palmiter version of Martin-Berdahl model

The clear sky emissivity is corrected to account for cloud cover by the following algorithm, developed by Larry Palmiter (with Berdahl's imprimatur), that represents the Martin and Berdahl model when weather tape values of cloud ceiling height, and total and opaque cloud fractions are available.

$$\epsilon_{sky} = \varepsilon_0 + (1 - \varepsilon_0)(n_{op}\varepsilon_{op}\Gamma_{op} + n_{th}\varepsilon_{th}\Gamma_{th})$$

Equation 70

where,

n_{op} = the opaque cloud fraction

n_{th} = the thin cloud fraction: $n_{th} = n - n_{op}$

n = the total sky cover fraction

ε_{op} = the opaque cloud emittance is assumed to be 1.

ε_{th} = the thin cloud emittance; assumed to be 0.4.

The cloud factor Γ is used to adjust the emissivity when the sky is cloudy due to the increasing cloud base temperature for decreasing cloud altitudes. The cloud base temperature is not available on the weather tapes, so assuming a standard lapse rate of 5.6°C/km, Γ is correlated with the more commonly measured cloud ceiling height, h (in meters), giving by the general expression:

$$\Gamma = e^{-\frac{h}{8200}}$$

For thin clouds, Γ_{th} is determined using an assumed cloud height of 8000-m, so,

$$\Gamma_{th} = e^{-\frac{8000}{8200}} = 0.377$$

Equation 71

For opaque clouds,

$$\Gamma_{op} = e^{-\frac{h}{8200}}$$

Equation 72

If ceiling height data is missing (coded 99999 on TMY2), the Palmiter model assumes that the opaque cloud base is at $h = 2000\ m$. If ceiling height is unlimited (coded as 77777) or cirroform (coded 88888), it is assumed that the opaque cloud base is at $h = 8000\ m$.

Using the assumed cloud cover and emissivity factors, Equation 70 becomes:

$$\epsilon_{sky} = \epsilon_0 + (1 - \epsilon_0)\left[n_o \Gamma_{op} + (n - n_o) * 0.4 * 0.377\right]$$

or,

$$\epsilon_{sky} = \epsilon_0 + (1 - \epsilon_0)\left[n_o e^{-\left(\frac{h}{8200}\right)} + 0.151(n - n_o)\right]$$

Equation 73

1.5.4.2 When opaque cloud cover data, n_o, is missing

In this case it is assumed that the cloud cover is opaque, $n_o = n$, when the ceiling height is less than 8000-m, and half opaque, $n_o = \frac{n}{2}$, when the ceiling height is equal or greater than 8000. That is,

for $h < 8000\ m$ (from Equation 73 with $n_o = n$):

$$\epsilon_{sky} = \epsilon_0 + (1 - \epsilon_0) n e^{-\left(\frac{h}{8200}\right)}$$

Equation 74

For $h \geq 8000\ m$ (from Equation 73 with $n_{op} = n_{th} = \frac{n}{2}$):

$$\epsilon_{sky} = \epsilon_0 + (1 - \epsilon_0) n \left[\frac{1}{2} e^{-\left(\frac{h}{8200}\right)} + 0.0754\right]$$

Equation 75

1.5.4.3 When both opaque cloud cover and ceiling height data is missing

When only total sky cover is available using an h of 2000-m reduces Equation 74 to:

$$\epsilon_{sky} = \epsilon_0 + 0.784(1 - \epsilon_0) n$$

Equation 76

1.6 DISTRIBUTION OF SW AND LW RADIATION INSIDE THE ZONE

1.6.1 Long Wave Radiation Distribution

1.6.1.1 Carroll model

The radiant model used in CSE is based on the "MRT Network Method" developed by Joe Carroll (see Carroll 1980 & 1981, and Carroll & Clinton 1980 & 1982). It was chosen because it doesn't require standard engineering view factors to be calculated, and yet gives a relatively accurate radiant heat distribution for typical building enclosures (see Carroll 1981).

It is an approximate model that simplifies the "exact" network (see Appendix C) by using a mean radiant temperature node, Tr, that act as a clearinghouse for the radiation heat exchange between surfaces, much as does the single air temperature node for the simple convective heat transfer models. For n surfaces this reduces the number of circuit elements from (n-1)! in the exact case, to n with the Carroll model.

For black surfaces the radiant network is shown in Figure 8. For n surfaces, T_r floats at the conductance, $A_i F_i$, weighted average surface temperature:

$$T_r = \frac{\sum_1^n A_i F_i T_i}{\sum_1^n A_i F_i}$$

Equation 77

The actual areas, A_i , need not be equal, nor limited to three.

Figure 8: Carroll Network for Black Surfaces

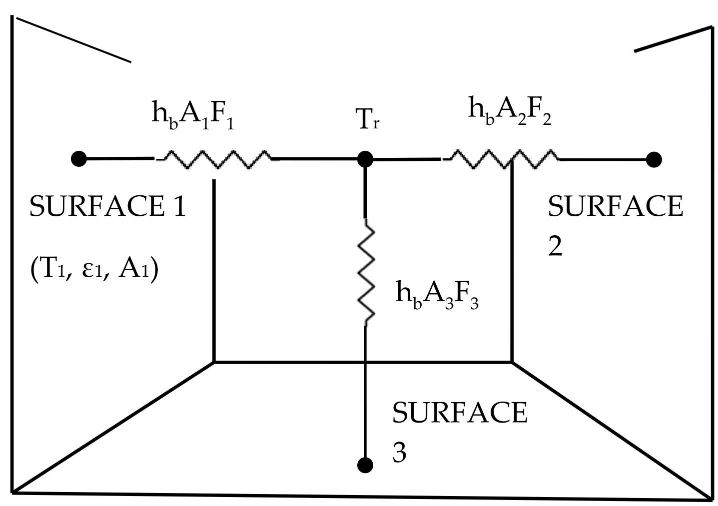

The factor F_i, in the radiant conductance between the T_i surface node and the T_r node is Carroll's "MRT view factor", that corrects for the self-weighting (see Appendix D) of T_i in the temperature T_r. The F_i factors are obtained from the set of n nonlinear equations for n surfaces:

$$F_i = \frac{1}{1 - \frac{A_i F_i}{\sum_1^n A_j F_j}}$$

Equation 78

Given the surface areas, these equations are easily solved at the beginning of the simulation by successive substitution, starting with all $F_i = 1$. This converges for realistic enclosures, but won't necessarily converge for enclosures having only two or three surfaces, particularly if there are large area disparities.

> F_i is always larger than 1 because it's role is to raise the conductance between T_r and T_i to compensate for the potential difference $|T_r - T_i|$ being smaller than it would be had T_i not been part of the conductance weighted average T_r. The F_i values can be seen to be close to 1, since

Equation 78 is roughly approximated by $F_i \approx 1 + (A_i / A_{all\ surfaces})$.

The net radiant heat transfer [Btu/hr] from surface i is:

$$q_i = h_b A_i F_i (T_i - T_r)$$

Equation 79

Using a Y-Δ transformation, the Figure 8 circuit can put in the form of the exact solution network of Figure C- 1 in Appendix C, showing the implicit view factors F_{ij} to be:

$$F_{ij} = \frac{F_i A_j F_j}{\sum_{k=1}^n A_k F_k}$$

Equation 80

Thus the implicit view factors are independent of the relative spacial disposition of the surfaces, and almost directly proportional to the surface area Aj of the viewed by surface i. Also, without special adjustments (see Carroll (1980a)), all surfaces see each other, so coplanar surfaces (a window and the wall it is in) radiate to each other.

> Equation 79 is exact (i.e., gives same answers as the Appendix C model) for cubical rooms; for which

Equation 78 gives $F_i = 1.20$. Substituting this into Equation 80 gives the implied $F_{ij} = 0.2$. This is the correct F_{ij} for cubes using view-factor equations Howell(1982). It is likely accurate for all of the regular polyhedra.

Grey surfaces

Carroll's model handles gray surfaces, with emissivities ε_i, by adding the Oppenheim surface conductance $\frac{A_i\varepsilon_i}{1-\varepsilon_i}$ in series with the conductances $h_bA_iF_i$. As shown in Figure 9, the conductance between T_i and T_r becomes $h_bA_iF_i'$, where the F_i' terms are:

$$F_i' = \frac{1}{\frac{1}{F_i} + \frac{1-\varepsilon_i}{\varepsilon_i}}$$

Equation 81

The net radiant heat transfer [Btu/hr] from surface i is given by:

$$q_i = h_bA_iF_i'(T_i - T_r)$$

Equation 82

where for grey surfaces T_r is the "$h_bA_iF_i'$" weighted average surface temperature given by:

$$T_r = \frac{\sum_1^n A_iF_i'T_i}{\sum_1^n A_iF_i'}$$

Equation 83

Similar to Equation 77 for a black enclosure, Equation 83 shows that T_r for grey surfaces is the conductance, A_iF_i', weighted average surface temperatures.

The role of F_i hasn't changed, but since the conductance A_iF_i is now connected to the radiosity node rather than the surface node, $E_r(=\sigma T_r^4)$ can be thought of as the A_iF_i-weighted average radiosity of the surfaces, rather than the A_iF_i-weighted average emissive power of the surfaces as in the black enclosure case.

Figure 9: Carroll Radiant Network for Grey Surfaces

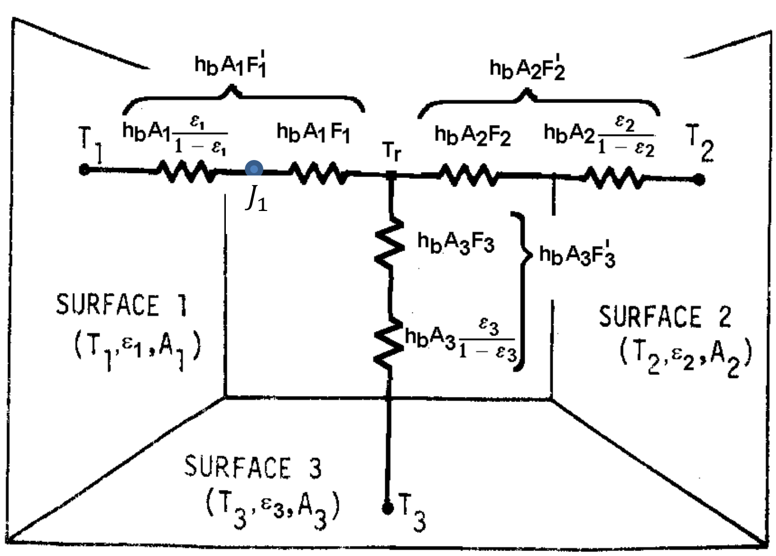

This completes the description of the basic Carroll model. The principle inputs are the interior surface areas in the zone, the emissivities of these surfaces, and the typical volume to surface area ratio of the zone (see Section 1.6.1.3). All of the interior surfaces, including ducts, windows, and interior walls, are assumed to exchange heat between each other as diffusely radiating gray body surfaces.

Longwave radiant internal gains can be added, in Btu/hr, to the radiant node Tr. This distributes the gains in proportion to the conductance $A_i F_i'$.

Conversion to delta

Using a Y-Δ transformation, the radiant network of Figure 9 can be converted to the Appendix C, Figure C- 3 circuit form, eliciting the F_{ij}' interchange factors implicit in Carroll's algorithm. Similar in form to Equation 80,

$$A_i F_{ij}' = \frac{A_i F_i' A_j F_j'}{\sum_{k=1}^{n} A_k F_k'}$$

Equation 84

Using these $A_i F_{ij}'$ values, q_{ij} can be obtained from

$$q_{ij} = h_b A_i F_{ij}' (T_i - T_j)$$

Equation 85

The total net heat transfer from surface *i* (i.e., the radiosity minus the irradiation for the un-linearized circuit) is given by summing Equation 85 for all the surfaces seen by surface i:

$$q_i = \sum_{j=1}^{n} h_b A_i F_{ij}' (T_i - T_j)$$

Equation 86

which will agree with the result of Equation 82.

1.6.1.2 Accuracy of Carroll model

The Carroll model of Figure 9 is exact for cubical enclosures with arbitrary surface emissivities. It is surprisingly accurate for a wide variety of shapes, such as hip roof attics and geodesic domes.

Carroll (1981) compared his model, and other simplified models, with the exact solution for the enclosure shown in Figure 10. Half the south wall and half of the west wall are glass with ε = 0.84, and the rest of the interior surfaces have ε = 0.9.

Figure 10: Test Room of Walton (1980)

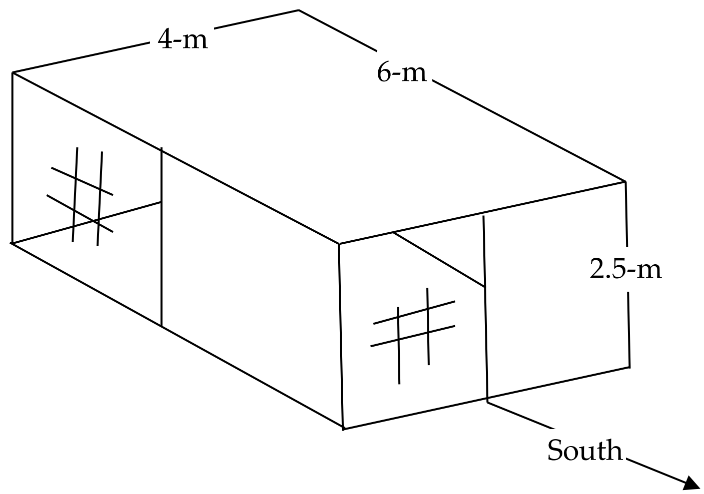

Comparisons were made primarily regarding three types of errors:

Heat balance errors

The first law requires that the sum of the net radiation emitted by each of the surfaces, plus any internal gain source of long-wave radiation, must equal zero. That is, $q_{int} + \sum_{i=1}^{n} q_i = 0$.

Due to their fixed conductance circuits, both the Carroll method and the Walton(1983) method are inherently free of heat balance errors. Carroll found BLAST and NBSLD algorithms to have rms heat balance errors of 9.8% (12%) and 1.7%(3.4%) for the Figure 10 enclosure.

Individual surface net heat transfer errors

For a given enclosure, these are errors in an individual surfaces net heat flow, q_i, compared to the exact method. For Carroll's method, this finds the error in q_i determined from the $A_i F'_{ij}$ values ofEquation 84, compared to the q_i values found using the exact $A_i F'_{ij}$ values (obtainable from Figure C- 3 of Appendix C).

Carroll found the % rms error in the q_i values for a given enclosure in two different ways.

The first method, Equation 87, gives the rms error of q_i for each surface divided by the rms of the n net heat transfers from each surface:

$$Err = \left(\frac{\frac{1}{n} \sum_{i=1}^{n} \Delta q_i^2}{\frac{1}{n} \sum_{i=1}^{n} \bar{q}_i^2} \right)^{\frac{1}{2}} * 100$$

Equation 87

where

$\Delta q_i = q_i - \bar{q}_i$, is the error in q_i.

$q_i = \sum_{j=1}^{n} h_b A_i F'_{ij}(T_i - T_j)$, using F'_{ij} values from Carroll's model, Equation 87.

$\bar{q}_i = \sum_{j=1}^{n} h_b A_i F'_{ij}(T_i - T_j)$, using the exact F'_{ij} values of Figure C- 3 of Appendix C

$T_i - T_j = 1^0 F$ assumed in all cases.

n = the number of surfaces

The second method, Equation 88, gives the rms of the percentage error in q_i of each surfaces. This method increases the weight of smaller surfaces such as windows.

$$Err = \frac{1}{n}\sum_{i=1}^{n}\left(\frac{\Delta q_i}{q_i}\right)^2 * 100$$

Equation 88

Results

For the enclosure of Figure 10, Carroll found his method gives *Err* = 0.11% for the first method and 0.19% for the second method.

These results are shown in Table 4, along with the results for other shape enclosures, and the errors determined by Carroll using the radiant interchange algorithms of Walton (1980) and NBSLD and BLAST simplified models.

Table 4: Err = % rms Error in q_i from Equation 87 and Equation 88 in Parenthesis

	Figure 10 room 2.5:4:6 ε = 0.9 (.84 wdws)	Corridor 10:1:1 ε = 0.9	Warehouse 10:10:1 ε = 0.9
Carroll	0.11 (0.19)	0.06(0.05)	0.07 (0.04)
Walton(1980)	1.9 (1.30)	0.6 (0.6)	4.4 (3.0)
NBSLD, BLAST	3.2 (2.1)	3.2 (2.6)	7.5 (4.4)

Errors in an individual surface's distribution of heat transfer to other surfaces

These are errors in q_{ij}, the heat exchanged between surfaces i and j (both directly and by reflections from other surfaces), relative to the exact total net heat transfer from surface *i* given by Figure C- 3 of Appendix C.

Carroll gives two percentage error results.

By the first method, for each surface i, the rms of the error, Δq_{ij}, in heat exchange to each of the *n-1* other *j* surfaces is obtained. Then the rms of these n rms error values is obtained, giving a representative distribution error for the enclosure. Dividing this by the rms value of the exact net surface heat transfers, q_i, of all the surfaces gives the final distribution error in percent:

$$Err = \frac{\sqrt{\sum_{i=1}^{n}\left(\frac{\sum_{j=1}^{n}\Delta q_{ij}^{2}}{n(n-1)}\right)}}{\sqrt{\sum_{i=1}^{n}\left(\frac{\bar{q}_i^{2}}{n}\right)}} * 100$$

Equation 89

where

$\Delta q_{ij} = q_{ij} - \bar{q}_{ij}$,

$q_{ij} = h_b A_i F'_{ij}(T_i - T_j)$ with F'_{ij} values from Equation 84.

$\bar{q}_{ij} = h_b A_i F'_{ij}(T_i - T_j)$ with the exact F'_{ij} values of Figure C- 3 of Appendix C.

By the second method, for each surface i, the rms of the percentage error in heat exchange q_{ij}, relative to the exact net heat transfer from that surface, $\bar{q}_i$, is obtained.

$$Err = 100 * \sqrt{\sum_{i=1}^{n}\left(\frac{\sum_{j=1}^{n}\left(\frac{\Delta q_{ij}}{\bar{q}_i}\right)^{2}}{n(n-1)}\right)}$$

Equation 90

Distribution error results

For the Figure 10 room, Carroll's model gives errors of 2.1% and 3.9% for methods 1 and 2 respectively. Walton's model has corresponding errors of 2.4% and 3.7%. Equation 91 was used for the results in parenthesis.

Table 5: % rms Error in q_i from Equation 90

	Figure 10 room 2.5:4:6 ε = 0.9 (.84 wdws)	Corridor 1:10:1 ε = 0.9	Warehouse 1:10:10 ε = 0.9
Carroll	2.1 (3.9)	3.3 (2.8)	0.6 (1.9)
Walton(1980)	2.4 (3.7)	3.3 (2.8)	2.8 (3.0)
BLAST	2.8 (4.4)	3.4 (4.4)	3.4 (15)
NBSLD	1.7 (3.5)	1 (0.83)	3.3(1.9)

(Equation 91 was used for the results in parenthesis.)

Carroll's model is seen to give very respectable results, despite giving no special treatment to coplanar surfaces.

1.6.1.3 Air absorption

The Carroll model also accounts for the absorption of long-wave radiation in the air, so that the air and mrt nodes are thermally coupled to each other as well as to the interior surfaces. Carroll (1980a) gives an air emissivity by the following dimensional empirical equation that is based on Hottel data from McAdams(1954):

$$\varepsilon_a = 0.08\varepsilon_s \ln\left(1 + \left(\frac{4V}{\varepsilon_s A} R P_{atm}\right) e^{(TaF-32)/30.6}\right)$$

Equation 91

The logarithm is natural, and,

ε_s = the area-weighted average long-wave emissivity for room surfaces, excluding air.

V/A = the room volume to surface area ratio, in meters.

R = the relative humidity in the zone. (0 ≤ R ≤ 1).

Patm = atmospheric pressure in atmospheres.

Ta = zone air temperature, in °F.

Following a heuristic argument Carroll assigns an effective area A_a to the air that is the product of ε_a and the sum of all of the zone surface areas, as if the absorbing part of the air were consolidated into a surface of area A_a.

$$A_a = \varepsilon_a \sum A_i$$

Equation 92

Using this area, the value of F_a for this 'surface' can be calculated along with the other F_i by Equation 80. The value of the conductance between the air and radiant nodes in Figure 11 is given by:

$$C_x = h_b A_a F_a$$

Equation 93

Figure 11: Like Figure 9 but with Convective Network Added

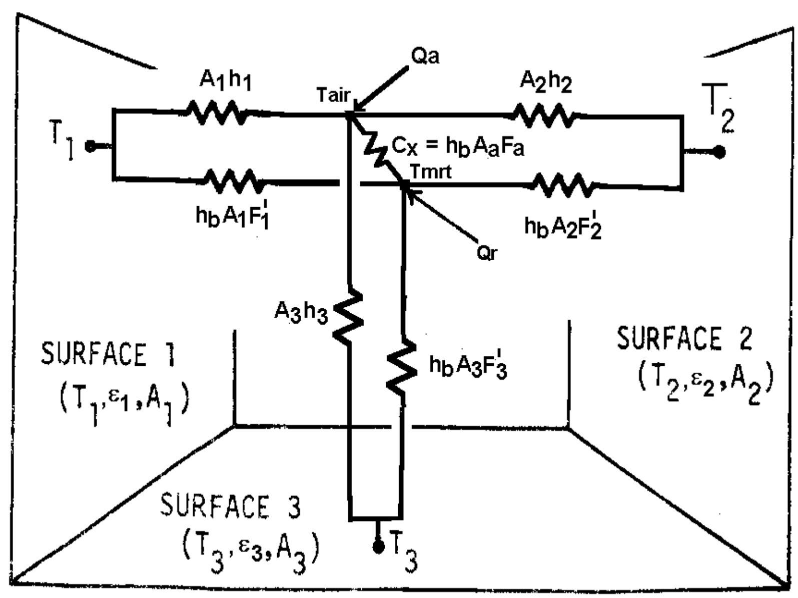

Facets

Suppose one of the interior surfaces of total area A_i is composed of N_i identical flat sub-surfaces, each at the same temperature, and similar views to each other, like the facets of a geodesic dome. The F_i values would be the same if each facet is treated as a separate surface. To avoid redundant solutions to Equation 80, it is easy to show that A_i can be treated as one surface in Equation 6-4 if N_i is introduced into Equation 80 as follows:

$$F_i = \frac{1}{1 - \dfrac{A_i \cdot F_i / N_i}{\Sigma(A_i \cdot F_i)}}$$

Equation 94

The facet feature is utilized in the simulation to represent attic truss surfaces. True?

1.6.2 Short Wave Radiation Distribution

This routine was used in the development code for this program. It is not currently implemented in CSE, being replaced by a simplified but similar routine.

The short wave radiation (solar insolation from hourly input) transmitted by each window can, at the users discretion, be all distributed diffusely inside the zone, or some of the insolation from each window can be specifically targeted to be incident on any number of surfaces, with the remaining untargeted radiation, if any, from that window, distributed diffusely. The insolation incident on any surface can be absorbed, reflected, and/or transmitted, depending on the surface properties inputted for that surface. The radiation that is reflected from the surfaces is distributed diffusely, to be reflected and absorbed by other surfaces ad infinitum.

Since some of the inside surfaces will be the inside surface of exterior windows, then some of the solar radiation admitted to the building will be either lost out the windows or absorbed or reflected by the widows.

1.6.2.1 Radiation removed at each surface of a zone by a single source of targeted insolation

Assume a spherical zone with total insolation S(Btu/hr) admitted into the zone through one window. Assume that the portion $a_i Q_i$ (ft^2*Btu/(hr-ft^2)) of S(Btu/hr) is targeted to surface i with area a_i such that,

$$\sum_i a_i Q_i = S$$

Equation 95

where the sum is over all surfaces i. The total spherical area is $a_S = \sum_i a_i$. Also incident on surface i will be the irradiation G_i (Btu/hr-ft^2) from other surfaces that have reflected a portion of the radiation they have received. We distinguish between the Q_i incident on the surface directly from the window, and the irradiation G_i which is composed of radiation reflected to i from all the surfaces, and that reflected by windows. All radiation (including Incident beam) is assumed to be reflected diffusely.

Each surface i will also reflect short-wave radiation, with a radiosity J_i [Btu/hr-sf].

Figure 12: Radiation Terminology

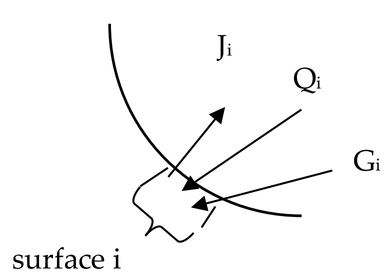

The derivation below determines the equations to obtain J_i and G_i for known Q_i values, for all the surfaces of the sphere, i = 1 to n.

First a relationship between Gi and Ji is developed:

Since G_i is composed only of reflected radiation,

$$a_i G_i = \sum_k J_k a_k F_{ik}$$

Equation 96

where the sum is over all surfaces n of the sphere of area a_S.

Using the view-factor reciprocity principle,

$$a_k F_{ki} = a_i F_{ik}$$

G_i becomes

$$G_i = \sum_k J_k F_{ik}$$

For spherical geometry, the view factor is $F_{ik} = a_k / a_S$, where $a_S = \sum a_k$, so G_i can be written

$$G_i = \frac{1}{a_S} \sum_k J_k a_k$$

Equation 97

The right hand side is the area-weighted average radiosity, showing that G_i is independent of i,

$$G_i = \bar{J}$$

Equation 98

Next a separate relationship between J_i and G_i is obtained, G_i eliminated and J_i solved for explicitly:

The radiosity of surface *i* is composed of the reflected part of both the irradiation and the targeted solar

$$\mathrm{J_i} = \rho_\mathrm{i}(\mathrm{G_i} + \mathrm{Q_i})$$

Equation 99

Substituting Equation 97 for G_i gives

$$\frac{J_i}{\rho_i} = \frac{1}{a_S} \sum_k J_k a_k + Q_i$$

Equation 100

Since by Equation 98 G_i is independent of i, then Equation 99 shows that the radiosity of any surface i is related to the radiosity of any surface k by the relationship

$$\frac{J_i}{\rho_i} - Q_i = \frac{J_k}{\rho_k} - Q_k$$

Substituting this into Equation 100 gives

$$\frac{J_i}{\rho_i} = \frac{1}{a_S}\sum_k \left(a_k\rho_k\left(\frac{J_i}{\rho_i} + Q_k - Q_i\right)\right) + Q_i$$

This can be solved explicitly for J_i:

$$J_i = \frac{\frac{1}{a_S}\rho_i}{1-\bar{\rho}}\left(\sum_k a_k\rho_k Q_k\right) + Q_i\rho_i$$

Equation 101

From Equation 101, the area weighted average J is

$$\bar{J} = \frac{\frac{1}{a_S}\bar{\rho}}{1-\bar{\rho}}\left(\sum_k a_k\rho_k Q_k\right) + \frac{1}{a_S}\sum_i a_i Q_i\rho_i$$

Equation 102

where $\bar{\rho}$ is the area weighed average reflectivity.

Now that J_i and G_i are known an energy balance will give the net heat transfer:

The net energy rate (Btu/hr) absorbed and/or transmitted by surface i, is:

$$Qnet_i = (G_i + Q_i - J_i)a_i = (\bar{J} - J_i + Q_i)a_i$$

Equation 103

Substituting Equation 101 and Equation 102 into this gives

$$Qnet_i = \frac{a_i}{a_S}\left(\frac{1-\rho_i}{1-\bar{\rho}}\right)\sum_k a_k\rho_k Q_k + a_i Q_i(1-\rho_i)$$

Equation 104

The first term in Equation 104 is from the absorption and/or transmission of radiation that reached and is absorbed by surface i after having been reflected, ad infinitum, by the interior surfaces. The second term is from the absorption of the "initially" incident insolation Q_i on surface i.

If none of the insolation is specifically targeted, and instead S is assumed to be distributed isotropically then Q_i is the same for each surface:

$$Q_i = \frac{S}{a_S}$$

Equation 105

Substituting this into Equation 104 gives Qnet$_i$ for isotropically distributed insolation:

$$Qnet_i = \frac{a_i}{a_S}\left(\frac{1-\rho_i}{1-\bar{\rho}}\right)S$$

Equation 106

1.6.2.2 Radiation removed at each surface of a zone by multiple window sources of targeted insolation

The targeting can be different for each window. Adding an additional subscript "j" to Equation 104 allows it to represent the energy removal for each surface separately for each window j. That is, Equation 104 becomes Equation 107, the rate of energy removal at each surface due to insolation *S$_j$*, that is distributed according to the assigned targeted values Q_{ji}.

$$Qnet_{ji} = \frac{a_i}{a_S}\left(\frac{1-\rho_i}{1-\bar{\rho}}\right)\sum_k a_k\rho_k Q_{jk} + a_i Q_{ji}(1-\rho_i)$$

Equation 107

The targeting fractions H_{jk}, to be user input, are defined as the fraction of insolation from window *j* that is incident on surface k:

$$H_{jk} = \frac{a_k Q_{jk}}{S_j}$$

Equation 108

With this definition, Equation 107 can be written as

$$Qnet_{ji} = a_i S_j(1-\rho_i)\left(\frac{H_{ji}}{a_i} + \frac{1}{a_S(1-\bar{\rho})}\sum_k \rho_k H_{jk}\right)$$

Equation 109

The effective absorptivity of the targeted surfaces is defined as

$$\alpha effT_{ji} = Qnet_{ji}/S_j$$

Equation 110

Replacing the spherical surfaces a$_i$ in Equation 109 by $a_i = A_i F_i$, and substituting Equation 109 into Equation 110 gives the targeted gain equation used in the CZM code:

$$\alpha effT_{ji} = A_i F_i(1-\rho_i)\left(\frac{H_{ji}}{A_i F_i} + \frac{1}{(1-\bar{\rho})\sum_i A_i F_i}\sum_k \rho_k H_{jk}\right)$$

Equation 111

If $\sum_k H_{jk} < 1$ then it is assumed that the remaining insolation $S_j(1 - \sum_k H_{jk})$is distributed isotropically. From Equation 105 it is

$$isotropic\ Qnet_{ji} = \frac{a_i}{a_S}\left(\frac{1-\rho_i}{1-\bar{\rho}}\right)S_j(1 - \sum_k H_{jk})$$

Equation 112

The definition of the effective absorptivity for isotropic insolation is:

$$\alpha effI_{ji} = Qnet_{ji}/S_j$$

Equation 113

Changing Equation 112 to utilize zone areas, $a_i = A_i F_i$, and substituting Equation 112 into Equation 113 gives the amount of the diffuse part of the insolation from each window j that is absorbed in each surface i. This is used in the CZM code.

$$\alpha effI_{ji} = \frac{A_i F_i}{\sum_k A_k F_k}\left(\frac{1-\rho_i}{1-\bar{\rho}}\right)(1 - \sum_k H_{jk})$$

Equation 114

Note that no distinction has been made between surfaces that are opaque like walls, and partially transparent window surfaces. They are treated equally. The difference is that the energy removed by an opaque wall is absorbed into the wall, whereas that removed by the window surfaces is partly transmitted back out the window, and partly absorbed at the window inside surface. The CZM development code lets the user specify a fraction of the radiation that is absorbed in the room-side surface of the window, which slightly heats the window and thus the zone.

Adding Equation 111 and Equation 114 gives the total effective absorptivity of surface i from the insolation admitted through window j:

$$\alpha eff_{ji} = A_i F_i (1-\rho_i)\left(\frac{1}{(1-\bar{\rho})\sum_k A_k F_k}\left[1 - \sum_k (1-\rho_k) H_{jk}\right] + \frac{H_{ji}}{A_i F_i}\right)$$

Equation 115

The net radiation absorbed in surface i from window j is thus

$$Qnet_{ji} = A_i F_i (1-\rho_i) S_j \left(\frac{1}{(1-\bar{\rho})\sum_k A_k F_k}\left[1 - \sum_k (1-\rho_k) H_{jk}\right] + \frac{H_{ji}}{A_i F_i}\right)$$

Equation 116

Summing this over all windows gives the total SW radiation absorbed and/or transmitted by surface i as:

$$Qnet_i = A_i F_i (1 - \rho_i) \sum_j \left[S_j \left(\frac{1}{(1 - \bar{\rho}) \sum_k A_k F_k} \left[1 - \sum_k (1 - \rho_k) H_{jk} \right] + \frac{H_{ji}}{A_i F_i} \right) \right]$$

Equation 117

1.7 WINDOW MODEL

The ASHWAT algorithm is used to model complex windows with diatherminous layers and curtains, etc. (Wright and Kotey 2006, Wright, J.L. 2008). Given the environmental conditions on each side of the window, ASHWAT determines the long wave, short wave and convection heat transfers to the conditioned space.

For the following input and output discussion, ASHWAT is treated as a black box.

1.7.1 Inputs

Each time step, for each window, ASHWAT is given the environmental inputs:

I = insolation incident on window system.

I_{refl} =insolation reflected diffusely from the other room surfaces.

$T_{a,out}$ = outside dry bulb air temperature.

$T_{a,in}$ = inside dry bulb air temperature.

$T_{r,in}$ = the temperature of the indoor plate.

$T_{r,out}$ = the temperature of the outdoor plate.

Figure 13: ASHWAT Inputs and Nomenclature

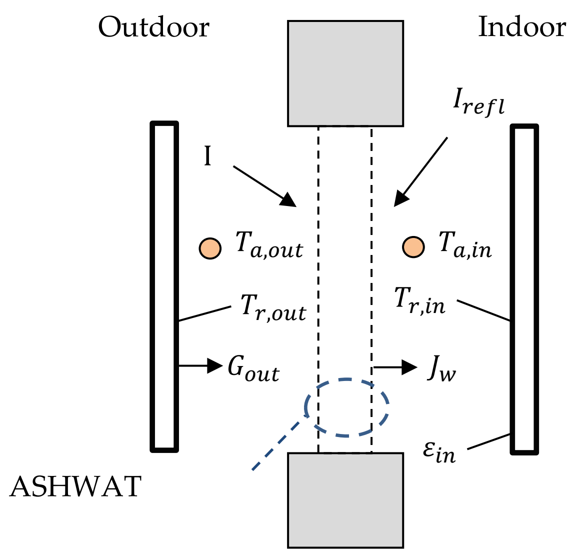

1.7.2 Outputs

ASHWAT's output gives heat transfer rates and circuit elements of Figure 14. The circuit of Figure 14 is part of the conditioned zone radiant network of Figure 2 and Figure 3 (with some different nomenclature).

Figure 14: Window System Representation in CSE

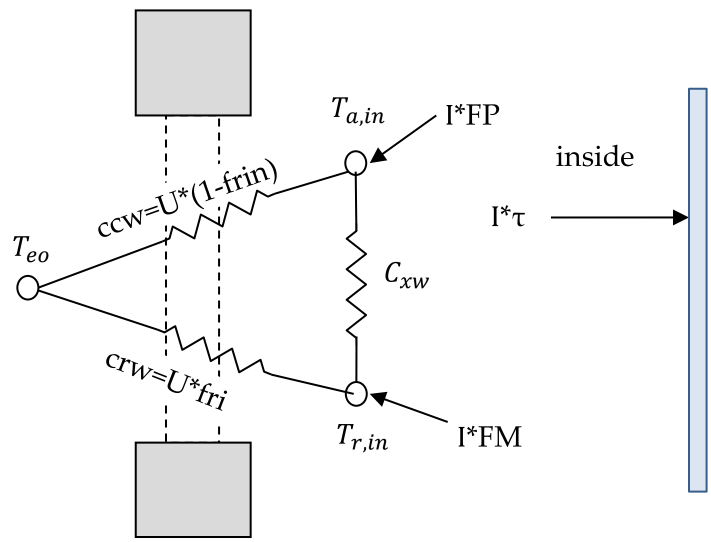

In Figure 14,

FP = fraction of the heat from Insolation absorbed in the various window layers that ends up being transferred to the inside radiant node.

FM = fraction of the heat from Insolation absorbed in the various window layers that ends up being convected to the inside air node.

$frin$ = fraction of total non-solar heat transfer that goes to the inside radiant node; dimensionless.

frout = fraction of non-solar heat transfer to the outside that goes to the outside radiant node.

U = conductance between the inside and outside effective temperatures T_{ei} and T_{eo}; Btu/(hr-sf-F), where $T_{ei} = T_{a,in}(1 - frin) + T_{r,in}frin$.

$T_{eo} = T_{a,out} * (1 - frout) + T_{r,out} * frout$ = the effective outdoor temperature; F.

C_{xw} = the cross coupling term; Btu/(hr-sf-F).

τ = the short wave transmissivity of the window system.

Note that the solar heat gain coefficient is: $SHGC = \tau + FP + FM$.

Net energy into zone via window, per unit COG area = + $I\ (\tau + FP + FM)$ - I_{refl} + $U(T_{eo} - T_{ei})$

1.7.3 Matching ASHWAT to CSE Radiant Network

1.7.3.1 Outside boundary conditions

ASHWAT models the irradiation on the outside of the window system as if it were emitted by a black plate parallel to the window at temperature $T_{r,out}$, as shown in Figure 13. The irradiation on the window system from the outside plate is thus $G_{out} = \sigma T_{r,out}^4$, so

$$T_{r,out} = \left(\frac{G_{out}}{\sigma}\right)^{0.25} = \left[F_{sky}\beta\, T_{sky}^4 + \left[F_{gnd} + F_{sky}(1-\beta)\right]T_{air}^4\,\right]^{0.25}$$

Equation 118

where G_{out} has been replaced by Equation 67.

1.7.3.2 Inside boundary conditions

From Figure 13, the equivalent network between the radiosity of the window system, J_w, and the inside plate is shown in Figure 15. The circuit parameters are in the conductance form. The "1" is the view factor between the plate and the window.

Figure 15: Equivalent Network between the Radiosity of the Window System, J_w, and the Inside Plate

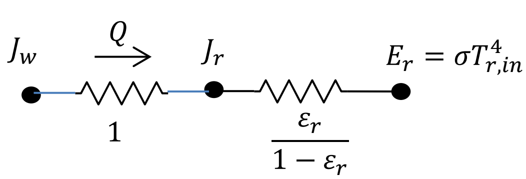

Figure 15 reduces to:

Figure 16: Reduced Figure 15

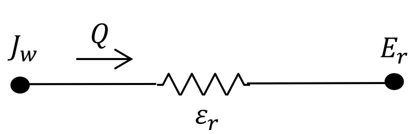

Thus the heat transfer rate per unit area, with Q positive from window to room, is:

$$Q = \varepsilon_r(J_w - E_r)$$

Equation 119

From Figure 9 the network between the radiosity of a surface and the mean radiant temperature node is shown in Figure 17. This corresponds to Figure 16 for the ASHWAT algorithm:

Figure 17: Network between the Radiosity of a Surface and the Mean Radiant Temperature Node

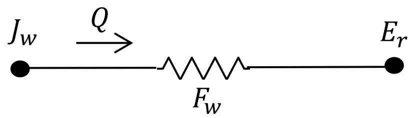

with the corresponding heat transfer rate:

$$Q = F_w(J_w - E_r)$$

Equation 120

Comparing Equation 119 and Equation 120 shows that to obtain the heat flow consistent with the Carroll network ASHWAT must model the window by setting inside plate's emissivity to the value of F_w.

$$\varepsilon_r = F_w$$

Equation 121

F_w is the Carroll MRT view factor defined in Section 1.6.1. F_w is slightly larger than 1, and serves to increase the heat transfer between J_w and E_r to compensate for the fact that $|J_w - E_r|$ is smaller than it would if $T_{r,in}$ had not included the window temperature in its average. This MRT view factor effect cannot be simulated by a parallel plate model without the trick of artificially raising the emissivity of the inside plate to the value F_w.

1.8 SLAB MODEL

1.8.1 Bajanac Simplified Model

The CZM slab model is partly based on the Simplified Method for the calculation of heat flow through foundations, presented by Bazjanac et al. (2000). They divide a slab into two regions.

1.8.1.1 Perimeter region

The perimeter area of the slab is defined as a 2 ft wide strip along external walls. Through this perimeter path, the interior air is assumed to be coupled via conductances α_1, α_2, and α_3 to three environmental temperatures: T_{week}, , T_{ground}, *and* T_{year}:

Figure 18: Perimeter Coupling

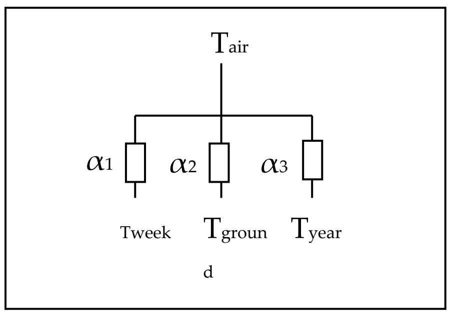

Thus the instantaneous heat flow from the room Temp node to perimeter slab, in Btu/hr-sf-F, is given by:

$$Qperim = \left[\alpha_1(T_{air} - T_{week}) + \ \alpha_2\left(T_{air} - T_{ground}\right) + \alpha_3\left(T_{air} - T_{year}\right)\right]$$

Equation 122

where,

T_{air} = the current interior-space effective temperature (involving both Ta and Tr).

T_{week} = the average outside air temperature of the preceding two-weeks.

T_{ground} = the current average temperature of the earth from the surface to a 10 ft depth.

T_{year} = the average yearly dry bulb temperature.

$\alpha's$ = conductances from Table 3 of Bazjanac et al; Btu/sf-hr-F.

1.8.1.2 Core region

The core region couples T to T_{ground} and T_{year}, via conductances α_4 and α_5.

Figure 19: Core Coupling

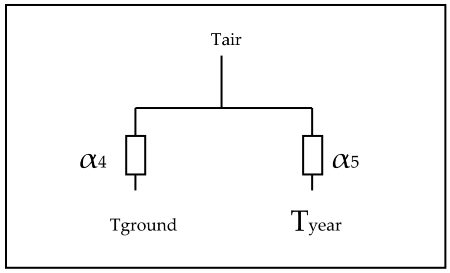

$$Qcore = [\alpha_4(T_{air} - T_{ground}) + \alpha_5(T_{air} - T_{year})]$$

Equation 123

Bazjanac et al. determined the conductances α_1, through α_5 by multi-linear regression analysis of the numerical results from a two-dimensional finite-difference slab-earth model. The conductances were determined for 52 slab foundation conditions and given in their Table 3.

1.8.1.3 Properties

The Bozjanac Table 3 conductances were obtained assuming the following properties:

1. Properties of earth:
   - conductivity = 1 Btuh/ft-F. (The k chosen was justified by assuming that lawns and other vegetation around California houses was watered during the dry season).
   - density =115 lbm/ft^3
   - specific heat = 0.2 Btu/lbm-F
   - thermal diffusivity = 0.0435 ft^2/hr.
2. Slab: "heavy construction grade concrete"
   - thickness = 4-inches
   - conductivity = 0.8
   - density = 144
   - specific heat = 0.139
3. Rrug = 2.08 hr-ft^2-F/Btu (ASHRAE 2005HF, p.25.5 'carpet fibrous pad').
4. Rfilm = 0.77 Btu/hr-ft^{2}F, the inside surface-to-room-temperature combined convective and radiative conductance.

1.8.1.4 Ground temperature

The above model uses the ground temperature determined by Kusuda and Achenbach (1965). Using the classical semi-infinite medium conduction equations for periodic surface temperature variation (Carslaw and Jaeger), they found the average ground temperature from the surface to a depth of 10 ft to be given by:

$$\mathrm{T_{ground}} = \mathrm{T_{yrAve}} - \mathrm{GM}\left(\frac{\mathrm{TyrMax-TyrMin}}{2}\right) cos\left(\left(\frac{2\pi}{8760}\right)\theta - PO - \phi\right)$$

Equation 124

where,

$\mathrm{T_{yrAve}}$ = average outdoor temperature over year; F.

$\mathrm{T_{yrMax}}$ = highest average monthly outdoor temperature for the year; F.

$\mathrm{T_{yrMin}}$ = lowest average monthly outdoor temperature for the year; F.

$\mathrm{GM} = \sqrt{\frac{\mathrm{e^{-2\beta} - 2e^{-\beta}} \, cos\, \beta + 1}{2\beta^2}}$ = dimensionless amplitude for integrated depth average.

$\beta = \mathrm{L}\sqrt{\frac{\pi}{\mathrm{D*PY}}}$ = dimensionless depth.

L = 10 ft, the depth over which average is taken.

D = thermal diffusivity of soil, $\mathrm{ft^2/hr}$.

PY = 8760 hr = period of 1 year.

$\theta = 24\left(\frac{365\mathrm{M}}{12} - 15\right)$ ≈ elapsed time from Jan-1 to middle of month M; hours.

M = month, 1→12.

$\phi = atan\left(\frac{1-e^{-\beta}(cos\beta + sin\beta)}{1-e^{-\beta}(cos\beta - sin\beta)}\right)$ = phase angle for depth averaged $\mathrm{T_{ground}}$; radians.

PO = 0.6 *radians* = phase lag of ground surface temperature (assumed equal to air temperature) relative to January 1. From measured data, see Fig. 7 in Kusuda and Achenbach.

1.8.2 Addition of a Layered Slab and Earth

The Bazjanac model assumes a constant indoor temperature, so cannot be applied directly to a whole building thermal-balance simulation model that allow changing indoor temperatures. To apply this model to CZM, with changing indoor temperatures, requires incorporating the dynamic effects of the slab and earth due to changing inside conditions.

This is done by putting a one-dimensional layered construction, representing the slab and some amount of earth mass, into the steady-state Bazjanac model circuit--replacing part of its resistance by a thermal impedance (which is equal to the resistance for steady state conditions). In this way the correct internal temperature swing dynamics can be approximated.

First, the circuit of Figure 18 is alternately expressed as shown in Figure 20(a), with Equation 122 taking the form:

$$Q = A * U_g (T_{air} - T_{geff})$$

Equation 125

where T_{geff} is the α-weighted average ground temperature:

$$T_{geff} = \frac{\alpha_1 T_{week} + \alpha_2 T_{ground} + \alpha_3 T_{yrAve}}{\alpha_1 + \alpha_2 + \alpha_3}$$

Equation 126

and

$$R_g = \frac{1}{\alpha_1 + \alpha_2 + \alpha_3}$$

Equation 127

Similarly for the core region,

$$T_{geff} = \frac{\alpha_4 T_{ground} + \alpha_5 T_{yrAve}}{\alpha_4 + \alpha_4}$$

Equation 128

$$R_g = \frac{1}{\alpha_4 + \alpha_5}$$

Equation 129

Now a one-dimensional layered construction is added into the circuit as shown in Figure 20(b), consisting of a surface film layer, a carpet (if any), the concrete slab, and earth layer. The bottom of the earth layer is then connected to T_{geff} through the what's left of R_g.

A one-dimensional representation of the mass is appropriate for the core region. It is a bit of a stretch for the perimeter slab modeling, because the real perimeter heat flow is decidedly 2-dimensional, with the heat flow vectors evermore diverging along the path of heat flow.

Figure 20: Addition of Film, Rug, Slab, and Earth

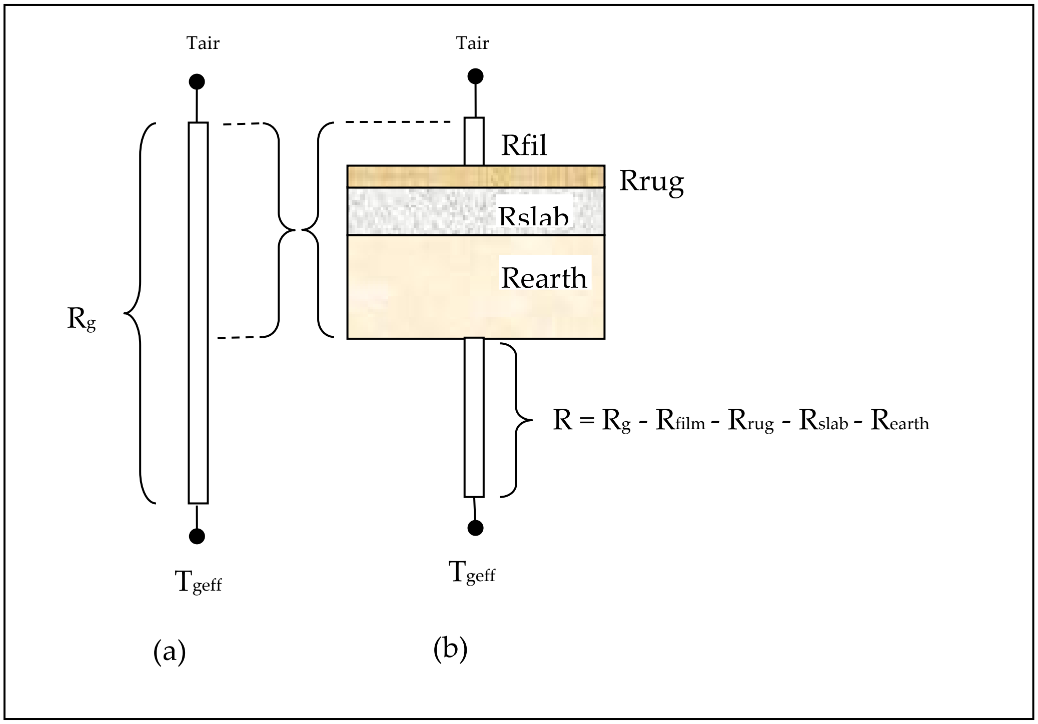

The earth thicknesses required to adequately model the dynamic interaction between the room driving forces (sun and temperature) and the slab/earth model was determined by considering the frequency response of the slab earth model of Figure 20(b). In the frequency domain, the periodic heat flow from the Tair node is given by Equation 130.

$$\tilde{Q}_{air} = \tilde{T}_{air}X - \tilde{T}_{geff}Y \;.$$

Equation 130

where,

X = the driving point admittance at the air (or combined air/radiant effective temp) node, in the units of Btu/hr-sf-F. It is the contribution to $\tilde{Q}_{air}$ per degree amplitude of $\tilde{T}_{air}$. X and Y are complex numbers determined from the layer properties (conductivity, heat capacity, density) of the circuit layers in Figure 20(b). See Carslaw and Jaeger; Subbarao and Anderson.

Y = the transfer admittance at the air node. It is the contribution to $\tilde{Q}_{air}$ per degreee amplitude of $\tilde{T}_{geff}$. [The same value of transfer admittance applies to the $\tilde{T}_{geff}$ node, even if the circuit is not symmetrical, being the contribution to the $\tilde{T}_{geff}$ node per degree amplitude of $\tilde{T}_{air}$]

$\tilde{Q}_{air}$ = the amplitude (Btu/hr-ft^2-F) and phase of the heat transfer rate leaving $\tilde{T}_{air}$, and is composed of the contribution from all of the frequencies that may be extant in the driving temperatures $\tilde{T}_{air}$ and $\tilde{T}_{geff}$.

Note that the layers shown, when modeled as a mass construction, may need to be subdivided into thinner layers, particularly the earth, in order to satisfy the discretization procedure discussed in Section 1.4; but this subdivision is irrelevant to the slab model discussion in this section.

The maximum possible thickness of the earth layer is limited by the need for R to be positive. The limiting maximum possible thickness value, dmax, occurs in the perimeter case, when the foundation is uninsulated (i.e., the foundation insulation value R-0 in Bazjanac et al), and the slab is uncarpeted. In this case, dmax = 2.9 ft. The corresponding numbers for an uncarpeted core slab case is 11.8 ft

A depth of 2 ft is implemented in the code, for both the perimeter and core slab earth layers.

The 2 ft value was chosen primarily because, for the frequencies of concern, the magnitude of the X admittance from the Tair node was almost independent of earth layer depth for earth layer depths greater than 2 ft. See Figure 21. The phase shift is similarly essentially independent of depth after 2 ft. This was also the case for the core region.

This is the case for all indoor driving frequencies periods of up to at least 384-hr = 16-days. Thus 2 ft of earth is able to portray the dynamics resulting from a cycle of 8-cloudy days followed by 8 sunny days.

Figure 21: Room Node X Admittance

The transfer admittance Y shown in Figure 22 also contributes to $\tilde{Q}_{air}$ according to the frequencies extant in the driving temperature $\tilde{T}_{geff}$.

Figure 22: Room Node Y Admittance

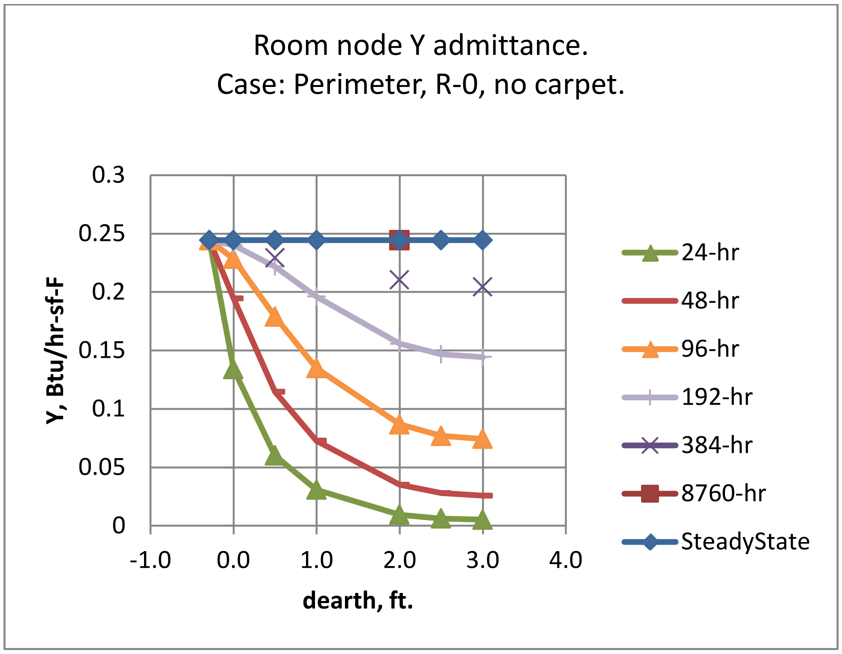

As seen in Equation 128, for the slab core region, $\tilde{T}_{geff}$ has the same frequency content as T_{ground} and T_{year}. T_{year} is a constant, i.e., zero frequency, steady-state.

As seen in Equation 124, T_{ground} contains only the annual 8760-hr period. Figure 22 shows that the 8760-hr waves are transmitted unaffected by the mass layer. That is, Y becomes essentially equal to the steady state transfer admittance which is the U factor of the assembly, the reciprocal of the R_g value. Thus, for the core region, the magnitude of the slab loss rates produced by Equation 125 are preserved and unaffected by the added earth layers.

However, although the mass layers don't affect the magnitude of the Bazjanac model slab losses, they do introduce a time lag that is in addition to that already implicit in the $\tilde{T}_{geff}$ values. For a 2 ft earth layer the lag is ~40-hours. A 22-day lag is already included by ϕ of Equation 124. To eliminate double-counting, the 40-hrs could be subtracted from phi, but this has not been done since 40-hr is inconsequential compared to 22 days.

For the perimeter region, $\tilde{T}_{geff}$ has the the additional frequency content of the T_{week}, the two-week running average outdoor temperature. T_{week} is dominated by the annual period, but has small amplitude 6-month period component, and a bit of signal at higher frequencies. Like the annual cycle, the 6-month period component is transmitted through the layered construction without damping, but again with a small but inconsequential phase lag.

Thus it was concluded that 2 ft of earth thicknesses below a 4-inch concrete slab adequately models changes in room side conditions, and at the same time adequately preserves the same average "deep earth" slab losses and phase lags of the Bazjanac model.

The validity of the response of the core slab construction is expected to be better than for the perimeter slab construction since the perimeter layers added do not properly account for the perimeter two-dimensional effects.

1.8.2.1 Warm-up time

The longest pre-run warm-up time is expected to be for a carpeted core slab with the 2 ft earth layer. Using the classical unsteady heat flow charts for convectively heated or cooled slabs (Mills) , the time to warm the slab construction 90% (of its final energy change) was found to be about 20-days. Most of the heat-up heat transfer is via the low resistance rug and air film, with less through the higher ground resistance (R in Figure 20(b)), so the 20- day estimate is fairly valid for the complete range of foundation insulation options given in Bazjanac's Table 3.

1.8.2.2 Input properties

Strictly speaking, the same properties assumed in the Bazjanac model in Section 1.8.1.3 should also be used in describing the rug, the concrete slab, and the earth in the layered constructions inputs.

This is particularly true for the carpet, if a carpet is specified, because the regression coefficients (the conductances a1, a2...) obtained for the carpeted slabs were sensitive to the Rrug value used. While inputting a different value than Rrug = 2.08 may give the desired carpeted room admittance response, the heat conducted from the deep ground will still give the heat flow based on Rrug = 2.08.

Small differences between the inputted and above properties is less important for the other layers, and is violated in the code with regard to Rfilm; its value is calculated each time-step and is used instead of 0.77, even though 0.77 is still the value subtracted from Rg in the code. This allows the correct modeling of the admittance of the slab floor, at the expense of a slight error in the overall resistance of the slab earth circuit.

1.9 VENTILATION AND INFILTRATION AIR NETWORK

1.9.1 Overview

This section describes the flow network algorithm used to model infiltration and ventilation air flows between conditioned zones, unconditioned zones, and the outdoors based on pressure and density differences and leakage areas between the zones.

Figure 23 shows the flow network interconnecting two conditioned zones (Z1 and Z2), the unconditioned attic and crawl space zones (Z3 and Z4), and the outside zone (Z5).

Figure 23. Schematic of Flow Network

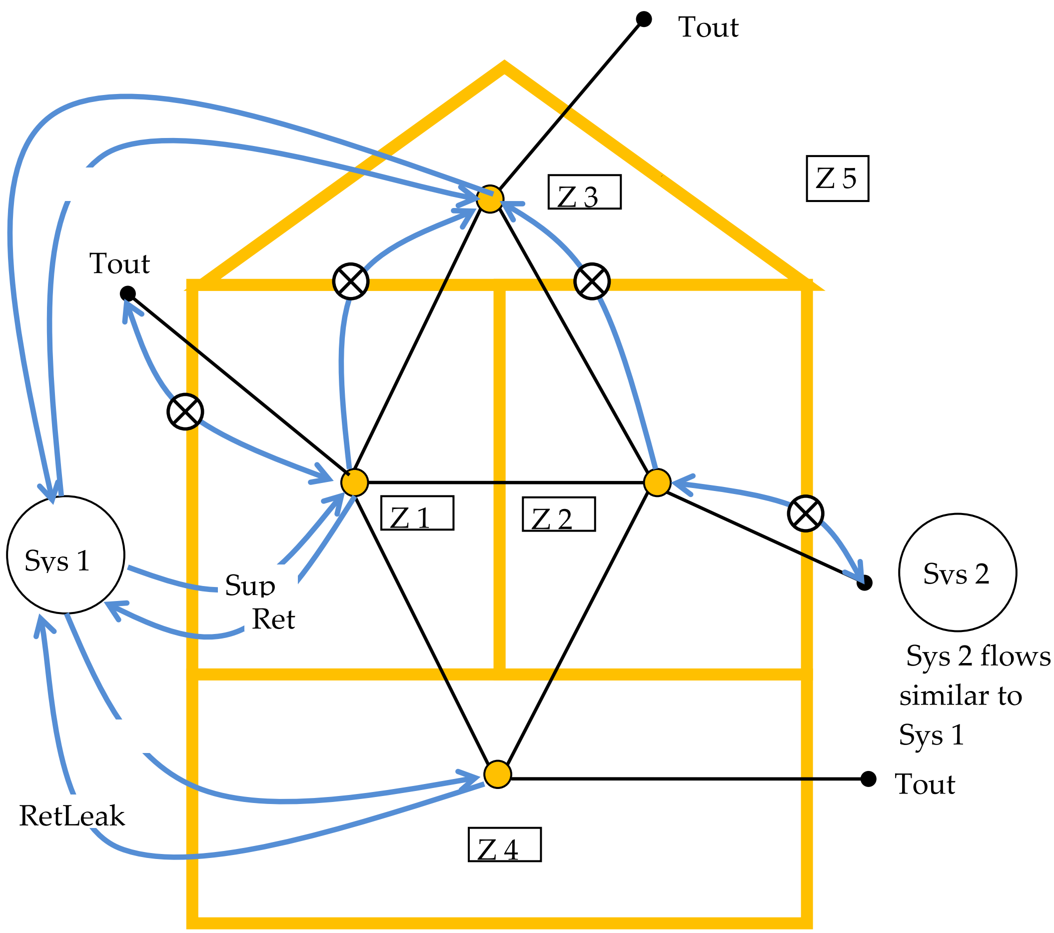

The black lines represent one or more pressure difference driven and/or buoyancy driven flows between zones.

The blue lines in Figure 23 represent scheduled fan flows not directly dependent on zone-to-zone pressure differences. These include individual house fans (circled x's) and fan driven duct system supply, return, and leakages flows. The fans will affect the zone pressures, but the pressures won't affect the fan flow. The duct flows, determined by the load and air handler capacity, are ~~also~~ assumed to not constitute leakage paths when the air handler is not operating.

Small leakage or ventilation openings will be modeled as orifices using a power law equations of Section 1.9.3 with an exponent of 0.5. Infiltration leaks are modeled with the power law equation exponent of 0.65.

Large vertical holes or infiltration surfaces, large enough that the vertical pressure difference distribution allows two-way flow, are modeled as two vertically separated small holes using the Wolozyn method (see Section 1.9.5– Large Vertical Openings).

The following kind of elements are modeled using the power law equations:

- Wall infiltration for vertical envelope walls, vertical interzone walls, and roof decks
- Ceiling, floor, and wall base infiltration
- Interzone doors, door undercuts, jump ducts, relief vents
- Openable window flow
- Attic soffit vents, gable vents, roof deck vents, ridge vents
- Crawl space vents
- Trickle Vents
- Fire Place leakage.
- Infiltration to garage.

Additional equations are used to model large horizontal openings, like stairwells; Section 1.9.4. This type of opening would typically be between zones Z1 and Z2 in Figure 23 when the zones are stacked vertically. The algorithm used is based on that implemented in Energy Plus (2009). In addition to using the power law equation above, the algorithm calculates buoyancy induced flows that can occur when the density of the air above the opening is larger than the density of the air below the opening, causing Rayleigh-Taylor instability.

To determine the flow rates at each time step, the flow through each flow element in the building is determined for an assumed set of zone reference pressures. If the flow into each zones does not match the flow out of the zone, the pressures are adjusted by the Newton-Raphson iterative method until the flows balance in all the zones within specified tolerances.

1.9.1.1 Wind direction independent air-network solution

For energy standards application, the air network for the four zone building model is designed to give results that are wind direction independent. In computing ventilation or infiltration air flows from holes in vertical walls exposed to outdoors, the program automatically calculates the sum of the flows through 4 holes each ¼ the area, one with each cardinal compass orientation, or an offset thereof. Thus, there will be wind induced flows through the envelope leakages that approximate the average flow expected over long periods, and they will be independent of wind direction. This approach is applied to all zone ventilation or infiltration flow elements connected to the outdoor conditions.

1.9.2 Vertical Pressure Distribution

The pressure at a given elevation in a zone, including outdoors, is a combination of stack and wind effects added to the zones reference pressure. The difference in pressure in the zones on each side of a leakage element connecting the zones determines the flow rate through the element.

The pressure on the zone i side of a flow element is given by:

$$p_i = Pz_i - \rho_i g z_i$$

Equation 131

z_i is the height of the element above some datum $z = 0$. The datum is arbitrary but is nominally taken as ground level. Pz_i is zone $i's$ reference pressure. This is the pressure zone i would have at elevation $z = 0$, regardless of whether the zone actually extends to this level. For the interior zones the Pz_i reference pressures are the unknowns that are solved for using the Newton-Raphson method. This method determines what values of zone pressures simultaneously result in a balanced flow in each zone. The value of Pz_i for the outdoor side of a flow element is given by (i is 5 if there are 4 conditioned and unconditioned zones):

$$Pz_i = \mathrm{patm} + CP * Pu$$

Equation 132

The weather tape atmospheric pressure, patm, is assumed to exist at the elevation z = 0 far from the building. Patm is taken as zero so that the unknown zones pressures will be found relative to the weather tape atmospheric pressure. Of course the actual weather tape atmospheric pressure is used in determining inside and outside zone air densities.

The wind velocity pressures, Pu, is:

$$Pu = \rho_{out}(S * U)^2/2$$

Equation 133

where,

U is the wind velocity at eave height.

S is the shelter coefficient equal to SC of Table 2: Local Shielding Parameters.

ρ_{out} is the outside air density.

CP is the orientation sensitive pressure coefficient.

1.9.2.1 Pressure coefficients used

The wall pressure coefficients in Table 6 are those used by Walker et al. (2005). They are for the four vertical walls of an isolated rectangular house, with the wind perpendicular to the long wall (short wall = ½ long wall). As discussed in regard to hip roofs below, only data for the normal wind direction is used. These coefficients are used for all ventilation and infiltration holes in the walls. Soffit vents also use these values since they are assumed to have the same pressure coefficient as the walls under them. This assumption is roughly corroborated by the data of Sharples (1997).

Table 6: Pressure Coefficients for Wind Normal to One Wall

Wind Pressure Coefficient, *CP*		
Upwind wall	Side walls	Downwind Wall
+0.6	-0.65	-0.3

Table 7 gives hip roof's pressure coefficients for a range of roof angles. These are used to determine the outside pressure on ridge vents and roof deck vents.

There is little data available for hip roof surface pressure coefficients, or for ridge pressure coefficients (needed to model ridge vents) for any roof type. The data in Table 7 is a simplified synthesis of the data given by Xu (1998) and Holmes (1993, 2003, etc.), informed by a review of ASHRAE, EU AIVC, and other data sets and research papers.

Xu used a wind tunnel to measure pressure coefficients for a hip roofed building which was otherwise identical to the gable roof building wind tunnel data obtained by Holmes. The building had an aspect ratio of 2:1, with 0^o wind direction normal to the long side (and normal to the gable ridge and hip roof top ridge). The building eave height was 0.4 the length of the short side. The building had a relatively large eave overhang of about 35% of the eave height. Xu and Holmes presented data for this building for roof pitch angles of 15, 20, and 30^o . Other Holmes data, for both larger and smaller roof angles was used to estimate the pressure coefficients beyond the 15 to 30 degree range. Neither Xu nor Holmes presented average surface pressures, so the average surface data and average ridge pressures given in the table are based on estimates from their surface pressure contour data.

The table is for wind normal to the long side of the building. Similar tables were obtained from Xu's data for the 45 and 90 degree wind angles. Table 7 would ideally be wind direction independent, implying some kind of average pressure coefficient; for example, for each surface take the pressure coefficient that is the average for the 0, 45, and 90 degree angles. However, infiltration flows depend on pressure differences, and the average of the pressure differences is not necessarily indicative of the difference of the average pressures. The soffit vents flows, driven by the pressure difference between the adjacent wall and the various roof vents complicate any averaging schemes.

Comparison of the pressure coefficients for the three wind directions, while showing plausible differences, arguably does not show a discernable pattern that would obviate just using the normal wind direction data. Given the variety of roofs and building shapes that will be represented by these coefficients, the variety of vent locations and areas, and the deficiencies of the data, using a consistent set of data for only one wind direction is deemed appropriate.

Table 7: Hip Roof Wind Pressure Coefficients

Roof Pitch ψ	Hip Roof Wind Pressure Coefficient, *CP*			
	Upwind roof	Side hip roofs	Downwind Roof	Ridge
$\psi < 10^o$	-0.8	-0.5	-0.3	-0.5
$10 \leq \psi < 15$	-0.5	-0.5	-0.5	-0.8
$15 \leq \psi < 25$	-0.3	-0.5	-0.5	-0.5
$25 \leq \psi < 35$	+0.1(pos)	-0.5	-0.5	-0.3
$35 \leq \psi < 50$	+0.3 (pos)	-0.5	-0.5	-0.2

1.9.2.2 Density

Zone i's air density ρ_i is assumed to be only a function of zone temperature T_i. That is, assuming the air is an ideal gas, at standard atmospheric conditions, the pressure change required to change the density by the same amount as a change in temperature of 1°F is $\frac{\partial\rho}{\partial T} / \frac{\partial\rho}{\partial p} = -\rho R_{air}$, which is approximately - 200 Pascals/F. Since zone pressure changes are much smaller than 200 Pa, they are in the range of producing the same effect as only a fraction of a degree F change in zone temperature; thus the density is assumed to always be based on patm. (This has been changed in code so that ρ_i depends on both T_i and Pz_i).

Using the ideal gas approximation, with absolute temperature units,

$$\rho_i = \frac{P_{atm}}{R_{air}T_i}$$

Equation 134

The pressure difference across the flow element is given by

$$\Delta p_{ij} = p_i - p_j = Pz_i - Pz_j - gz_i(\rho_i - \rho_j)$$

Equation 135

1.9.3 Power Law Flow Equation

1.9.3.1 Orifice flow power law

For an orifice, with fixed density of air along the flow path (from inlet to vena contracta), Bernoulli's equation gives:

$$m = C_D A\sqrt{2\rho_{in}g_c}\,(\Delta p)^{\frac{1}{2}}$$

Equation 136

where

C_D is the dimensionless orifice contraction coefficient.

$C_D = \frac{\pi}{\pi+2}$ = Kirchoff's irrotational flow value for a sharp edge orifice.

$C_D =$ 0.6 default for CSE windows

$C_D =$ 1 for rounded inlet orifice as used in ELA definition, and consistent with no vena contracta due to rounded inlet.

A = Orifice throat area, ft^2.

ρ_{in} = density of air entering the orifice; lb_m/ft^3.

$g_c = 32.2 \frac{lb_m ft}{lb_f\ sec^2}$

1.9.3.2 Infiltration flow power law

The following is based on Sherman (1998). English units are used herein. Measured blower door infiltration data is expressed empirically as a power law:

$$Q = \kappa \Delta P^n$$

Equation 137

or

$$m = \rho_{in} \kappa \Delta P^n$$

Equation 138

where

Q = volume flow in ft^3/sec.

m = mass flow in lb_m/sec.

ρ_{in} = entering air density, lb_m/ft^3

ΔP = pressure difference in $lb_f/ft^2 = psf$.

n= measured exponent, assumed to be n = 0.65 if measured value is unavailable.

κ = measured proportionality constant.

Equation 137 and Equation 138 are dimensional equations. Thus κ is not a dimensionless number but implicitly has the dimensions $ft^{3+2n}/(sec{*}lb_f^n)$. See Section 1.9.3.8–Converting Units of κ.

Sherman defines equivalent leakage area, ELA, as the area of a rounded-entrance orifice that gives the same flow as the infiltration of Equation 137 when the pressure difference ΔP is equal to the reference pressure P_r = 0.08354 psf (= 4 Pa) By Equation 136, a rounded-entrance nozzle with throat area ELA and $\Delta P = P_r$ has a flow rate:

$$m = ELA\sqrt{2\rho_{in}g_c}\,(\mathrm{P_r})^{\frac{1}{2}}$$

Equation 139

Equation 137 and Equation 139 with $\Delta P = P_r$ gives the ELA as:

$$ELA = \kappa {P_r}^{n-\frac{1}{2}}\sqrt{\frac{\rho_{in}}{2g_c}}$$

Equation 140

Solving Equation 140 for κ, gives

$$\kappa = ELA\sqrt{\frac{2g_c}{\rho_{in}}}P_r^{\frac{1}{2}-n}$$

Equation 141

Substituting Equation 140 into Equation 137 gives the general equation, equivalent to Equation 137, that is the infiltration flow at any pressure difference ΔP:

$$m = ELA\sqrt{2\rho_{in}g_c}P_r^{\frac{1}{2}-n}\Delta P^n$$

Equation 142

(Note that substituting Equation 140 into Equation 142 recovers the empirical Equation 137).

1.9.3.3 General power law flow equation

CSE uses Equation 136 to model flow through elements such as windows, doors, and vents. Equation 142 is used for infiltration flows for elements with a defined ELA.

Both equations are special cases of the generalized flow power law Equation 143. For flow from zone i to zone j.

$$m_{i,j} = SP * A_e\sqrt{2\rho_{in}\,g_c}\,|\Delta p_{i,j}|^{n_g}$$

Equation 143

SP is the sign of the pressure difference $\Delta p_{i,j} = p_i - p_j$, utilized to determine the sign of the flow, defined as + from i to j. The exponent is n_g, "g" for generalized.

Equation 143 reduces to the orifice Equation 136 if:

- $A_e = A * C_D$ with $C_D = 0.6$.

- $n_g = \frac{1}{2}$

Equation 143 reduces to the infiltration Equation 142 if:

- $A_e = \left(P_r^{\frac{1}{2}-n}\right)ELA$, where n here is the measured exponent.
- $n_g = n$
- $P_r = 0.08354\frac{lb_f}{ft^2}$

[Although C_D is dimensionless in Equation 136, the generalization to Equation 143 requires C_D to implicitly have the units of$(lb_m)^{\frac{1}{2}-n_g}(ft)^{2n_g-1}$].

1.9.3.4 Dealing with unbounded derivative at $\Delta P = 0$

The partial derivative of the mass flow of Equation 143 with respect to the pressure in zone i is given by:

$$\frac{\partial \mathrm{m_{i,j}}}{\partial \mathrm{p_i}} = \mathrm{A_e n_g}\sqrt{2\rho_{\mathrm{in}}}|\Delta \mathrm{p_{i,j}}|^{\mathrm{n_g}-1}$$

Equation 144

Since $n_g < 1$ this derivative →∞ as ΔP→ zero, potentially causing problems with the Newton-Raphson convergence. In order to make the derivative finite for small pressure drops, whenever the pressure difference is below a fixed value, ΔP_L, the power law is extended to the origin by a linear power law ($n_g = 1$),

$$m_{i,j} = SP * A_{elinear}\sqrt{2\rho_{in}\, g_c}\,|\Delta p_{i,j}|^1$$

Equation 145

as shown in Figure 24.

So that the flow rates match when $\Delta P = \Delta P_L$, $A_{elinear}$ is determined by equating Equation 145 to Equation 143 with $\Delta p = \Delta P_L$, giving:

$$A_{elinear} = A_e \Delta P_L{}^{ng-1}$$

Equation 146

Note that the derivative of m will be discontinuous when $\Delta p = \Delta P_L$, which conceivably could also cause Newton-Raphson problems, but during extensive code testing, none have occurred.

Figure 24: Mass Flow m versus Pressure Drop ΔP

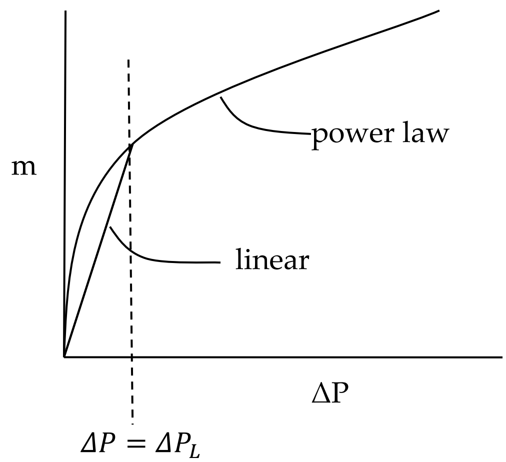

1.9.3.5 Summary of inputs to the generalized flow equation

The generalized flow equation, Equation 143,

$$m_{i,j} = SP * A_e\sqrt{2\rho_{in}\, g_c}\,|\Delta p_{i,j}|^{ng}$$

is used with the following parameter values, depending on element type and pressure drop ΔP.

1.9.3.6 For windows, doors, and vents

If $\Delta P > \Delta P_L$:

- $A_e = A * C_D$
- A = area of flow element; ft^2.
- $C_D = 0.6$.
- $n_g = \frac{1}{2}$

If $\Delta P < \Delta P_L$:

- $Ae\ = C_D\ A * {\Delta P_L}^{0.5-1}\ = C_D\ A/\sqrt{\Delta P_L}$
- A = area of flow element; ft^2.
- $C_D = 0.6$
- $n_g = 1$
- ΔP_L = determined by computational experiment.

1.9.3.7 For infiltration leakage elements

If $\Delta P > \Delta P_L$:

- $A_e = \left(P_r^{\frac{1}{2}-n}\right) ELA$, n here is the measured exponent, or 0.65 if not known. (Note that if $n = 0.65$, $A_e = 1.45 * ELA$, used in CEC ACM manual).
- $n_g = n$
- $P_r = 0.08354 \frac{lb_f}{ft^2}$
- ELA is determined from either:
  - the measured parameters κ and n using Equation 140. See Section 1.9.3.8–Converting units of κ.
  - code regulations, in which case $n = 0.65$ is assumed.

If $\Delta P < \Delta P_L$:

- $A_e = \Delta {P_L}^{n-1} \left(P_r^{\frac{1}{2}-n}\right) ELA$, where n here is the measured value, or 0.65.
- $n_g = 1$
- $P_r = 0.08354 \frac{lb_f}{ft^2}$

1.9.3.8 Converting units of κ

The κ in Equation 137 is not dimensionless, so κ changes value depending on the units of Q and ΔP in Equation 137. The analysis herein (Section 1.9) assumes Q in ft^3/sec and ΔP in lb_f/ft^2.

However, conventionally κ is obtained from measured data with Q in $\left(\frac{ft^3}{\min}\right)$ and ΔP in $Pascals$. With these units Equation 137 takes the form:

$$Q[cfm] = \kappa'(\Delta P(Pa))^n$$

Equation 147

Using dimensional analysis the value of κ to be used in Equation 137 with Q in $(\mathrm{ft}^3/\sec)$ and ΔP in $\left(\frac{\mathrm{lb_f}}{\mathrm{ft}^2}\right)$ is:

$$\kappa = \left(\frac{47.88^n}{60}\right)\kappa'$$

Equation 148

where the numbers are from the conversion factors $47.88 \frac{\mathrm{Pa}}{\mathrm{lb_f/ft^3}}$ and 60 sec/min. $\kappa = 0.206\kappa'$ for $\mathrm{n} = 0.65$.

κ' = the measured value from data with Q in $\left(\frac{ft^3}{\min}\right)$ and ΔP in $Pascals$.

1.9.3.9 ACM Manual relationship between CFM50 and ELA

Using Equation 142 (in volume flow form) the infiltration volume flow, CFS50, with 50 Pa pressurization is:

$$\text{CFS50} = \text{ELA}\sqrt{\frac{2g_c}{\rho}}P_r^{\frac{1}{2}-n}\Delta P^n = ELA\sqrt{\frac{64.4}{0.075}}0.08354^{-0.15}\,1.04428^{0.65} = 43.738 * ELA$$

Equation 149

where

ΔP = 50 Pa = 1.04428 psf

CFS50 = flow in units of ft^3/sec.

For cfm units, and ELA in square inches,

CFM50 = (60/144)CFS50 = 18.224*ELA

Equation 150

or alternately,

ELA [in^2] = 0.055*CFM50

Equation 151

This is the equation used to get ELA from blower door data at 50 Pa pressure difference.

1.9.3.10 Heat Flow

When the flow $m_{i,j}$ is positive, the heat delivered to zone j by this flow is given by

$$Q_j = m_{i,j}C_p(T_i - T_j),$$

Equation 152

while the heat delivered to zone *i* by the flow $m_{i,j}$ is zero:

$$\mathrm{Q_i} = 0$$

Equation 153

When the flow $m_{i,j}$ is negative, the heat delivered to zone j is zero,

$$Q_j = 0$$

Equation 154

while the heat delivered to zone *i* by the flow $m_{i,j}$ is:

$$Q_i = m_{i,j}C_p(T_i - T_j)$$

Equation 155

1.9.4 Large Horizontal Openings

An additional set of equations is needed to model large horizontal openings such as stairwells. The algorithm used is similar to that implemented in Energy Plus, which is based on that given by Cooper (1989). In addition to pressure driven flow using the power law equations of Section 1.9.3.3 this algorithm involves buoyancy induced flows that can occur when the density of the air above the opening is larger than the density of the air below the opening, causing Rayleigh-Taylor instability.

For a given rectangular opening this algorithm can produce three separate flows components between the zones:

a) a forced orifice flow in the direction dictated by the zone to zone pressure difference, Δp. This flow is independent of the following instability induced flows.
b) a buoyancy flow downward when the air density in the upper zone is greater than that is the lower zone, i.e., $T_{upper\text{-}zone} < T_{lower\text{-}zone}$. This flow is maximum when Δp is zero, and linearly decreases with increasing Δp until the buoyancy flow is zero, which occurs when the pressure difference is large enough that the forced flow "overpowers" the instability flow. The latter occurs if Δp is greater than the "flooding" pressure ΔpF.
c) an upward buoyancy flow equal to the downward buoyancy flow.

These three flows are modeled by two flow-elements. The first element handles the forced flow (a) and in addition whichever of the buoyancy flow component, (a) or (c), that is in the same direction as the forced flow. The second element handles the alternate buoyancy flow component.

1.9.4.1 Pressure driven flow

The pressure forced flow is modeled as orifice flow using Equation 143, except the area A in the Section 1.9.3.5 is replaced by:

$$Aeff = L1 * L2 * sin(StairAngle) * (1 + cos(StairAngle))$$

Equation 156

L1 and *L2* are the dimensions of the horizontal rectangular hole. To include the effect of stairs, a $StairAngle$ can be set, where $StairAngle = 90\ deg$ corresponds to vertical stairs. The angle can be set to 90 degrees to exclude the effect of the stairs.

Equation 144 is used for the partial derivative of the flow, with the area A_e using *Aeff* in place of A.

1.9.4.2 Buoyancy flow

When the zone on top has a higher density than the zone on the bottom, the maximum possible buoyancy flow, mbm, occurs when the pressure difference across the hole is zero:

$$mbm = 0.055\sqrt{g\bar{\rho}|\Delta\rho|Dhyd^5}$$

Equation 157

The 0.055 factor is dimensionless ; g = 32.2 ft/s^2.

The hydraulic diameter of the hole is defined as:

$$Dhyd = 2 * Aeff/(L1 + L2)$$

Equation 158

When the zone on top has a higher density than the zone on the bottom, and the pressure difference is lower than the flooding pressure, then the buoyancy flow is given by:

$$mb \ = \ mbm * \left(1 - \frac{|\Delta p|}{\Delta pF}\right)$$

Equation 159

The flooding pressure difference ΔpF is defined as:

$$\Delta pF = C_s^2 g|\Delta\rho|Dhyd^5/(2\mathrm{A}_{\mathrm{eff}}^2)$$

Equation 160

The shape factor C_s is

$$C_s = 0.942\left(minimum\left(\frac{L1}{L2}, \frac{L2}{L1}\right)\right)$$

Equation 161

If the top zone density is lower than the bottom zones, or if $|\Delta p| > \Delta pF$ then the buoyancy flow mb is zero.

The partial derivatives of the buoyancy flows with respect to adjacent zone pressures are all zero since the buoyancy flows are equal and opposite. That is, although the buoyancy flow magnitudes are sensitive to zone pressures, they have no influence on the zone mass balance.

Although the buoyancy flows don't directly influence zone pressures, they do affect the heat transfer rates.

When buoyancy flows exists, the heat transfer due to the buoyancy flow to the upper zone, *i* say, is

$$\mathrm{Q_i} = \ \mathrm{mb} * \mathrm{C_p}(\mathrm{T_j} - \mathrm{T_i})$$

Equation 162

and to the lower zone is

$$\mathrm{Q_j} = \ \mathrm{mb} * \mathrm{C_p}(\mathrm{T_i} - \mathrm{T_j})$$

Equation 163

1.9.5 Large Vertical Openings

The flow through large vertical rectangular openings are handled using the method suggested by Woloszyn (1999).

Woloszyn uses a simplified version of the common integrate-over-pressure-distribution scheme as used by Walker for example. Rectangular holes are divided in two, with the flow through the top half driven by a constant Δp equal to the pressure difference ¾ the way up the opening (the midpoint of the top half of the opening area). Similarly, the flow through the bottom half uses the Δp at ¼ the way up the hole, and assumes it is constant over the bottom half. Although approximate compared to the integration methods, it is expected to be able to reasonably accurately, if not precisely, portray one and two way flows through such elements. This procedure has the virtue of eliminating the calculation of the neutral level, thereby greatly reducing the number of code logic branches and equations. It also eliminates a divide by zero problem when $\Delta\rho \rightarrow 0$ in the exact integration methods.

Besides being used for large vertical holes, like open windows and doorways, the method is also used for distributed infiltration. That is, a rectangular wall with an effective leakage area ELA is represented by two holes, each of area ELA/2, located at the ¼ and ¾ heights. These holes are then modeled using Equation 138, Equation 141, Equation 144, and Equation 145.

1.9.5.1 Triangular surfaces

The method is generalized further to treat the tilted triangular surfaces assumed for hip roofs. In this case the lower Woloszyn hole, of area ELA/2, is placed at the height that is above ¼ of the area of the triangle. This can be shown to be a height of:

$$H_{lower\ hole} = Z_{soffit} + \left(1 - \frac{\sqrt{3}}{2}\right)(Z_{ridge} - Z_{soffit})$$

Equation 164

Similarly, the top hole is placed at the height above ¾ of the area of the triangle:

$$H_{upper\ hole} = Z_{soffit} + (1/2)(Z_{ridge} - Z_{soffit})$$

Equation 165

1.9.6 Newton-Raphson Solution

Assume there are a total of *nuc* conditioned and unconditioned zones with unknown pressures. The outside conditions, of known pressure, are assigned a zone number *nout* = *nuc*+*1*.

The mass flow rate from zone *i* to zone *j* (including *j*=*nout*) is designated as $m_{i,j}$, and can be positive (flow out of zone i) or negative (flow into zone i).

$$m_{i,j} = \sum_{k=1}^{K_{i,j}} m_{i,j,k}$$

Equation 166

where $m_{i,j,k}$ is the flow rate through the *k*'th element of the $K_{i,j}$ elements in surface *i,j*. By symmetry,

$$m_{i,j,k} = -\, m_{j,i,k}$$

Equation 167

and

$$\mathrm{m_{i,j}} \;\; = -\, \mathrm{m_{j,i}}$$

Equation 168

From Equation 167, $\mathrm{m}_{\mathrm{i,j},k}$ values are functions of the zone pressure difference $(P_i - P_j)$.

$$\mathrm{m_{i,j,k}} = +\,\mathrm{A_e}\sqrt{2\rho_{\mathrm{in}}}\left(\mathrm{P_i} - \mathrm{P_j}\right)^{\mathrm{n}} \qquad \text{for positive } \Delta\mathrm{P}$$

$$\mathrm{m_{i,j,k}} = -\mathrm{A_e}\sqrt{2\rho_{\mathrm{in}}}\left(\mathrm{P_j} - \mathrm{P_i}\right)^{\mathrm{n}} \qquad \text{for negative } \Delta\mathrm{P}$$

Equation 169

This shows that in general,

$$\frac{\partial m_{i,j,k}}{\partial P_i} = -\frac{\partial m_{i,j,k}}{\partial P_j}$$

Equation 170

The net flow leaving zone *i* (*i=1 to nuc)* is the defined as the residual r_i:

$$r_i = \sum_{j=1, j\neq i}^{nout} m_{i,j} = \sum_{j=1, j\neq i}^{j=nout} \sum_{k=1}^{K_{i,j}} m_{i,j,k}$$

Equation 171

The $j \neq i$ criterion on the sums eliminates summing $m_{i,i}$ terms which are zero by definition. The zone pressures $\mathrm{P_i}$ are to be determined such that the residuals $\mathrm{r_i}$ all become zero.

Equation 169 and Equation 171 constitute a set of n = nuc nonlinear equations with n = nuc unknown pressures. To linearize the equations, a Taylor's series is used to determine the residual r_i' at the pressure $P_j{}'$ near the guessed value of pressures P_j, where the residual is r_i. Keeping only first order terms:

$$r_i' = r_i + \sum_{j=1}^{nuc} \frac{\partial r_i}{\partial P_j} \left(P_j{}' - P_j \right)$$

Equation 172

In matrix form this is written:

$$\boldsymbol{r}' = \boldsymbol{r} + \boldsymbol{J}(\boldsymbol{P}' - \boldsymbol{P})$$

Equation 173

where $\boldsymbol{r}'$ is the vector with elements r_i', and $\boldsymbol{r}$ is the vector with elements r_i.

$\boldsymbol{J}$ is the nuc-by-nuc Jocobian matrix with elements:

$$J_{i,l} = \frac{\partial r_i}{\partial P_l} = \sum_{j=1}^{nout} \frac{\partial m_{i,j}}{\partial P_l} = \sum_{j=1, j \neq i}^{j=nout} \sum_{k=1}^{k=K_{i,j}} \frac{\partial m_{i,j,k}}{\partial P_l}$$

Equation 174

where $i = 1\ to\ nuc, and\ l = 1\ to\ nuc$.

Setting $r_i' = 0$ and solving for $P_j{}'$, Equation 173 becomes

$$\boldsymbol{P}' = \boldsymbol{P} - \boldsymbol{J}^{-1}\boldsymbol{r}$$

Equation 175

$$\boldsymbol{P}' = \boldsymbol{P} - \boldsymbol{C}$$

Equation 176

where $\boldsymbol{C}$ is the correction vector:

$$\boldsymbol{C} = -\boldsymbol{J}^{-1}\boldsymbol{r}$$

Equation 177

$$P_i{}' = P_i - C_i$$

Equation 178

Equation 178 gives the pressures $P_i{}'$ that are predicted to make r_i' zero.

1.9.6.1 Convergence

Convergence is attained when the residuals r_i are sufficiently small. As employed by Energy Plus and Clarke, both absolute and relative magnitude tests are made.

Convergence is assumed when the absolute magnitude of the residual in each zone i is less than a predetermined limit *ResMax*:

$$|res_i| < ResMax$$

Equation 179

OR, the magnitude of the residual divided by the sum of the magnitudes of the flow through each element connected to zone i, is less than a predetermined limit $ResErr$:

$$\frac{|res_i|}{resmag_i} < ResErr$$

Equation 180

where

$$resmag_i = \sum_{j=1}^{nout} |m_{i,j}|$$

Equation 181

(code uses: sum of magnitude of flows to & from zone iz, resmag(iz) += ABS(mdot(iz,jz,ke)).

1.9.6.2 Relaxation

Equation 178 is more generally written as

$$P_i{}' = P_i - relax * C_i$$

Equation 182

where $relax$ is the relaxation coefficient, a factor less than one that reduces the correction applied to P_i. Relaxation factors on the order of 0.75 have been shown to reduce the number of iterations in cases normally having slowly decreasing and oscillating corrections. But a fixed value of 0.75 can slow what were formerly rapidly converging cases. The following approach is used to reduce the relaxation factor only when necessary.

Following Clarke, when the corrections C_i from one iteration to the next changes sign, and the latest C_i has a magnitude over half as big as the former C_i, then it is assumed that the convergence is probably slow and oscillating. This symptom is typically consistent over a few iterations, and if this were precisely the case, the correction history would follow a geometric progression with a negative common ratio $\frac{C_i}{C_i^{last}}$. Thus by extrapolation a better estimate of correct solution will be obtained if the relaxation factor is taken as the sum of the infinite termed geometric progression:

$$relax = \frac{1}{1 - \frac{C_i}{C_i^{last}}}$$

Equation 183

Thus, whenever, during an iteration for zone i,

$$\frac{C_i}{C_i^{last}} < -0.5$$

Equation 184

then Equation 178 is replaced by

$$P_i{}' = P_i - \frac{1}{1 - \frac{C_i}{C_i^{last}}} * C_i$$

Equation 185

Insofar as the extrapolation is warranted, this should give a better prediction of the pressure $P_i{}'$ than would using *relax* = 1 for this iteration. For the iteration following that using Equation 185, *relax* = 1 is reverted to (i.e., Equation 178) so that only unrelaxed correction values are used to evaluate $\frac{C_i}{C_i^{last}}$. The following iteration, if any, is then again tested by Equation 184. The first iteration is always done with *relax = 0.75* since at this point there is no value available for C_i^{last}.

It would be reasonable to add a max Ci limit; i.e., max pressure change allowed, a la Clarke, but code testing has not shown the need.

1.9.6.3 Off diagonal terms

Consider Equation 174 for off-diagonal terms. Since $i \neq l$, zone i's flow $m_{i,j}$ varies with P_l only if *j* = *l*. Thus setting *j* = *l*, and $i \neq l$, Equation 174 reduces to:

$$J_{i,l,i\neq l} = \sum_{k=1}^{K_{i,l}} \frac{\partial m_{i,l,k}}{\partial P_l}$$

Equation 186

where $i = 1\ to\ nuc, and\ l = \ 1\ to\ nuc.$

Equation 186, along with Equation 170, shows that all off diagonal terms have a negative magnitude. Since $m_{i,l,k} = -\ m_{l,i,k}$,

$$J_{i,l,i\neq l} = \sum_{k=1}^{K_{i,l}} \frac{\partial m_{i,l,k}}{\partial P_l} = -\sum_{k=1}^{K_{i,l}} \frac{\partial m_{l,i,k}}{\partial P_l}$$

Equation 187

Using Equation 170, Equation 187 becomes:

$$J_{i,l,i\neq l} = \sum_{k=1}^{K_{i,l}} \frac{\partial m_{l,i,k}}{\partial P_i} = J_{l,i,i\neq l}$$

Equation 188

Thus the Jacobian matrix is symmetric:

$$J_{i,l} = J_{l,i}$$

Equation 189

Thus only the upper (or lower) diagonal terms need be determined, with the other half determined by transposition. The off diagonal terms only involve partials of flows between zones with unknown pressures.

1.9.6.4 Diagonal terms

For $i = j$ Equation 174 gives:

$$J_{i,i} = \frac{\partial r_i}{\partial P_i} = \sum_{j=1}^{nout} \frac{\partial m_{i,j}}{\partial P_i} = \sum_{j=1}^{j=nout} \sum_{k=1}^{k=K_{i,j}} \frac{\partial m_{i,j,k}}{\partial P_i}$$

Equation 190

where $i = 1\ to\ nuc$.

Equation 190 terms can be regrouped to show a simpler numerical way to determine $J_{i,i}$, by using the off diagonal terms already calculated:

$$J_{i,i} = \frac{\partial m_{i,nout}}{\partial P_i} - \sum_{k=1,k\neq i}^{k=nuc} J_{k,i}$$

Equation 191

This shows that the diagonal elements use the derivatives of mass flows to the outdoors minus the off diagonal terms in the same column of the Jacobian.

Equation 191 shows that matrix will be singular if $\frac{\partial m_{i,nout}}{\partial P_i} = 0$, so that at least one connection to outdoors is necessary.

1.10 DUCT SYSTEM MODEL

1.10.1 Description of Model

The duct model builds on the procedure given by Palmiter (see Francisco and Palmiter, 2003), that uses a steady state heat exchanger effectiveness approach to get analytical expressions for instantaneous duct loss and system efficiencies. The duct model, developed for this program by Palmiter, makes use of many of the same fundamental steady state equations and approach, but given the considerable complexity of the multiple duct systems, does not do a simultaneous solution of all the equations which a generalized Francisco and Palmiter scheme may imply. Instead the approach takes advantage of the small time steps used in the code, and in effect decouples the systems from each other and the zone by basing all losses and other heat transfers occurring during the time step on the driving conditions of Tair and Tmrt known at the beginning of the time step, similar to how heat transfers are determined during mass temperature updates .

Other assumptions made in the duct program: mass and thermal siphon effects in the duct system are ignored.

The duct system performance is analyzed at every time step. The duct air temperatures are calculated assuming they are operating at steady state, in equilibrium with the thermal conditions at the beginning of the time-step in the attic. Heat capacity effects of the ducts are ignored.

During each time step, the following steps are taken to find the duct system operating conditions such as the air temperatures in each duct, the losses, the heating or cooling delivered, etc.

Initially, for each time step, the duct systems performance is determined when operating at full capacity, independent of the load. The procedure starts at the return registers in each conditioned zone, where the duct air temperatures are the current timesteps conditioned zone air temperatures. The conditioned zone air entering the return register heats or cools, or both, as it traversed through each component of the duct system: the return duct, the return plenum, the heating/cooling device, and the supply ducts. That is, the duct air temperature rises or drops immediately downstream of the return register (where returns leaks are assigned to occur) due to mixing of leakage air at the air temperature in the unconditioned zone in which the return duct is located with the return air from the conditioned zone. It may also increase or decrease in temperature in the return plenum as it mixed with the air from the return duct in another unconditioned zone. After being heated or cooled by the air handler at its applicable heating/cooling capacity, it is then additionally heated or cooled by supply duct conductive gains/losses to the interior of the unconditioned zone.

Summing all the gains and losses in temperature of the duct air as it travels through the system gives the supply temperature for the supply duct, allowing the heat delivered at full capacity, $Qdel$, to be determined.

If the above useful heat delivered at full capacity is more than required by the load, then the equipment capacity is reduced to meet the load by assuming the system is only running the fraction $Qload/\,Qdel$ of the time step. The needed capacity, $Qneed$, is this fraction of the nominal capacity. The duct losses for the time step are also reduced by this fraction.

The above calculations are done each time step and the average Qneed summarized in the hourly output.

The above steps are presented in detail in the following sections, in the same sequence as described above.

1.10.2 Duct System Inputs

1.10.2.1 Subscripts

In most cases in this section, the subscripted variables stand for arrays.

The subscript u stands for the unconditioned zone in which the duct is located.

The subscript c stands for conditioned zone number and its associated air handler system.

The subscript m stands for the mode of air handler operation: 0 off, 1 heating, 2 cooling.

1.10.2.2 Annual run inputs

The following data is input to model the duct/air handler system(s):

Duct inside areas

$Asd_{c,u}$ = supply duct inside area for air handler c in unconditioned zone u.

$Ard_{c,u}$ = return duct inside area for airhandler c in unconditioned zone u.

Duct insulation rated R values

$Rsd_{c,u}$ = supply duct rated R for air handler c in unconditioned zone u; hr-ft^2-F/Btu.

$Rrd_{c,u}$ = return duct rated R for air handler c in unconditioned zone u; hr-ft^2-F/Btu.

Inside duct area and inside area based resistance, and the outside duct area and outside area based resistance when there is a single duct segment in the return and supply branches

Consider one duct of constant inside diameter, d_i, and length L. The duct is insulated with insulation having a thermal conductivity k, and rated R value, R_{rate}. All R values herein are in the units of (hr-ft2-F/Btu).

Layed flat, the thickness the insulation layer is:

$$t = Rrate * k$$

Equation 192

If the insulation is wrapped at this thickness around a duct of diameter d_i, the outside diameter, d_o, of the insulation will be:

$$d_o = d_i + 2 * Rrate * k$$

so,

$$\frac{d_o}{d_i} = 1 + \frac{2kR_{rate}}{d_i}$$

Equation 193

Conduction heat transfer texts gives the overall conductance C of length L of an annular insulation layer as:

$$C = \frac{2\pi kL}{ln\left(\frac{d_o}{d_i}\right)}$$

Equation 194

Dividing this by inside area, $A_i = \pi d_i L$, gives the conductance per unit inside area:

$$C_i = \frac{2k}{d_i ln\left(\frac{d_o}{d_i}\right)}$$

The duct resistance value per unit inside area is the reciprocal,

$$R_i = \frac{d_i ln\left(\frac{d_o}{d_i}\right)}{2k}$$

Equation 195

This can be written in terms of areas, and length L, as:

$$R_i = \frac{A_i ln\left(\frac{A_o}{A_i}\right)}{2\pi kL}$$

Equation 196

The duct resistance value based on outside area can be determined from R_i and A_i as:

$$R_o = \frac{d_o}{d_i} R_i$$

Equation 197

$$A_o = \frac{d_o}{d_i} A_i$$

The R values of Equation 195 and Equation 197, divided by R_{rated}, are plotted in Figure 25 as a function of the inside diameter of the duct branch.

Figure 25: Ratio of Actual R to Rated R

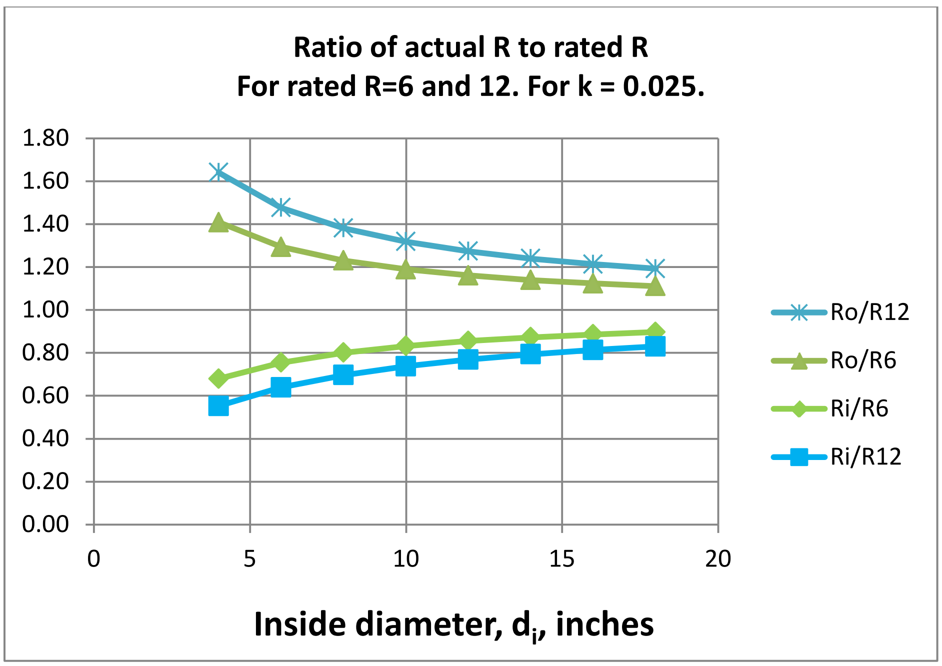

Duct system composed of multiple segments in the supply and return branches

Suppose the supply ducts from an air handler system are branched, with each branch having different sizes, lengths, rated insulation Rrate, and conductivity k values, and all the branches are in one unconditioned zone. These could be combined into one equivalent duct as follows.

The duct branches, j=1→ n, are combined, each of inside areas $A_i(j)$, outside areas $A_o(j)$, conductivities $k(j)$, and inside area based resistances $R_i(j)$. Using the method of Palmiter and Kruse (2003), the overall conductance of the branched duct system, based on inside area, is the sum of the conductances of each branch:

$$'UA' = \sum_{j=1\rightarrow n} \left(\frac{A_i(j)}{R_i(j)} \right)$$

Equation 198

where R_i for each branch segment j is given by Equation 196 as

$$R_i(j) = \frac{A_i(j)ln\left(\frac{A_o(j)}{A_i(j)}\right)}{2\pi k(j)L(j)}$$

Equation 199

With $A_i(j) = \pi d_i(j)L(j)$, and using Equation 193, this can be written as

$$R_i(j) = \frac{d_i(j)ln\left(1 + \frac{2k(j)R_{rate}(j)}{d_i(j)}\right)}{2k(j)}$$

Equation 200

The total branch inside area is:

$$A_i = \sum_{j=1\rightarrow n} A_i(j)$$

Equation 201

The effective overall resistance of the branched duct, based on inside area A_i, is thus:

$$R_i = \frac{A_i}{'UA'} = \frac{A_i}{\sum_{j=1\rightarrow n}\left(\frac{A_i(j)}{R_i(j)}\right)} = \frac{A_i}{\sum_{j=1\rightarrow n}\left[\frac{A_i(j)}{\frac{d_i(j)ln\left(1 + \frac{2k(j)R_{rate}(j)}{d_i(j)}\right)}{2k(j)}}\right]}$$

Equation 202

The values of the terms needed for each branch segment, shown on the right hand side of Equation 202 are not available since the former ACM manual only requires that the following R is known:

$$\text{"R"} = \frac{A_i}{\sum_{j=1\rightarrow n}\frac{A_i(j)}{R_{rate}(j)}}$$

Equation 203

Equation 202 and Equation 203 would be equivalent if Equation 203 had the term $R_i(j)$ in place of $R_{rate}(j)$. As it is, Equation 203 gives the area weighted average R_{rate}, not $R_i(j)$.

The total outside area is:

$$A_o = \sum_{j=1 \to n} A_o(j)$$

Equation 204

Based on outside area, the effective duct system resistance would be:

$$R_o = \frac{A_o}{A_i} R_i$$

Equation 205

1.10.2.3 Emissivities

$epss_{c,u}$ = supply duct emissivity for air handler c in unconditioned zone u.

$epsr_{c,u}$ = return duct emissivity for air handler c in unconditioned zone u.

1.10.2.4 Duct leakage

$Ls_{c,u}$ = the fraction of the flow through the system c air handler fan that is leaked from the supply duct in unconditioned zone u. The leak is assigned to occur near the supply register so that the leakage air is at the supply register temperature.

$Lr_{c,u}$ = the fraction of the flow through the system c air handler fan that is leaked into the return duct in unconditioned zone u. The leak is assigned to occur at the return register. The air leaking into the duct is at the unconditioned zone temperature.

1.10.2.5 System flow

$Flow_{m,c}$ = the flow rate in cfm (at standard conditions) through the air handler for the cooling and heating modes, for of each system.

1.10.2.6 Flow distribution

How much of the air handler flow of system c goes through each of its return and supply ducts is given by the per run input flow fractions:

$Fmr_{c,u}$ = fraction of flow of system c in the return duct located in unconditioned zone u.

$Fms_{c,u}$ = fraction of flow of system c in the supply duct located in unconditioned zone u.

$Fmrc_c$ = fraction of flow of system c in the return duct located in conditioned zone c.

$Fmsc_c$ = fraction of flow of system c in the supply duct located in conditioned zone c.

For a given system c, the sum of the return duct fractions must add to one: $Fmr_{c,1}$ + $Fmr_{c,2}$ + $Fmrc_c$ = 1. Similarly for the supply duct fractions.

1.10.3 Return Duct Air Temperatures

Following the procedure indicated in Section 1.10.1, the return duct air temperatures are determined first. Utilizing the heat exchanger effectiveness approach (see Mills (1992), and Appendix A), the temperature of the system c return duct air entering the return plenum from a return duct located in unconditioned zone number u is given by:

$$Tout_{c,u} = Er_{m,c,u} Teqr_{c,u} + (1 - Er_{m,c,u}) \cdot Tmix_{c,u}$$

where $Er_{m,c,u}$ is the effectiveness of the return duct of system c in unconditioned zone u when operating in mode m:

$$Er_{m.c.u} = 1 - e^{\frac{-Urtot_{c,u}}{Mcpr_{m,c,u}}}$$

where $Urtot_{c,u}$ is the total conductance between the return duct air and the equivalent surroundings temperature $Teqr_{c,u}$:

$$Teqr_{c,u} = (Frda_{c,u} \cdot Tair_u + Frdr_{c,u} \cdot Tmrt_u),$$

$Frda_{c,u}$ is the fraction of return duct (dissolved surface node) conductance that goes to the $Tair_u$ node.

$$Frda_{c,u} = \frac{Urc_{c,u}}{(Urc_{c,u} + Urr_{c,u}}$$

$Frdr_{c,u}$ is the fraction of the conductance from the c,u return duct air that goes to the $Tmrt_u$ radiant node.

$$Frdr_{c,u} = \frac{Urr_{c,u}}{Urc_{c,u} + Urr_{c,u}}$$

The U terms are the conductances from the duct air to the mrt and air nodes, determined as described in Appendix A. These conductance values, and the similar supply duct values of Section 1.10.6 are used in the energy balance of the unconditioned zone(s) containing ducts.

Urr_{cu} = conductance from return duct air to Tmrt.

$Urc_{c,u}$ = conductance from return duct air to Tair.

$$Urtot_{c,u} = Urc_{c,u} + Urr_{c,u}$$

The term $Mcpr_{m,c,u}$ is the flow conductance (see below) for the return duct flow:

$$Mcpr_{m,c,u} = Mcp_{m,c} Fmr_{c,u}$$

The total system flow, $Mcp_{m,c}$ is in the "flow conductance" form with the units Btu/hr-F:

$$Mcp_{m,c} = Flow_{m,c} \cdot c_p$$

where c_p is the volumetric heat capacity, which is taken as 1.08 Btu/(hr-F-cfm) for dry air at the ASHRAE standard conditions of density = 0.075 lb_m/ft^3 and c_p = 0.24 Btu/lb_m-F.

The term $Tmix_{c,u}$ is the mixed air just downstream of the return duct leakage, given by:

$$Tmix_{c,u} = Lr_{c,u}Tair_u + (1 - Lr_{c,u})Temp_c$$

where $Temp_c$ is the temperature of conditioned zone c's air, assumed to be well-mixed.

1.10.4 Return Plenum Temperature and Return Duct Conductive Heat Losses

The heat loss rate from the return duct via convection and radiation, needed in the unconditioned zone energy balance, is:

$$qlr_{c,u} = Mcpr_{m,c,u} \cdot (Tmix_{c,u} - Tout_{c,u})$$

The final return plenum temperature of system c is found by summing the contributions to its plenum temperature from the return ducts in each unconditioned zone and the return ducts located in the conditioned zone. That is,

$$Trp_c = Fmrc_c \cdot Temp_c + \sum_{all\ u} Fmr_{c,u} \cdot Tout_{c,u}$$

1.10.5 Temperature Rise through Air Handler Heating or Cooling Equipment

If the mode is heating or cooling, the temperature rise through the air handler heating or cooling equipment of system c at sensible capacity Cap_c is given by:

$$dte_c = \frac{Cap_c}{Mcp_{m,c}}$$

Equation 206

The program considers no heat losses or gains from the air handler components other than from the ducts.

1.10.6 Supply Plenum and Supply Register Temperatures

The supply plenum temperature is given by:

$$Tsp_c = Trp_c + dte_c$$

Equation 207

The supply register temperature for the supply duct of system c in unconditioned space u is:

$$Tsr_{c,U} = Teqs_{c,u} + (1 - Es_{m,c,u}) \cdot (Tsp_c - Teqs_{c,u})$$

Equation 208

where $Es_{m,c,u}$ is the effectiveness of the supply duct of system c in unconditioned zone u when operating in mode m:

$$Es_{m,c,u} = 1 - e^{\frac{-Ustot_{c,u}}{Mcps_{m,c,u}}}$$

Substituting the Tsp_c equation above into Equation 208and rearranging gives:

$$Tsr_{c,u} = (1 - Es_{m,c,u})dte_c + Tsrhx_{m,c,u}$$

Equation 209

where

$$Tsrhx_{m,c,u} = \left(1 - Es_{m,c,u}\right)Trp_c + Es_{m,c,u}Teqs_{c,u}$$

$Tsrhx$ is the temperature that would be delivered to the supply register with the current mode's flow rate but with zero capacity such that $dte_c = 0$. The duct system is then acting as a heat exchanger (thus the 'hx') between the connected conditioned and unconditioned zones.

The term $s_{c,u}$, similar to $Teqr_{c,u}$ of Section 1.10.3, is an equivalent environmental temperature defined by

$$Teqs_{c,u} = (Fsda_{c,u} \cdot Tair_u + Fsdr_{c,u} \cdot Tmrt_u),$$

where

$$Fsda_{c,u} = \frac{Usc_{c,u}}{Usc_{c,u} + Usr_{c,u}}$$

$$Fsdr_{c,u} = \frac{Usr_{c,u}}{Usc_{c,u} + Usr_{c,u}}$$

$Usr_{c,u}$= conductance from supply duct air to Tmrt.

$Usc_{c,u}$ = conductance from supply duct air to Tair.

$$Ustot_{c,u} = Usc_{c,u} + Usr_{c,u}$$

The supply duct flow rate is:

$$Mcps_{m,c,u} = Mcp_{m,c} \cdot Fms_{c,u}$$

1.10.7 Heating/Cooling Delivered and Supply Duct Conductive Heat Loss

Given $Tsr_{c,u}$, from above, the heat delivered to the conditioned zones by way of the supply ducts located in one or more of the unconditioned zones is given by summing the sensible heat delivered via each unconditioned zones:

Q delivered from ducts $= \sum_u Mcpsr_{m,c,u} \cdot (Tsr_{c,u} - Temp_c)$

Equation 210

where $Mcpsr_{m,c,u}$, the flow out the supply register after the supply leakage is removed, is given by:

$$Mcpsr_{m,c,u} = (1 - Ls_{c,u}) \cdot Mcps_{m,c,u}$$

The heat delivered to the conditioned zones by way of ducts in the conditioned zone, which are assumed to have no losses or unbalanced leakage, is given by:

$$\text{Q delivered directly to conditioned zone} = Fmsc_c \cdot Cap_c$$

Equation 211

Adding the Q's of Equation 210 and Equation 211 gives the net heating (+), or cooling (-), delivered by the system c as:

$$Qdel_c = Fmsc_c \cdot Cap_c + \sum\nolimits_{\text{over } u}[Mcpsr_{m,c,u} \cdot (Tsr_{c,u} - Temp_c)]$$

Substituting the expression for $Tsr_{c,u}$ from Equation 209 into this, $Qdel_c$ can be put in the form:

$$Qdel_c = Qdel1_c + Qdel2_c,$$

where $Qdel1_c$ is the part of Qdel that is independent of air handler capacity. That is, it is the Q delivered if dte is zero, and is the heat exchanged between the unconditioned and conditioned zones via the duct system:

$$Qdel1_c = \sum_{all\ u} [Mcpsr_{m,c,u}(Tsrhx_{m,c,u} - Temp_c)]\,.$$

$Qdel2_c$ is the part of $Qdel$ that is linearly dependent on the air handler capacity:

$$Qdel2_c = Fmsc_c \cdot Cap_c + \sum_{over\ u} [Mcpsr_{m,c,u} \cdot (1 - Es_{m,c,u}) \cdot dte_c]$$

The rate of supply duct conduction losses this time step is given by:

$$qls_{c,u} = Mcps_{m,c,u} \cdot (Tsp_c - Tsr_{c,u})$$

1.10.8 Duct System Performance when the Load is Less than the Heat Delivered at Full Capacity

If Qld_c is smaller than the capacity $Qdel_c$, then the system runs only part of the time step. In this case the run time fraction is:

$$Frun_c = \frac{Qld_c}{Qdel_c}$$

The capacity required to meet the load is $Qneed_c$:

$$Qneed_c = Frun_c \cdot Cap_c$$

The duct conductive and leakage losses are also reduced by the same $Frun_c$ fraction.

1.10.9 Duct System Performance when the Load is Greater than the Heat Delivered at Full Capacity

In principle this won't occur because the conditioned zone load is limited to the system capacity when it is calculated by the conditioned zone thermostat logic However, the capacity thus calculated is based on the duct efficiency [defined as η=Qload/Qneed] determined for the unconditioned zone during the last time-step, and as a result the load might exceed the capacity determined by the duct model efficiency this time-step.

That is, when the conditioned zone energy balance is performed, and for example heating is called for, then the output capacity of the heating system needs to be known, which requires knowing the duct system efficiency. But the duct efficiency is only known after the attic simulation is run.

To avoid iteration between the conditioned zone and attic zone modules, the most recent duct efficiency is used to determine the capacity in the conditioned zones thermostat calculations. When the attic simulation is next performed, if the conditioned zone was last running at capacity, and if the efficiency now calculated turns out to be higher than was assumed by the thermostat calculations, then the load will have exceeded the limiting capacity by a small amount depending on the assumed vs. actual efficiency. In cases like this, to avoid iteration, the limiting capacity is allowed to exceed the actual limit by a small amount, so that the correct air handler input energy demand is determined for the conditioned zone load allowed.

In this case, the system is set to run for the full sub-hour time step and the air handler meets the load by increasing its capacity with the following procedure. This procedure, a carryover from the 2008 Residential Building Standards ACM procedures, wherein no capacity limits were imposed on the air handler systems, is as follows.

From the $Qdel1$ and $Qdel2$ equations it can be seen that the capacity needed in this case is:

$$Qneed_c = \frac{Qld_c - Qdel1_c}{Qdel2_c} Cap_c$$

Thus, the temperature rise through the air handler needs to be:

$$dte_c = \frac{Qneed_c}{Mcp_{m,c}}$$

The supply plenum temperature becomes:

$$Tsp_c = Trp_c + dte_c$$

The supply register temperatures is determined reusing Equation 208:

$$Tsr_{c,u} = Teqs_u + (1 - Es_{m,c,u}) \cdot (Tsp_c - Teqs_{c,u})$$

The supply duct losses now become:

$$qls_{c,u} = Mcps_{m,c,u} \cdot (Tsp_c - Tsr_{c,u})$$

The $Qneed_c$'s from each of the time steps during the hour are summed over the hour and reported in the output as $Qneed_c$. The supply and return duct conduction loss terms $qls_{c,u}$ and $qlr_{c,u}$ are used in the energy balance of the unconditioned zone each time step.

1.11 VARIABLE INSULATION CONDUCTIVITY

The following correlation is used. It is based on the correlation used in EnergyGauge USA (Parker, et al, 1999) which is based on Wilkes (1981) data:

$k = (kn) \cdot (1 + 0.00418(T_{insul} - 70))$; temperatures in °F.

where,

k = insulation conductivity (Btu/hr-ft-R) at the average insulation temperature, T_{insul}(F).

kn = nominal insulation conductivity (Btu/hr-ft-R) for insulation at 70 F.

1.12 CEILING BYPASS MODEL

A simple model was implemented to simulate ceiling bypass heat transfer, the heat that is transported from the conditioned zone to the attic via miscellaneous inter-wall cavities in the conditioned zone that may be partially open to the attic, as for example around a fireplace unit. Natural convection in the cavity when the conditioned zone is hotter than the attic is assumed to be the main mechanism for the bypass heat transfer. The conductance, when the conditioned zone air temperature $Tair_c > Tair_u$, the attic air temperature:

$$qbp = U(Tair_c - Tair_u)$$

where, the conductance follows a simple power law dependence on the temperature difference:

$$U = U_{bp}(Temp_1 - Tair_u)^{nbp}$$

Ubp is a coefficient depending on the cavity geometry. Although an exponent of nbp on the order of 1/4 can be assumed for laminar convection, there is no current empirical basis for determining the exponent. If the ACM rule of $U = 0.02Aceil$ were implemented, then nbp would be chosen as zero.

1.13 ZONE HUMIDITY BALANCE

1.13.1 Zone Humidity Balance

Given a zone with various flows, m_j, with humidities w_j, entering the zone, and with a scheduled source of water vapor, m_{sched}, a water mass balance on the zone gives:

$$\frac{dMw}{dt} = \sum_j m_j(w_j - w) + m_{sched}$$

Equation 212

which can be written as:

$$M\frac{dw}{dt} = \sum_j m_j(w_j - w) + m_{sched} - w\frac{dM}{dt}$$

Equation 213

where,

M = mass of dry air in the zone; lbm of dry air.

$\frac{dw}{dt}$ = the rate of change of humidity ratio in zone.

m_j = air flow rate from source j into zone; lbm-dry-air/unit-time. Source j can be outdoors, a supply register, adjacent zone, etc.

w_j = humidity ratio of air coming from source *j*; lbm H_2O/lbm dry air.

w = humidity ratio of air in zone; lbm H_2O/lbm dry air.

m_{sched} = scheduled rate of moisture addition to zone; lbm H_2O/unit time.

Using the air perfect gas equation the last term in Equation 213 can be written

$$w\frac{dM}{dt} = -w\frac{M}{T}\frac{dT}{dt}$$

so that Equation 213 becomes

$$M\frac{dw}{dt} = \sum_j m_j(w_j - w) + m_{sched} + w\frac{M}{T}\frac{dT}{dt}$$

Equation 214

where T is the air temperature in absolute degrees.

This equation is solved using a forward difference rather than a backward or central difference since a forward difference uncouples the moisture balance equations of each of the zones.

Integrating from time t to time $t + \delta t$, where δt is the time step, using a forward difference, gives:

$$w(t+\delta t) = \left(m_{sched}(t) + \sum_j m_j(t) w_j(t)\right)\frac{\delta t}{M(t)} + w(t)\left(1 - \frac{\delta t}{M(t)}\sum_j m_j(t) - \frac{T(t+\delta t) - T(t)}{T(t)[\deg R]}\right)$$

Equation 215

Notice that all of the values on the right hand side of Equation 215 are determined at t (the beginning of the integration period) except for the $T(t + \delta t)$ term which represents the zone air temperature at the end of the integration period. $T(t + \delta t)$ is known from the zone energy sensible energy balance at time t (see Section 1.3). The term $\frac{T(t+\delta t)-T(t)}{T(t)[\deg R]}$ is assumed to be negligible and not included in the CSE code.

1.13.2 Stability of Solution

The time series solution of Equation 215 will become unstable unless the second term is positive. That is, stability requires

$$\left(\frac{\delta t}{M(t)}\sum_j m_j(t) + \frac{T(t+\delta t) - T(t)}{T(t)[\deg R]}\right) < 1$$

Equation 216

Solving for δt, stability requires

$$\delta t < \frac{M(t)}{\sum_j m_j(t)}\left(1 - \frac{T(t+\delta t) - T(t)}{T(t)[\deg R]}\right)$$

Equation 217

Since the zone air changes per unit time is $AC = \frac{\sum_j m_j(t)}{M(t)}$ then the stability requirement can be written in terms of air changes as:

$$AC < \frac{1}{\delta t}\left(1 - \frac{T(t+\delta t) - T(t)}{T(t)[\deg R]}\right)$$

Equation 218

If the solution is unstable at the given δt, the zone air mass M(t) can be temporarily boosted up such that:

$$M(t) > \frac{\delta t \sum_j m_j(t)}{\left(1 - \frac{T(t+\delta t) - T(t)}{T(t)[\deg R]}\right)}$$

This will lead to a higher latent capacity for the zone air, introducing some error in the zone humidity prediction. This will also lead to a zone latent heat imbalance unless this artificial increase in zone air is accounted for.

1.13.3 Hygric Inertia of Zone

The absorption/desorption of moisture in the zone is accounted for using the hygric inertial model of Vereecken et al. whereby a multiplier X is added to the M(t) term of Equation 10 and Equation 11. An appropriate value of X can be measured for the complete zone and all of its furnishings by using the protocol given by [Vereecken E, Roels S, Janssen H, 2011. In situ determination of the moisture buffer potential of room enclosures, Journal of Building Physics, 34(3): 223-246.]

1.13.4 Saturation

~~If the humidity, w, predicted by **Error! Reference source not found.** is greater than wsat(Tzone), then the amount of moisture that must be removed this time step is:~~

~~water condensed = $M(w - w_{sat})$ lbm H2O.~~

~~heat to air = (LatentHeat/lbmH2O)* $M(w - w_{sat})$ Btu~~

~~Then the predicted w is reset to w_{sat} for the next time step calculation.~~

1.14 ZONE COMFORT ALGORITHM

CSE includes an implementation of the ISO 7730 comfort model. The model is documented in ASHRAE Standard 55-2010 (ASHRAE 2010) among other places. The model calculates Predicted Mean Vote (PMV) and Predicted Percent Dissatisfied (PPD) for each zone at each time step. These statistics are averaged over days, months, and the full year.

The inputs to the ISO 7730 model are:

- Air dry-bulb temperature
- Air humidity ratio
- Mean radiant temperature
- Air velocity
- Occupant metabolic rate
- Occupant clothing level

Zone conditions calculated by CSE are used for the first three of these inputs. The remaining inputs are set by user input. They can be varied during the simulation using the CSE expression capability.

1.15 HVAC EQUIPMENT MODELS

Air conditioning systems shall be sized, installed, tested and modeled according to the provisions of this section.

1.15.1 Compression Air-Conditioner Model

The Compliance Software calculates the hourly cooling electricity consumption in kWh using Equation 219. In this equation, the energy for the air handler fan and the electric compressor or parasitic power for the outdoor unit of a gas absorption air conditioner are combined. The Compliance Software calculates the hourly cooling gas consumption in therms using Equation 219.

$$AC_{kWh} = \frac{Fan_{Wh} + Comp_{Wh}}{1{,}000}$$

Equation 219

Where:

AC_{kWh} = Air conditioner kWh of electricity consumption for a particular hour of the simulation. This value is calculated for each hour, combined with the TDV multipliers, and summed for the year.

Fan_{Wh} = Indoor fan electrical energy for a particular hour of the simulation, Wh.

$Comp_{Wh}$ = Electrical energy for all components except the indoor fan for a particular hour of the simulation, Wh. This value includes consumption for the compressor plus outdoor condenser fan and is calculated using Equation 221.

CSE calculates the energy for electrically driven cooling using the algorithms described in this section.

Primary model parameters. The following values characterize the AC unit and are constant for a given unit:

Cap95 = AHRI rated total cooling capacity at 95 °F, Btuh

$CFM_{per\ ton}$ = Air flow rate per ton of cooling capacity, cfm/ton.

$$= \frac{\text{Operating air flow rate, cfm}}{\text{Cap95 / 12000}}$$

EFan = Fan operating electrical power, W/cfm. Default = 0.365.

SEER = AHRI rated Seasonal Energy Efficiency Ratio, Btuh/W. EER shall be used in lieu of the SEER for equipment not required to be tested for a SEER rating.

EER = AHRI rated energy efficiency ratio at 95 °F, Btuh/W. If EER is not available, it is derived from SEER as follows:

If SEER	>=16	>=13 & <16	<13
EER	13	11.3 + 0.57 x (SEER-13)	10+0.84×(SEER– 11.5)

F_{chg} = Refrigerant charge factor, default = 0.9. For systems with a verified charge indicator light (Reference Residential Appendix RA3.4) or verified refrigerant charge (Reference Residential Appendix RA3), the factor shall be 0.96.

F_{size} = Compressor sizing factor, default = 0.95. For systems sized according to the Maximum Cooling Capacity for compliance software Credit (see Section <TODO>), the factor shall be 1.0.

Derived model parameters. The following values are used in the formulas below and depend only on model parameters.

Tons = Nominal cooling capacity defined as Cap95 / 12000

$QFan_{rat}$ = Assumed fan heat included at AHRI test conditions, Btuh

Fan motor type	$QFan_{rat}$
PSC	500 x Cap95 / 12000
BPM	283 x Cap95 / 12000

$QFan_{op}$ = Fan heat assumed during operation (i.e., during simulation), Btuh

$$QFan_{op} = \frac{CFM_{per\ ton} \times Cap95 \times EFan \times 3.413}{12000}$$

Equation 220

Model inputs. The following values vary at each time step in the simulation and are used in the formulas below to determine AC unit performance under for that time step.

DB_t = Dry bulb temperature of air at the condensing unit, °F (typically outdoor air temperature).

WB_{ec} = Coil entering air wet bulb temperature, °F (return air temperature adjusted for blow-through fan heat if any)

DB_{ec} = Coil entering air dry bulb temperature, °F (return air temperature adjusted for blow through fan heat if any)

Qneed = Cooling system sensible cooling output, Btuh. Qneed is calculated across the unit and thus includes both the building load and distribution losses.

Compressor energy for a particular time step of the simulation shall be calculated using Equation 221.

$$Comp_{wh} = \frac{QFan_{op} + Qneed}{CE_t}$$

Equation 221

Where:

Fan_{wh} = Fan power for this time step, Wh.

CE_t = Sensible energy efficiency at current conditions, Btuh/W. This is calculated using Equation 222 below.

$$CE_t = EER_t \times SHR$$

Equation 222

Where:

EER_t = Energy efficiency ratio at current conditions, Btuh/W. EER_t is calculated using Equation 226 below.

SHR = Sensible Heat Ratio (sensible capacity / total capacity), derived as follows:

$$\begin{aligned} SHR = \text{minimum}(1,\ & A_{SHR} \times DB_{ec} + \\ & B_{SHR} \times WB_{ec} + \\ & C_{SHR} \times DB_t + \\ & D_{SHR} \times CFM_{per\ ton} + \\ & E_{SHR} \times DB_{ec} \times DB_t + \\ & F_{SHR} \times DB_{ec} \times CFM_{per\ ton} + \\ & G_{SHR} \times WB_{ec} \times DB_t + \\ & H_{SHR} \times WB_{ec} \times CFM_{per\ ton} + \\ & I_{SHR} \times DB_t \times CFM_{per\ ton} + \\ & J_{SHR} \times WB_{ec}^2 + \\ & K_{SHR} / CFM_{per\ ton} + \\ & L_{SHR}) \end{aligned}$$

SHR coefficients:

A_{SHR}	0.0242020
B_{SHR}	-0.0592153

C_{SHR}	0.0012651
D_{SHR}	0.0016375
E_{SHR}	0
F_{SHR}	0
G_{SHR}	0
H_{SHR}	-0.0000165
I_{SHR}	0
J_{SHR}	0.0002021
K_{SHR}	0
L_{SHR}	1.5085285

CAP_{nf} = Total cooling capacity across coil (that is, without fan heat) at current conditions, Btuh

$$CAP_{nf} = (Cap95 + QFan_{rat}) \times F_{chg} \times F_{size} \times F_{cond\_cap}$$

Equation 223

F_{cond_cap} =
$A_{CAP} \times DB_{ec}$ +
$B_{CAP} \times WB_{ec}$ +
$C_{CAP} \times DB_{t}$ +
$D_{CAP} \times CFM_{per\ ton}$ +
$E_{CAP} \times DB_{ec} \times DB_{t}$ +
$F_{CAP} \times DB_{ec} \times CFM_{per\ ton}$ +
$G_{CAP} \times WB_{ec} \times DB_{t}$ +
$H_{CAP} \times WB_{ec} \times CFM_{per\ ton}$ +
$I_{CAP} \times DB_{t} \times CFM_{per\ ton}$ +
$J_{CAP} \times WB_{ec}^{2}$ +
$K_{CAP} / CFM_{per\ ton}$ +
L_{CAP}

Coefficients as follows:

SHR Condition	SHR < 1	SHR = 1

A_{CAP}	0	0.009483100
B_{CAP}	0.009645900	0
C_{CAP}	0.002536900	-0.000600600
D_{CAP}	0.000171500	-0.000148900
E_{CAP}	0	-0.000032600
F_{CAP}	0	0.000011900
G_{CAP}	-0.000095900	0
H_{CAP}	0.000008180	0
I_{CAP}	-0.000007550	-0.000005050
J_{CAP}	0.000105700	0
K_{CAP}	-53.542300000	-52.561740000
L_{CAP}	0.381567150	0.430751600

CAP_{sen} = Sensible capacity including fan heat, Btuh

$$CAP_{sen} = CAP_{nf} \times SHR - QFan_{op}$$

Equation 224

CAP_{lat} = Latent capacity, Btuh

$$CAP_{lat} = CAP_{nf} - CAP_{sen}$$

Equation 225

Note: The air leaving the AC unit is limited to 95% relative humidity. If that limit is invoked, CAP_{lat} is reduced and CAP_{sen} is increase.

EER_t is calculated as follows:

When

$DB_t \leq 82$ ºF $EER_t = SEER_{nf}$

$82 < DB_t < 95$ °F $EER_t = SEER_{nf} + ((DB_t - 82)*(EER_{nf} – SEER_{nf}) / 13)$

$DB_t \geq 95$ °F $EER_t = EER_{nf}$

Equation 226

Where:

$SEER_{nf}$ = Seasonal energy efficiency ratio at current conditions without distribution fan consumption ("nf" = no fans). This is calculated using Equation 227.

EER_{nf} = Energy efficiency ratio at current conditions without distribution fan consumption ("nf" = no fans) and adjusted for refrigerant charge and airflow. This is calculated using Equation 228.

$$SEER_{nf} = \frac{F_{chg} \times F_{size} \times F_{cond\_SEER} \times (1.09 \times Cap95 + QFan_{rat})}{1.09 \times Cap95/SEER - QFan_{rat}/3.413}$$

Equation 227

$$\begin{aligned} F_{cond\_SEER} = F_{cond\_cap} / \; & (A_{SEER} \times DB_{ec} + \\ & B_{SEER} \times WB_{ec} + \\ & C_{SEER} \times DB_t + \\ & D_{SEER} \times CFM_{per\ ton} + \\ & E_{SEER} \times DB_{ec} \times DB_t + \\ & F_{SEER} \times DB_{ec} \times CFM_{per\ ton} + \\ & G_{SEER} \times WB_{ec} \times DB_t + \\ & H_{SEER} \times WB_{ec} \times CFM_{per\ ton} + \\ & I_{SEER} \times DB_t \times CFM_{per\ ton} + \\ & J_{SEER} \times WB_{ec}^2 + \\ & K_{SEER} / CFM_{per\ ton} + \\ & L_{SEER}) \end{aligned}$$

Coefficients as follows:

SHR Condition	SHR < 1	SHR = 1
A_{SEER}	0	0.0046103
B_{SEER}	-0.0202256	0
C_{SEER}	0.0236703	0.0125598
D_{SEER}	-0.0006638	-0.000512
E_{SEER}	0	-0.0000357
F_{SEER}	0	0.0000105
G_{SEER}	-0.0001841	0
H_{SEER}	0.0000214	0

I_{SEER}	-0.00000812	0
J_{SEER}	0.0002971	0
K_{SEER}	-27.95672	0
L_{SEER}	0.209951063	-0.316172311

$$EER_{nf} = \frac{Cap_{nf}}{F_{cond\_EER} \times (Cap95/EER - QFan_{rat}/3.413)}$$

Equation 228

Where:

$$\begin{aligned} F_{cond\_EER} = (&A_{EER} \times DB_{ec} + \\ &B_{EER} \times WB_{ec} + \\ &C_{EER} \times DB_t + \\ &D_{EER} \times CFM_{per\ ton} + \\ &E_{EER} \times DB_{ec} \times DB_t + \\ &F_{EER} \times DB_{ec} \times CFM_{per\ ton} + \\ &G_{EER} \times WB_{ec} \times DB_t + \\ &H_{EER} \times WB_{ec} \times CFM_{per\ ton} + \\ &I_{EER} \times DB_t \times CFM_{per\ ton} + \\ &J_{EER} \times WB_{ec}^2 + \\ &K_{EER} / CFM_{per\ ton} + \\ &L_{EER}) \end{aligned}$$

Coefficients as follows:

SHR Condition	SHR < 1	SHR = 1
A_{EER}	0	0.004610300
B_{EER}	-0.020225600	0
C_{EER}	0.023670300	0.012559800
D_{EER}	-0.000663800	-0.000512000
E_{EER}	0	-0.000035700
F_{EER}	0	0.000010500

G_{EER}	-0.000184100	0
H_{EER}	0.000021400	0
I_{EER}	-0.000008120	0
J_{EER}	0.000297100	0
K_{EER}	-27.956720000	0
L_{EER}	0.015003100	-0.475306500

1.15.2 Air-Source Heat Pump Model (Heating mode)

The air source heat pump model is based on methods presented in AHRI Standard 210/240-2008.

Primary model parameters. The following values characterize the ASHP and are constant for a given unit:

Cap47 = Rated heating capacity at outdoor dry-bulb temperature = 47 °F

COP47 = Coefficient of performance at outdoor dry bulb = 47 °F (if available, see below)

Cap35 = Heating capacity under frosting conditions at outdoor dry-bulb temperature = 35 °F (if available, see below)

COP35 = Coefficient of performance at outdoor dry bulb = 35 °F (if available, see below)

Cap17 = Rated heating capacity at outdoor dry-bulb temperature = 17 °F

COP17 = Coefficient of performance at outdoor dry bulb = 17 °F (if available, see below)

HSPF = Rated Heating Seasonal Performance Factor, Btuh/Wh

COPbu = COP of backup heating, default = 1 (electric resistance heat)

Capbu = Available backup heating capacity, Btuh

Derived model parameters.

Inp47 = Electrical input power at 47 °F = Cap47 / COP47, Btuh (not W)

Inp17 = Electrical input power at 17 °F = Cap17 / COP17, Btuh (not W)

Estimation of unavailable model parameters.

$$\mathrm{COP47} = 0.3038073 \times \mathrm{HSPF} - 1.984475 \times \frac{\mathrm{Cap17}}{\mathrm{Cap47}} + 2.360116$$

$$\mathrm{COP17} = 0.2359355 \times \mathrm{HSPF} - 1.205568 \times \frac{\mathrm{Cap17}}{\mathrm{Cap47}} - 0.1660746$$

$$Cap35 = 0.9 \times [Cap17 + 0.6 \times (Cap47 - Cap17)]$$

$$Inp35 = 0.985 \times [Inp17 + 0.6 \times (Inp47 - Inp17)]$$

$$COP35 = \frac{Cap35}{Inp35}$$

Simulation

Full-load capacity and input power of the ASHP is determined each time step as a function of outdoor dry-bulb temperature T, as follows --

If (17 °F < T < 45 °F)

$$Cap(T) = Cap17 + \frac{(Cap35 - Cap17) \times (T - 17)}{35 - 17}$$

$$Inp(T) = Inp17 + \frac{(Inp35 - Inp17) \times (T - 17)}{35 - 17}$$

Else

$$Cap(T) = Cap17 + \frac{(Cap47 - Cap17) \times (T - 17)}{47 - 17}$$

$$Inp(T) = Inp17 + \frac{(Inp47 - Inp17) \times (T - 17)}{47 - 17}$$

Resistance heat.

Load in excess of Cap(T) is met with backup heating at COPbu.

1.15.3 Equipment Sizing

CSE determines the capacity of HVAC equipment via an auto-sizing capability. Autosizing is conducted prior to the main annual simulation. It is done by using the hourly simulator for a set of design days and increasing capacity as needed to maintain thermostat set points. Each design day is repeated several times until the required capacity converges. The set of design days includes one cold day with no solar gain and several hot days at with clear-sky solar at different times of the year. This ensures that maximums of both heating and cooling loads will be found. Equipment characteristics other than capacity are specified on a per-unit basis (e.g. "cfm per ton"), so a full description of the system can be derived from the primary capacity.

The sizing procedure uses the equipment models in an inverse mode. For example, the sensible cooling load for a given set up conditions is back-converted to the required rated total capacity (Cap95) by using inverted forms of the model equations. The general simulation calculation sequence is used, but the logic of the HVAC models is altered during the autosizing phase.

Note that for air-source heat pumps, only the backup heating capacity is autosized. In addition, modeled duct sizes are not sized and must be specified.

The equipment sizes calculated by CSE are used for compliance analysis only and are not substitutes for load calculations used for selecting equipment or meeting other code requirements.

2 Compliance Manager

2.1 OVERVIEW

To be written

2.2 ONE-DIMENSIONAL ROOF EDGE HEAT TRANSFER MODEL

2.2.1 Construction Practice

This document describes the one-dimensional model used to represent the heat flow between the conditioned zone and the outdoors through the portion of the ceiling insulation, along the outside edge of the attic, through which the heat flows to the outdoors without passing through the attic air. This portion will be modeled in CSE as cathedral ceilings, and is referred herein as the roof edge. The rest of the heat flow path through the ceiling insulation will be modeled as part of the attic zone, and is not discussed here.

Two types of roof construction are considered, standard-heel and raised-heel trusses, shown in Figure 26 and Figure 27, with the geometries assumed to be representative of current practice. The roof trusses are assumed to be framed with 2x4's. Although the figures are for a roof with a 4-in-12 pitch, the 1-D model will handle any standard pitch. The distance between the wall plate and roof deck (shown, for example, as 12 inches in Figure 27) is also not restricted to the distances implied by Figure 26 and Figure 27.

The 1-D model is developed in order to simplify the heat transfer calculation for roof edges, while preserving the steady state and transient characteristics (layer mass) of the typical roof constructions addressed. The 1-D model produces the dimensions of the construction layers needed to represent the roof edges.

Figure 26: Standard-Heel Geometry

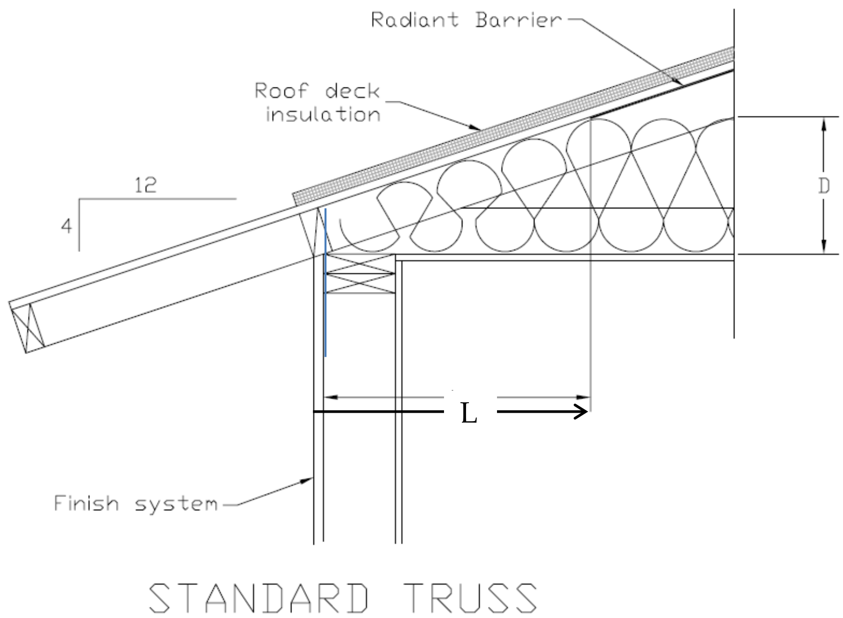

L and D determine where the top of the ceiling insulation meets the roof deck plane.

Figure 27: Raised-Heel Geometry

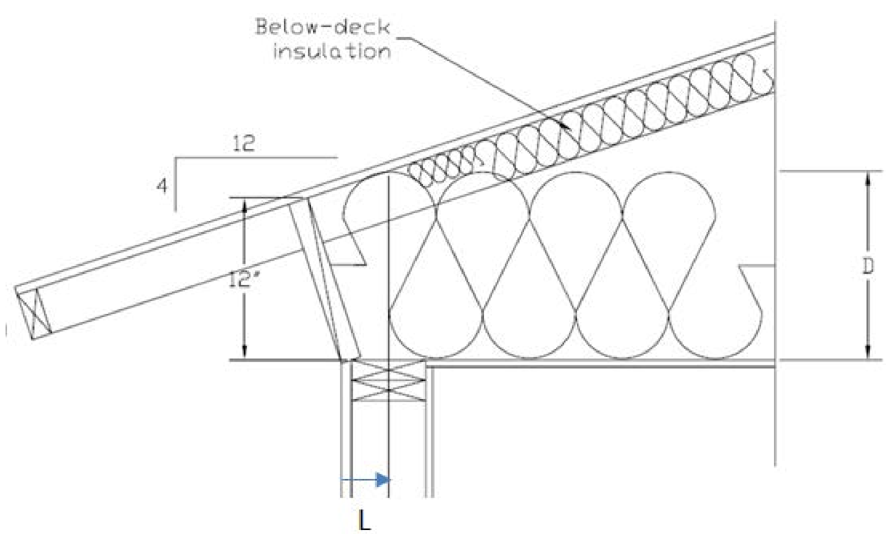

L and D determine where the top of the ceiling insulation meets the roof deck plane.

2.2.2 One-Dimensional Model

Using the parallel path method, the heat transfer is determined separately for the insulation and framing paths of the constructions.

First consider modeling the standard-heel truss of Figure 26.

2.2.2.1 Standard heel insulation path

For the path through the insulation, Figure 26 is approximated as the simpler 2-D configuration of Figure 28 and Figure 30, with the left vertical edge assumed to be adiabatic and of height Y. The right vertical edge is also assumed to be adiabatic. To partly compensate for not allowing heat flow out the left side tilted edge board in Figure 26, the ceiling is assumed to extend to the outer edge of the vertical wall.

The width, W_A of roof edge path A, is taken as the width of the vertical path of solid wood in the framing section view of Figure 30.

Figure 28: Standard-Heel Simplified Geometry for Insulation Path

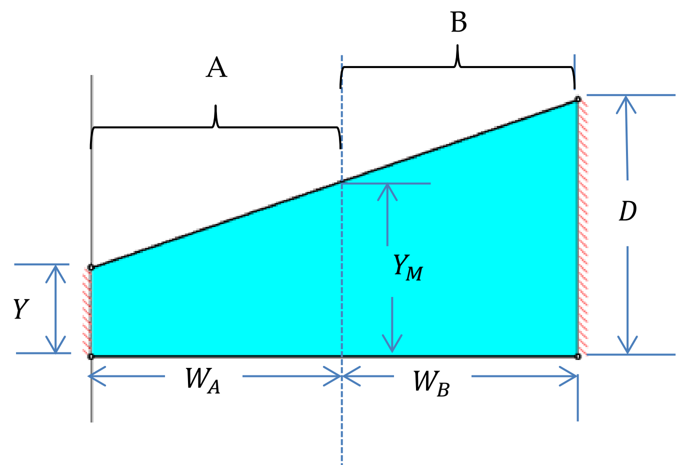

Figure 28 is then reduced to the 1-D form shown in Figure 29, where the layer thicknesses are taken as the average height of the layer in Figure 28.

Figure 29: Standard-Heel 1-D Geometry for Insulation Path

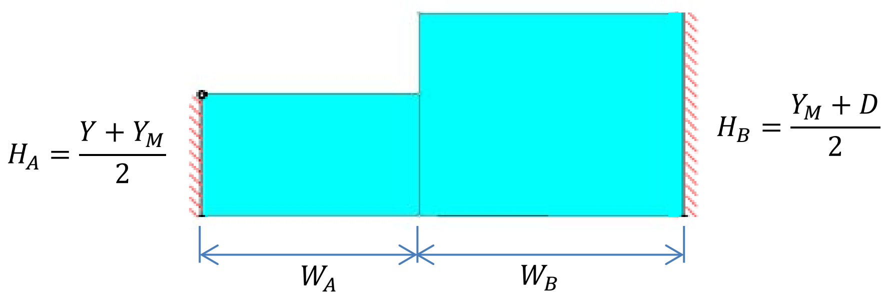

The left hand portion represents the insulation path of the 1-D model of roof edge A. The right side represents the insulation path of the 1-D model of roof edge B.

The 1-D model just considers the ceiling insulation and framing. When implemented as part of a cathedral ceiling in CSE, a sheetrock layer would be added to the bottom of Figure 29 paths. Layers added to the tops of the layers in Figure 29 would be decking, asphalt shingles, and tile, for example.

2.2.2.2 *Standard heel framing path*

Similar to the insulation path, the framing heat transfer path starts with Figure 30, which is reduced to Figure 31. The widths of A and B are the same as for the insulation path figures. H_{B1}, and H_{B3} are the vertical thickness of the 2x4's and H_{B2} is the average thickness of insulation.

Figure 30: Standard-Heel Simplified Geometry for Framing Path

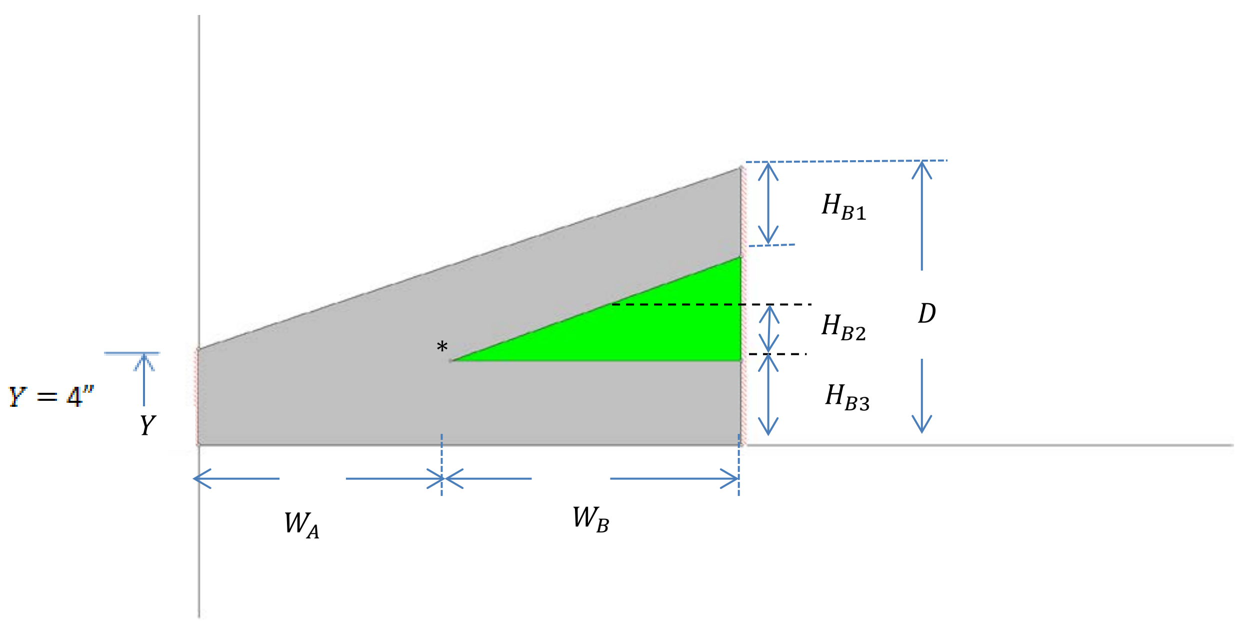

Figure 31: Standard-Heel 1-D Geometry for Framing Path

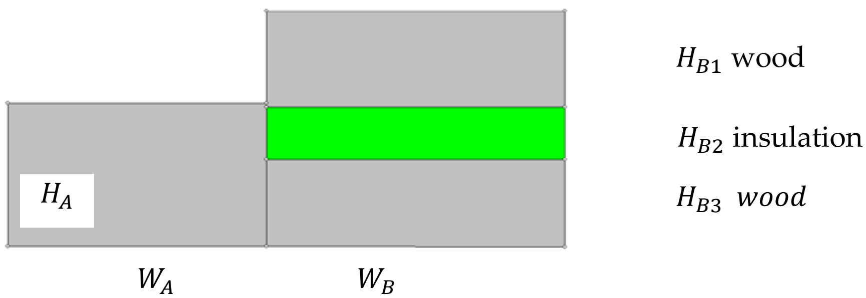

2.2.2.3 *Raised heel*

The 1-D model for the raised-heel case of Figure 27 is different than for the standard-heel case of Figure 26. The geometry is illustrated in Figure 32 and Figure 33 for a ceiling insulation of R38.

As the edge height, Y, in Figure 30 is increased, the deck and ceiling 2x4's separate vertically near the roof edge, and a vertical 2x4 is assumed to fill the gap. That is, as Y is increased, the standard truss geometry of Figure 28 and Figure 30 morphs into the raised truss geometry of Figure 32 and Figure 33. The 1-d roof edge algorithm below, gives the layering outputs for both the standard-heel truss and the raised-heel truss and everything in between.

2.2.2.4 *Raised heel insulation path*

Figure 32: Raised-Heel 1-D Insulation Path Geometry

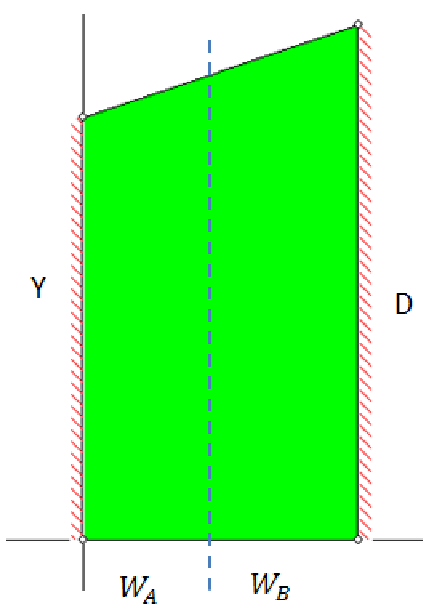

2.2.2.5 Raised heel frame path

Figure 33: Raised-Heel 1-D Framing Path Geometry

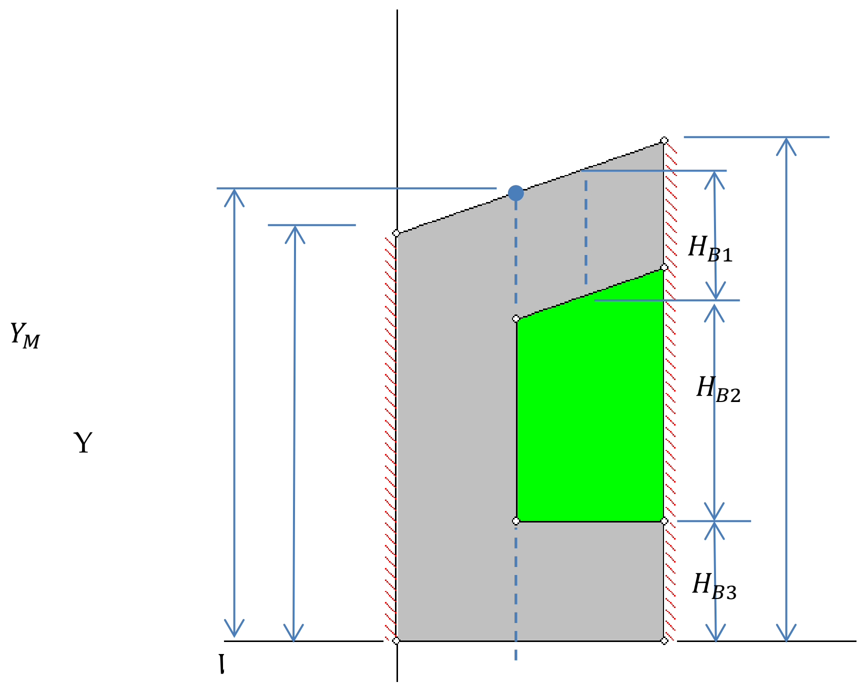

H_{B1}, and H_{B3} are the vertical thickness of the 2x4's and H_{B2} is the average thickness of insulation.

2.2.2.6 Roof edge algorithm

The following algorithm, written in succinct pseudo-code form, determines the layer widths and thicknesses for roof edge paths A and B. [This algorithm is implemented in RoodEdgeAlgorithm-1.xlsx].

All dimensions are assumed to be feet.

Input:

Y = edge height, ft.

w = framing width, ft. [nominally (3.5/12)-ft]

$Rtot$ = total R value of ceiling insulation, hr-ft^2-F/Btu.

R_{perin} = R value of the ceiling insulation for one inch thickness, hr-ft^2-F/Btu.

P = pitch = rise/12

Calculation of $\mathbf{W_A, W_B, H_A, H_B, H_{B1}, H_{B2}}$, and $\mathbf{H_{B3}}$:

$D = \frac{Rtot}{12*R_{perin}}$ insulation depth, ft

$Y_I = w\left(1 + \sqrt{1 + P^2}\right)$ vertical thickness at position $x = X_I$.

$X_I = \frac{Y_I - Y}{P}$ horiz distance from left edge to intersection of deck and ceiling 2x4's (see * in Figure 30). In Figure 33, the corresponding point would be outside the roof section, and near the left edge of the page, and as opposed to the * point, this X_I will is a negative number since it is to left of origin at outside surface of top wall plate.

IF $X_I \geq w$:

$Y_M = Y_I$ Y_M is the height of roof section at the vertical line between A and B.

ELSE $X_I < w$:

$Y_M = (w - X_I)P + Y_I$

END IF

IF $D \geq Y_M$:

$$W_B = \frac{D - Y_M}{P}$$

$$H_A = \frac{Y + Y_M}{2}$$

$$H_B = \frac{Y_M + D}{2}$$

$$H_{B1} = w\sqrt{1 + P^2}$$

$$H_{B2} = H_B - Y_I$$

$$H_{B3} = w$$

IF $X_I \geq w$:

$W_A = X_I$

ELSE $X_I < w$:

$W_A = w$

END IF

ELSE IF $D < Y_M$ AND $D > Y$:

$$W_A = \frac{D - Y}{P}$$

$$H_A = \frac{D + Y}{2}$$

$W_B = H_B = H_{B1} = H_{B2} = H_{B3} = 0$

ELSE (D ≤ Y)

$W_A = H_A = 0$

$W_B = H_B = H_{B1} = H_{B2} = H_{B3} = 0$

END IF

PRINT OUTPUT: $W_A, W_B, H_A, H_B, H_{B1}, H_{B2}, H_{B3}$

2.2.3 Roof Edge Model Validation

The roof edge heat transfer is basically a 3-D problem. The 1-D model makes a number of simplifications. For example, the parallel insulation and framing path assumption ignores lateral heat transfer between the insulation and framing path, and leads to an underestimation of the overall heat transfer. The assumption of an adiabatic right hand border, where in reality the heat flow lies are not quite vertical, also underestimates the heat transfer through the cathedral ceilings with an accompanying overestimation of the remaining heat transfer through the attic portion of the ceiling insulation. The assumption of the layer thicknesses taken as the average layer thickness ignores 2-D effects. The complicated 2-D heat transfer at the junction of the vertical wall and roof is simplified by assuming the left border is adiabatic, and the ceiling continuation to the outside of the wall. Corner effects for the roof edge, where vertical walls meet at right angles, results in a 3-D heat flow situation that can only be estimated.

Because of these complexities, it is difficult to assess the accuracy of the 1-D model.

However, in order to obtain some perspective on the accuracy of the 1-D model, the heat transfer was calculated for two cases, of different insulation depths, using both the 1-D roof edge algorithm, and a 2-D (using FEHT finite-element program) solution with the roof edge 2-D geometry of Figure 26. The 2-D model still requires many of the assumptions made in the 1-D model, including the parallel path assumption.

2.2.3.1 1-D model, Rtot = 30, Y = 4-inches

Using the 1-D Roof Edge Algorithm, the heat transfer rates through roof edges A and B was calculated for the following inputs.

Input to Roof Edge Algorithm

$R_{tot} = 30$ hr-ft^2-F/Btu.

$P = 4/12$

Y = 0.3333 ft

w = 0.2917 ft

R_{perin} = 2.6 hr-ft^2-F/Btu.

Output of Roof Edge Algorithm

W_A =0.797 ft

W_B = 1.087 ft

H_A =0.466 ft

H_B =0.780 ft

H_{B1} = 0.292 ft

H_{B2} = 0.182 ft

H_{B3} = 0.307 ft

Insulation Path Results

The insulation conductivity is $k = \frac{1}{12R_{perin}}$ = 0.03205 Btu/hr-ft-F.

The thermal resistance of A and B are:

$$R_A = \frac{H_A}{k_{insul}} = 14.546 \text{ hr-ft}^2\text{-F/Btu}$$

$$R_B = \frac{H_B}{k_{insul}} = 24.346 \text{ hr-ft}^2\text{-F/Btu}$$

If no additional layers are added (sheetrock, etc.), and the top and bottom surface temperature difference is 100 F, the heat transfer rate in this case, per foot of roof perpendicular to the section, becomes:

$$Q_A = \frac{W_A * \Delta T}{R_A} = \frac{0.797*100}{14.546} = 5.48 \text{ Btu/hr-ft}$$

$$Q_B = \frac{W_B * \Delta T}{R_B} = \frac{1.087*100}{24.346} = 4.465 \text{ Btu/hr-ft}$$

The total is:

$$Q_{insulpath} = Q_A + Q_B = 9.944 \text{ Btu/hr-ft}$$

Framing Path Results

Assume wood framing conductivity k = 0.084 hr-ft-F/Btu.

The thermal resistance of A, per foot of roof edge perpendicular to the section:

$$R_A = \frac{H_A}{k_{wood}} = 5.55 \text{ hr-ft}^2\text{-F/Btu}$$

The thermal resistance of path B; sum of layer resistances:

$$R_B = \frac{H_{B1}}{k_{wood}} + \frac{H_{B2}}{k_{insul}} + \frac{H_{B3}}{k_{wood}} = 3.66+5.654+3.473=12.786 \text{ hr-ft}^2\text{-F/Btu}$$

The sum of the heat transfers in this case is (from CathedralWorksheet.xlsx).

$$Q_A = \frac{W_A * \Delta T}{R_A} = \frac{0.797 * 100}{5.550} = 14.36$$

$$Q_B = \frac{W_B * \Delta T}{R_B} = \frac{1.087 * 100}{12.786} = 8.50$$

$Q_{framingpath} = Q_A + Q_B =$ 22.86 Btu/hr-ft

2.2.3.2 1-D model, Rtot = 60, Y = 4-inches

Input to Roof Edge Algorithm

Rtot = 60; other inputs the same as in Rtot = 30 case above.

Output of Roof Edge Algorithm

$\mathrm{W_A}$ = 0.797 ft

$\mathrm{W_B}$ = 3.972 ft

$\mathrm{H_A}$ = 0.466 ft

$\mathrm{H_B}$ = 1.261 ft

$\mathrm{H_{B1}}$ = 0.292 ft

H_{B2} = 0.662 ft

H_{B3} = 0.307 ft

Insulation Path Results

Similar to the Rtot = 30 case, the thermal resistance of A and B are:

$R_A = \frac{H_A}{k_{insul}} = 14.546$ hr-ft²-F/Btu

$R_B = \frac{H_B}{k_{insul}} = 39.346$ hr-ft²-F/Btu

The heat transfer rates are:

$$Q_A = \frac{W_A * \Delta T}{R_A} = \frac{0.797 * 100}{14.546} = 5.48$$

$$Q_B = \frac{W_B * \Delta T}{R_B} = \frac{3.972 * 100}{39.346} = 10.095$$

$Q_{framingpath} = Q_A + Q_B =$ 15.57 Btu/hr-ft

Framing path results

The thermal resistance of A, per foot of roof edge perpendicular to the section:

$R_A = \frac{H_A}{k_{wood}} = 5.55$ hr-ft²-F/Btu

The thermal resistance of path B is the sum of layer resistances. k = 0.084 hr-ft-F/Btu is assumed.

$$R_B = \frac{H_{B1}}{k_{wood}} + \frac{H_{B2}}{k_{insul}} + \frac{H_{B3}}{k_{wood}} = \text{hr-ft}^2\text{-F/Btu}$$

$$= 3.472 + 20.66 + 3.66 = 27.79$$

The sum of the heat transfers in this case is:

$$Q_A = \frac{W_A * \Delta T}{R_A} = \frac{0.797*100}{5.55} = 14.36$$

$$Q_B = \frac{W_B * \Delta T}{R_B} = \frac{3.972*100}{27.79} = 14.29$$

$$Q_{framingpath} = Q_A + Q_B = 28.65 \text{ Btu/hr-ft}$$

2.2.3.3 2-D Model, Rtot = 30, Y = 4-inches

Insulation Path

The Figure 26 case is modeled with the simplified geometry of Figure 34, shown for a ceiling insulation of R30. The top of the plate capping the vertical wall is assumed to be adiabatic. The tilted block assumed to be wood, exposed to ambient conditions on its outside sides. The outside of the wood and insulation assumed to be at a uniform 100F. The ceiling side of the insulation is set to at 0 F. The same material properties were used as in the 1-D model.

Figure 34: Standard Truss, Insulation Path, 2-Dimensional Heat Transfer Model Geometry

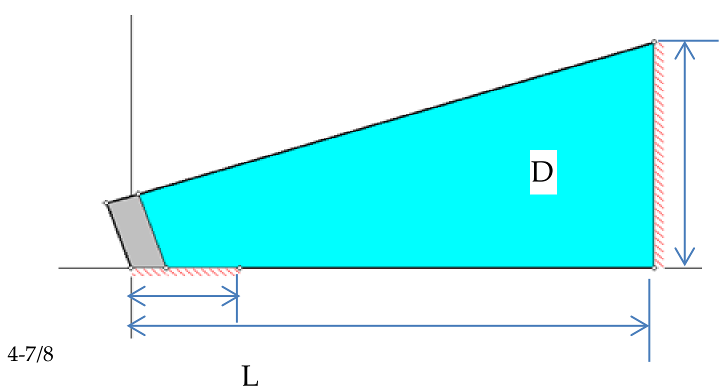

The resulting isotherms and heat transfer vectors are shown in Figure 35.

Figure 35: Standard-Heel, Insulation Path, 2-Dimensional Heat Transfer Isotherms and Heat Transfer Vectors

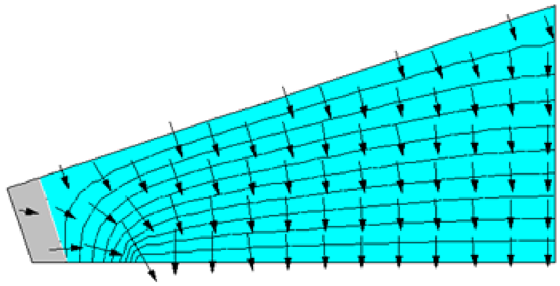

The overall heat transfer, per foot of perimeter, for this case was determined (RUN std30.FET) to be:

Q = 9.67 Btu/hr-ft

Equation 229

Framing Path

The frame path was modeled similarly, with the Figure 36 graphic results.

Figure 36. Standard-Heel, Frame Path, 2-Dimensional Heat Transfer Isotherms and Heat Transfer Vectors

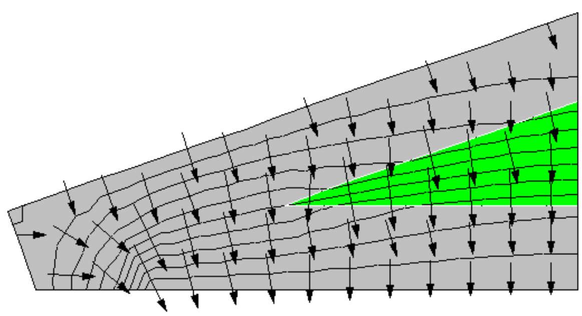

The overall heat transfer, per foot of perimeter, for this case was determined (RUN std30F.FET) to be:

Q = 21.94 Btu/hr-ft

Equation 230

2.2.3.4 2-D Model, Rtot = 60, Y = 4-inches

Similar to the R30 case above, Figure 37 and Figure 38 show the insulation and framing path 2-D results.

Figure 37: 2-D Results for Insulation Path of R-60 Standard-Heel

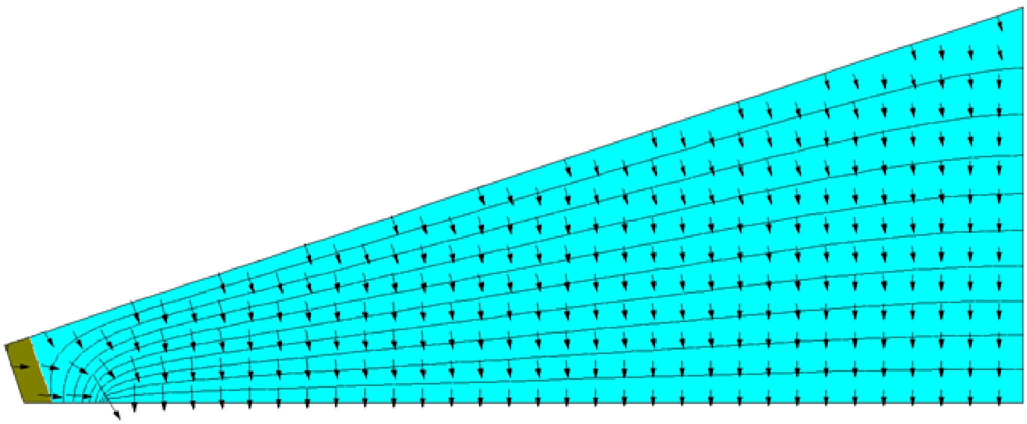

.

The overall heat transfer, per foot of perimeter, for this case was determined (RUN: std60.fet) to be:

Q = 16.342 Btu/hr-ft

Equation 231

Figure 38: 2-D Results for Framing Path of R-60 Standard-Heel

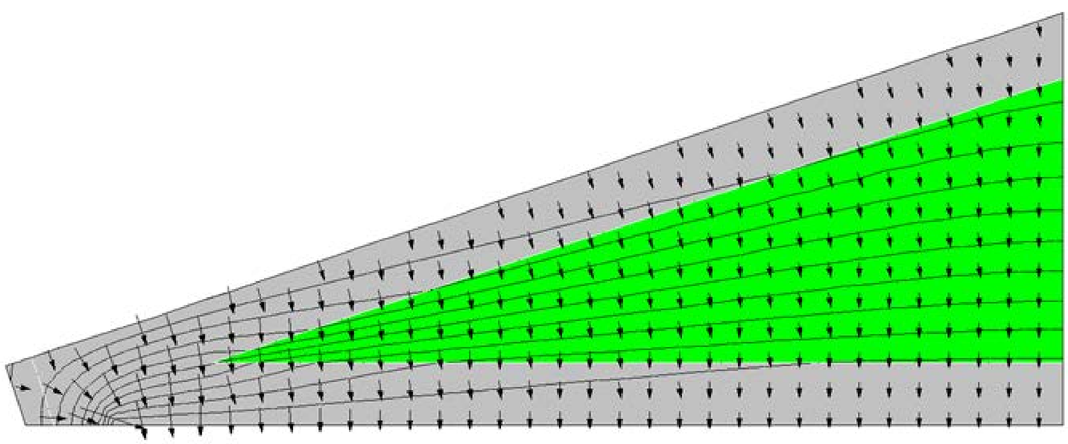

The overall heat transfer, per foot of perimeter, for this case was determined (RUN: std60F.FET) to be:

Q = 31.543 Btu/hr-ft

Equation 232

2.2.3.5 Comparison of 1-D and 2-D results

The above 2-D results are compared with the simplified 1-D model in Table 8.

Table 8: Comparison of 1-D and 2-D Results

	R30 ceiling insulation		**R60 ceiling insulation**	
	insulation path	framing path	insulation path	framing path
Q_{1D}	9.94	22.86	15.57	28.65
Q_{2D}	9.67	21.94	16.34	31.543
Q_{1D} is	3% $> Q_{2d}$	4% $> Q_{2d}$	5% $< Q_{2d}$	9% $< Q_{2d}$

Because the 2-D model used is itself of limited accuracy considering the numerous approximations made, the above results are not considered to be definitive. However they do indicate that a number of the assumptions made in the 1-D model are reasonably accurate. While this comparison is limited to steady state heat transfer performance, mass effects are expected to have comparable accuracy.

2.3 HOW TO BUILD AN AIRNET

BAW Rev 7 120910

Rev 4: Fixed error in 1b Leakage distribution that resulted in the total of the leaks being less than the input overall leakage.

Rev 5: Fixed error in 3d that had the cathedral ceiling leaking to the attic. Now to outside.

Rev 7: Undid the change in Rev 6 in 1a that converted ACH50 to ELA wrong

Rev 8: Modified the attic vent equations in 4a to clarify the area

Rev 9: Modified the attic leak equations in 3d to include the 1.45 conversion factor and clarify

2.3.1 Background

2.3.2 Approach

IZXFER is the building block input for an Airnet. There will be many IZXFERs in an input file, each representing a single air transfer object (leak, vent, window, fan, duct leak). Each IZXFER needs a unique name if detailed reports on its activity are needed. IZXFER is a command at the same level as HOLIDAY.

MATERIAL, CONSTRUCTION, METER, ZONE and REPORT which means that it can be located anywhere except inside another object (like a zone).

The main objects in the Airnet are:

- Infiltration
- Window ventilation
- IAQ ventilation
- Mechanical cooling ventilation
- Duct leakage

Units are ft^2.

CBECC inputs to add for Airnet:

WinHHTop	Head height of the highest windows in the zone. Used to get the vertical location of the window ventilation holes. In the development program this was done on a building wide basis: #define WnHeadHeight 7.67 // Average head height above the floor of operable windows
Ventilation Height Difference	This rule needs to be changed to refer to Zone instead of Building: "The default assumption for the proposed design is 2 feet for one story

	buildings and 8 feet for two or more stories. Greater height differences may be used with special ventilation features such as high, operable clerestory windows. In this case, the height difference entered by the user is the height between the average center height of the lower operable windows and the average center height of the upper operable windows. Such features shall be fully documented on the building plans and noted in the Special Features Inspection Checklist of the CF-1R." (2008 RACM pp 3-9)
Floor Height	The height of each floor over outdoors, crawl or garage is needed to set the Z dimension of the hole in the floor.
Soffit height	The height of the attic floor. Probably can be determined by the height of the ceiling below attic. Trouble for Split level?
Interzone Door	May need input for whether an interzone door exists between each 2 conditioned zones. Assuming it for now.
ReturnRegister	The conditioned zone(s) where the return/exhaust register is located. Make this an input on the HVAC System Data screen

2.3.2.1 Problems

- The window scheme doesn't work for 3 story zones!!!
- The Econ and NightBreeze cooling ventilation systems are multizone and use ducts. I suggest we set them up as part of the duct system.

2.3.3 Inputs

ACH50	7.6 (Air Changes per Hour at 50 Pascals pressure difference that leak through the envelope of the conditioned zones)
Avent	1/300 (ratio of "free area of attic vents to AceilGross)
Fraction High	0.3 (fraction of the attic vent area located in the upper part of the attic, check precise definition)

1. *Infiltration Setup.* Infiltration is uncontrolled air leakage through the cracks and intentional vents in the building. The first step is to determine the total size of the openings and then distribute them over the conditioned zones in proportion to surface areas.

   It is modeled in a single conditioned zones with 8 holes (IZXFERs) to represent the leakage in vertical walls and 1 hole each in the floor and ceiling.

Calculate:

a. For conditioned zones the total Effective Leakage Area ELAtot = CFA*ACH50/(2*10000) (CFA is conditioned floor area) //Rev 7 120907
b. Determine Envelope Areas
   1. ExCeiltotSF =sum (AceilGross + area of exterior ceilings) (exterior ceilings are surfaces in conditioned zones of type ceiling whose outside condition is Ambient, Ignore Knee walls for infiltration (walls between the conditioned zone and the attic)
   2. ExWalltotSF =sum (Gross Area of Exterior Walls) (walls in conditioned zones whose outside condition is Ambient)
   3. ExFloortotSF =sum (Gross Area of Exterior floors) (floors in conditioned zones whose outside condition is Ambient, Crawl or GROUND)
   4. ExFloorSlabSF =sum (Gross Area of Exterior slab on grade floors) (slab on grade floors in conditioned zones)
   5. SlabRatio =ExFloorSlabSF/ExFloortotSF
   6. GaragetotSF =sum (Gross Area of Surfaces to Garage) (walls and floors in conditioned zones whose outside condition is Garage)
c. Determine leakage distribution:
   1. ELAceilsf = ELAtot* (.4+.1*SlabRatio)/(AceilGross + area of exterior ceilings)
   2. ELAraisedFloorsf = ELAtot* (.2* 1-SlabRatio)/(ExFloortotSF-ExFloorSlabSF)

#If there is a garage zone

3. ELAGaragesf = ELAtot* 0.1/GaragetotSF
4. ELAwallsf = ELAtot* (.3 + .1*SlabRatio)/ExWalltotSF //Rev 4

#Else

3. ELAGaragesf = 0

4. ELAwallsf = ELAtot* (.4 + .1*SlabRatio)/ExWalltotSF //Rev 4

#endif

2. *Cooling Ventilation Setup:* Four types: Windows only (all types have windows for some part of the year), Whole house fan, Smart Vent, NightBreeze

Set up seasonal window control

#if Smart Vent or NightBreeze //Windows are on in Winter, but off in summer when mechanical ventilation is on

#redefine Windowmode select(@weather.taDbAvg07 >60., 0.00001,default 1.)

#define VentDiffMult select(@top.tDbOSh < (@znRes[Single].prior.S.tAir-VentDiff), 1,default 0.000001) //Vent off if Tin-Vendiff > Tout !! 110413 XXX

#Else //everything but Econ and NightBreeeze Windows are on year round

#reDefine Windowmode 1. //Always available

#Define VentDiff 0 // Differential. No differential for windows or WWF 110309 BAW

// multiplier for window and whole house fan vent availability, .00001 is proxy for Off Revised to start at dawn end at 11 PM.

#redefine Win_hr select($hour < 24, select($radDiff <1., select($hour>12,1.0, default .00001), default 1.0), default .00001)

3. *Airnet for Each Conditioned Zone:*
   a. Calculate

      ELA_Aceil(zone) = ELAceilsf * AceilGross(zone)

      ELA_Xceil(zone) = ELAceilsf * (AEdge(zone) + area of exterior ceilings(zone)) //AEdge is determined in the Ceiling Surface setup BAW 120517

      ELAXwall(zone) = ELAwallsf * Gross Area of Exterior Walls(zone)

      ELAGwall(zone) = ELAGaragesf * Gross Area of walls and floors next to the Garage(zone)

      ELAfloor(zone) = ELAraisedFloorsf * AreaExtfloor(zone) (gross area of floors whose outside condition is Ambient, Crawl)

      ZoneBotZ = Bottom(zone) - height of the lowest floor in the zone

      ZoneTopZ = ZoneBotZ + FloortoFloor(zone)*NumofStories(zone)

      ZoneHeightZ = ZoneTopZ - ZoneBotZ

      WinHHTop = ZoneBotZ + FloortoFloor(zone)*(NumofStories(zone)-1) + Window head height

   b. Exteror wall of conditioned zones infiltration objects Calculate height of bottom and top holes.

      // All infiltration leaks in walls are assumed to be spread uniformly over the exposed wall surfaces areas. There are no LEAKS associated with windows, doors etc.

//8 Wall Holes in each zone to Outdoors 1 upwind, 2 side walls, 1 downwind. Sidewalls are identical so combine them into 1 hole with 2*area

// Low is at 1/4 of wall height, high is at 3/4 of wall height //BAW 10/23

// izCpr (default = 0) = Wind Coef Upwind wall +0.6Side walls -0.65 Downwind Wall -0.3

ELAXwall(zone) = ELAwallsf * Gross Area of Exterior Walls(zone)

WH = ELAXwall(zone)*1.45/8 //Wall Hole size. Conversion from ELA to airnet infiltration opening is 1.45*

Write Airnet Objects to CSE Input WlLU stands for Wall Low Upwind etc.

IZXFER (ZoneName)WlLU izNVTYPE = AirNetExt izZN1 = (ZoneName) izALo = WH izHD = ZoneBotZ + (0.25 * ZoneHeightZ) izNVEff = 1 izExp=0.65 izCpr=0.6

IZXFER (ZoneName)WlLS izNVTYPE = AirNetExt izZN1 = (ZoneName) izALo = 2*WH izHD = ZoneBotZ + (0.25 * ZoneHeightZ) izNVEff = 1 izExp=0.65 izCpr=-.65

IZXFER (ZoneName)WlLD izNVTYPE = AirNetExt izZN1 = (ZoneName) izALo = WH izHD = ZoneBotZ + (0.25 * ZoneHeightZ) izNVEff = 1 izExp=0.65 izCpr=-0.3

IZXFER (ZoneName)WlHU izNVTYPE = AirNetExt izZN1 = (ZoneName) izALo = WH izHD = ZoneBotZ + (0.75 * ZoneHeightZ) izNVEff = 1 izExp=0.65 izCpr=0.6

IZXFER (ZoneName)WlHS izNVTYPE = AirNetExt izZN1 = (ZoneName) izALo = 2*WH izHD = ZoneBotZ + (0.75 * ZoneHeightZ)izNVEff = 1 izExp=0.65 izCpr=-.65

IZXFER (ZoneName)WlHD izNVTYPE = AirNetExt izZN1 = (ZoneName) izALo = WH izHD = ZoneBotZ + (0.75 * ZoneHeightZ) izNVEff = 1 izExp=0.65 izCpr=-0.3

c. Windows

// Operable window openings for ventilation. Assumes effect of screens is included in open area Revised 120409 BAW

// IZXFER izALo and izAHi are the min and max vent areas. Both are hourly.

//8 Window Holes in zone Single to Outdoors Assumes no orientation so 1/4 each orientation, 1/8 low and 1/8 high. Sidewalls are identical so combine them into 1 hole with 2*area

// high is at 1/2 default Hdiff below Window WinHHTop, Low is at WinHdiff below.high

//Note that this scheme doesn't work for 3 story zones!!!

Inputs

WnVentArea	// ft2, Nonzero - operable window open area. Default is 10 percent of the window area. Assume a single window is 4 feet high with openings centered at -1 and -3' from the top
WnVentHDiff 2.0	// Window vent height difference between center of high opening and low opening
WinHHTop	// Head height of highest windows in the zone

Calculate

WnHole = 0.5*(WnVentArea/8.)*Win_hr*Windowmode // 1/8th in each hole, ft2. 1/2 of nominal area to account for screens etc. Hourly and seasonal availability

Write Airnet Objects to CSE Input   WnLU stands for Window Low Upwind etc

IZXFER (ZoneName)WnLU izNVTYPE = AirNetExt izZN1 = (ZoneName) izALo=.00001 izAHi = WnHole izHD = WinHHTop - (3+ WnVentHDiff) izNVEff =.5 izCpr=0.6

IZXFER (ZoneName)WnLS izNVTYPE = AirNetExt izZN1 = (ZoneName) izALo=.00001 izAHi = 2*WnHole izHD = WinHHTop - (3+WnVentHDiff) izNVEff =.5 izCpr=-.65

IZXFER (ZoneName)WnLD izNVTYPE = AirNetExt izZN1 = (ZoneName) izALo=.00001 izAHi = WnHole izHD = WinHHTop - (3+WnVentHDiff) izNVEff =.5 izCpr=-0.3

IZXFER (ZoneName)WnHU izNVTYPE = AirNetExt izZN1 = (ZoneName) izALo=.00001 izAHi = WnHole izHD = (WinHHTop-1) izNVEff =.5 izCpr=0.6

IZXFER (ZoneName)WnHS izNVTYPE = AirNetExt izZN1 = (ZoneName) izALo=.00001 izAHi = 2*WnHole izHD = (WinHHTop-1) izNVEff =.5 izCpr=-.65

IZXFER (ZoneName)WnHD izNVTYPE = AirNetExt izZN1 = (ZoneName) izALo=.00001 izAHi = WnHole izHD = (WinHHTop-1) izNVEff =.5 izCpr=-0.3

d. Ceiling

Calculate

If ceiling below attic

ELA_Aceil(zone) = ELAceilsf * AceilGross(zone) //knee walls to attic not included in determining the conditioned to attic leakage distribution of

If Whole House fan, Ceiling leak through WWF when off

If Improved WHFela = .05 // Average of Motor Damper Models Rev 9

else WHFela = .11 // Average of Gravity Damper Models Rev 9

If ceiling to outside

ELA_Xceil(zone) = ELAceilsf * AEdge(zone) + area of exterior ceilings(zone)

CeilHole = (ELA_Aceil(zone) + WHFela)*1.45 //Ceil Hole size. Conversion from ELA to airnet infiltration opening is 1.45* Rev 9

CathCeilHole = ELA_Xceil(zone) * 1.45 //Cathedral Ceil Hole size. Conversion from ELA to airnet infiltration opening is 1.45* Rev 9

Write Airnet Objects to CSE Input

IZXFER (ZoneName)xAttic izNVTYPE = AirNetIZ izZN1=(ZoneName) izALo=CeilHole izHD = ZoneTopZ izNVEff=1. izExp=0.65 izZN2 = Attic Rev 9

IZXFER (ZoneName)CC izNVTYPE = AirNetExt izZN1=(ZoneName) izALo=CathCeilHole izHD = ZoneTopZ izNVEff=1. izExp=0.65 Rev 9

e. Floor over outside

For each floor over outside calculate:

ELAfloor(Name) = ELAraisedFloorsf * AreaExtfloor * 1.45 (floors whose outside condition is Ambiant)

Write Airnet Object to CSE Input

IZXFER (Name) izNVTYPE = AirNetExt izZN1 = (ZoneName) izALo = ELAfloor(Name) izHD = Floor Height izNVEff = 1 izExp=0.65 izCpr=0. // located at the Extfloor elevation, no wind effect

f. Floor over Crawl

For each floor over outside calculate:

ELAfloor(Name) = ELAraisedFloorsf * AreaCrawlfloor * 1.45 (floors whose outside condition is Crawl)

Write Airnet Object to CSE Input

IZXFER (Name)xCrawl izNVTYPE = AirNetIZ izZN1=(ZoneName) izALo=ELAfloor(Name) izHD = Floor Height izNVEff=1. izExp=0.65 izZN2 = Crawl

g. Floor over Garage

For each floor over garage calculate:

ELAfloor(Name) = ELAGaragesf * AreaGarfloor * 1.45 (floors whose outside condition is Garage)

Write Airnet Object to CSE Input

IZXFER (Name)xGarage izNVTYPE = AirNetIZ izZN1=(ZoneName) izALo=ELAfloor(Name) izHD = Floor Height izNVEff=1. izExp=0.65 izZN2 = Garage

h. Garage wall

Calculate:

GWH = ELAGaragesf * Gross Area of walls next to the Garage(zone)/2 // size of the 2 holes (high and low) betwen zone and garage

GWalltopZ = Min(ZoneTopZ(zone),(ZoneTopZ(Garage)) //The top of the shared wall

GWallBotZ = Max(ZoneBotZ(zone),(ZoneBotZ(Garage)) //The bottom of the shared wall

GwallH = GWalltopZ - GWallBotZ // Height of shared wall

GWHhZ = GwallBotZ + .75 GwallH // Height of top hole

GWHlZ = GwallBotZ + .25 GwallH // Height of bottom hole

Write Airnet Objects to CSE Input

IZXFER (ZoneName)xGarageH izNVTYPE = AirNetIZ izZN1=(ZoneName) izALo=GWH izHD = GWHhZ izNVEff=1. izExp=0.65 izZN2 = Garage

IZXFER (ZoneName)xGarageL izNVTYPE = AirNetIZ izZN1=(ZoneName) izALo=GWH izHD = GWHlZ izNVEff=1. izExp=0.65 izZN2 = Garage

4. *Airnet for Each Unconditioned Zone:*

   a. Attic

If Ventilated attic Calculate (4 soffit vents at attic floor elevation plus sloped deck vents at 2/3 of Attic high if frac high > 0

// Pitch types for roof wind pressure coeffs: 0 deg, <10deg, <15 deg,<25, <35 ,all the rest. Flat same as low slope.

#define PitchType select(Pitch <= 0, 1,Pitch <= 0.18, 1,Pitch <= 0.27, 2,Pitch <= 0.47, 3,Pitch <= 0.7, 4,default 5)

AventTot = AceilGross * AVent

SoffitVent 0.5*0.25 *(1.-FracHigh)*Max(AventTot, AtticRelief) //Attic relief is minimum vent needed to vent mechanical cooling air dumped to attic Rev 8

Deckvent 0.5*0.25*FracHigh*Max(AventTot, AtticRelief) Rev 8

If sealed attic To Be Developed

Write Airnet Objects to CSE Input

IZXFER AtticSU izNVTYPE = AirNetExt izZN1 = Attic izALo = SoffitVent izHD = SoffitHeight izNVEff = .6 izExp=0.65 izCpr=0.6

IZXFER AtticSS izNVTYPE = AirNetExt izZN1 = Attic izALo = 2*SoffitVent izHD = SoffitHeight izNVEff = .6 izExp=0.65 izCpr=-.65

IZXFER AtticSD izNVTYPE = AirNetExt izZN1 = Attic izALo = SoffitVent izHD = SoffitHeight izNVEff = .6 izExp=0.65 izCpr=-0.3

IZXFER AtticDU izNVTYPE = AirNetExt izZN1 = Attic izALo = DeckVent izHD = 0.67 * AtticHeight + SoffitHeight izNVEff=.6 izExp=0.5 izCpr=testx*choose(Pitchtype,-.5,-.8,-.5,-.3,.1,.3)

IZXFER AtticDS izNVTYPE = AirNetExt izZN1 = Attic izALo = 2*DeckVent izHD = 0.67 * AtticHeight + SoffitHeight izNVEff=.6 izExp=0.5 izCpr=testx*choose(Pitchtype,-.5,-.5,-.5,-.5,-.5,-.5)

IZXFER AtticDD izNVTYPE = AirNetExt izZN1 = Attic izALo = DeckVent izHD = 0.67 * AtticHeight + SoffitHeight izNVEff=.6 izExp=0.5 izCpr=testx*choose(Pitchtype,-.5,-.3,-.5,-.5,-.5,-.5)

b. Garage – Assume California garage with a water heater and combustion air vents so it is pretty leaky Guess 1 ft2 of free area. Ignore other infiltration

Calculate

Gvent = 1/4

Write Airnet Objects to CSE Input

IZXFER GarageU izNVTYPE = AirNetExt izZN1 = Garage izALo = Gvent izHD = GarageBotZ +1 izNVEff = .6 izExp=0.65 izCpr=0.6

IZXFER GarageS izNVTYPE = AirNetExt izZN1 = Garage izALo = 2*Gvent izHD = GarageBotZ +1 izNVEff = .6 izExp=0.65 izCpr=-.65

IZXFER GarageD izNVTYPE = AirNetExt izZN1 = Garage izALo = Gvent izHD = GarageBotZ +1 izNVEff = .6 izExp=0.65 izCpr=-0.3

c. Vented crawl space To Be Developed
d. Sealed crawl space To Be Developed
e. Basement To Be Developed

5. *Interzone Holes* – Assume an open door or stair between any twp conditioned zones with common surfaces, except between units in multi-family

If 2 or more conditioned zones

Error if not at least one common surface for every conditioned zone (a surface in zone A whose outside condition is another conditoned zone)

Door calculation for each pair of zones with a common wall surface (zoneA<>zoneB, zoneB<>zoneC, zoneA<>zoneC, etc)

DoortopZ = Min(ZoneTopZ(zone A),(ZoneTopZ(zone B)) //The top of the shared wall

DoorBotZ = Max(ZoneBotZ(zone A),(ZoneBotZ(zone B)) //The bottom of the shared wall

DoorH = DoortopZ - DoorBotZ // Height of shared opening

DH = 20/ // Area of half of assumed door

DHhZ = GwallBotZ + .75 GwallH // Height of top hole

DHHlZ = GwallBotZ + .25 GwallH // Height of bottom hole

For each zone pair write Airnet Objects to CSE Input

IZXFER (ZoneNameA)DHx(ZoneNameB)DH izNVTYPE = AirNetIZ izZN1=(ZoneNameA) izALo=DH izHD = DHhZ izNVEff=1. izExp=0.5 izZN2 = (ZoneNameB)

IZXFER (ZoneNameA)DLx(ZoneNameB)DL izNVTYPE = AirNetIZ izZN1=(ZoneNameA) izALo=DH izHD = DHlZ izNVEff=1. izExp=0.5 izZN2 = (ZoneNameB)

Stair calculation for each pair of zones with only a floor/ceiling surface (zoneA<>zoneB, zoneB<>zoneC, zoneA<>zoneC, etc)

StairZ = Max(ZoneBotZ(zone A),(ZoneBotZ(zone B)) //The height of the stair hole is at the upper floor

For each zone pair write Airnet Objects to CSE Input Note that izZN1 MUST be the lower of the 2 zones or the model doesn't work

IZXFER (ZoneNameA)Sx(ZoneNameB)S izNVType = AIRNETHORIZ izZN1=(ZoneName of lowerzone) izZN2 = (ZoneName of upper zone) izL1=3 izL1=10 izHD =StairZ

6. *IAQ ventilation*

Inputs for each zone

IAQVentCFM // CFM of IAQ vent

IAQfanWperCFM // W/CFM of IAQ vent

Type IAQExhaust // "IAQExhaust", "IAQSupply", "IAQBalanced" "NoIAQVent"

IAQVentHtRcv 0.0 // Heat recovery efficiency of Balanced type, frac

Write Airnet Objects to CSE Input

If Exhaust

IZXFER (Zone)IAQfan izNVTYPE = AirNetExtFan izZN1 = (Zone) izVFmin=-IAQVentCFM izVFmax=-IAQVentCFM izFanVfDs=IAQVentCFM izFanElecPwr=IAQfanWperCFM izFanMtr=IAQventMtr

If IAQSupply

IZXFER (Zone)IAQfan izNVTYPE = AirNetExtFan izZN1 = (Zone) izVFmin=IAQVentCFM izVFmax=IAQVentCFM izFanVfDs=IAQVentCFM izFanElecPwr=IAQfanWperCFM izFanMtr=IAQventMtr

If IAQBalanced // Needs heat recovery

IZXFER (Zone)IAQfanS izNVTYPE = AirNetExtFan izZN1 = (Zone) izVFmin=IAQVentCFM izVFmax=IAQVentCFM izFanVfDs=IAQVentCFM izFanElecPwr=IAQfanWperCFM izFanMtr=IAQventMtr

IZXFER (Zone)IAQfanE izNVTYPE = AirNetExtFan izZN1 = (Zone) izVFmin=-IAQVentCFM izVFmax=-IAQVentCFM izFanVfDs=IAQVentCFM izFanElecPwr=IAQfanWperCFM izFanMtr=IAQventMtr

7. Mechanical Cooling Ventilation // The following does not work for multi-zone systems with Econ, NightBreeze. Revise along with ducts model

For each Cooling Ventilation System

Inputs

CoolVentType //type of MECHANICAL cooling ventilation, Choice of WHF, Econ, NightBreeze

CoolVentCFM //Rated air flow of the mechanical cooling system

CoolVent W/CFM //

ReturnRegister // If WHF the conditoned zone where it is located

Calculate

Relief = CoolVentCFM/375 // The minimum size of the attic vents required to let the WHF flow out of the attic

If WHF // Whole House Fan

Calculate

Relief = CoolVentCFM/375 // The minimum size of the attic vent required for this fan to let the WHF flow out of the attic

Write Airnet Objects to CSE Input

IZXFER (Zone)WHF izNVTYPE=AirNetIZFan izZN1=(Zone) izVFmin=0. izVFMax=-CoolVentCFM*Win_hr izFanVfDs=CoolVentCFM izZn2=Attic izFanElecPwr=CoolVentWperCFM izFanMtr=CoolVentMtr

If Econ // Economizer ventilation option on the Central Forced Air System such as Smartvent

Calculate

Relief = CoolVentCFM/375 // The minimum size of the attic vent required for this fan to let the WHF flow out of the attic

Write Airnet Objects to CSE Input

ZXFER Econ# izNVTYPE=AirNetExtFan izZN1=(zone) izVFmin=0. izVFMax=CoolVentCFM*Coolmode*VentDiffMult izFanVfDs=CoolVentCFM izFanElecPwr=CoolVentWperCFM izFanMtr=CoolVentMtr //!! 110413

IZXFER Relief# izNVTYPE=AirNetIZFlow izZN1=ReturnRegister izZn2=Attic izVFmin=0 izVFmax=-CoolVentCFM*Coolmode*.9*VentDiffMult

If NightBreeze //Model for NightBreeze variable flow night ventilation system !!needs lower limit @ CFA<1000/unit and multiple systems @ CFA> 3333 ft2

Calculate

Relief = CoolVentCFM/375 // The minimum size of the attic vent required for this fan to let the WHF flow out of the attic

Write Airnet Objects to CSE Input

IZXFER NightBreeze izNVTYPE=AirNetExtFan izZN1=(zone) izVFmin=0. izFanMtr=CoolVentMtr

izFanVfDs=CoolVentCFM * CFA //CoolVentCFM = CFM/CFA for NightBreeze. Default is 0.6

izFanElecPwr = (616.47-0.6159*CFA + .000246 *CFA*CFA)/(CoolVentCFM * CFA) //W/CFM DEG 9/29/2010 Equation 1

izVFMax=CoolVentCFM*Coolmode*VentDiffMult*CFA / max((17.91554 - 3.67538 * logE(@weather.taDbPvPk)),1) //DEG 9/29/2010 Equation 3 110411

izFanCurvePy = 0, -0.026937155, 0.187108922, 0.839620406, 0 //Fit to DEG flow^2.85

IZXFER NBRelief izNVTYPE=AirNetIZFlow izZN1=ReturnRegister izZn2=Attic izVFmin=0 izVFmax=-CoolVentCFM * CFA * Coolmode*.9 *VentDiffMult

Next Zone

Calculate

AtticRelief = Sum(CoolVentCFM)/375 // The sum of all zonal cool vent CFM determines the minimum size of the attic vents required to let the vent air out of the attic

//Used in Attic Zone AirNet above

//Min Attic Vent area for relief Tamarac
http://www.tamtech.com/userfiles/Fan%20size%20and%20venting%20requirements(3).pdf

7. *Duct system leaks and pressurization.* These are generated by automatically by CSE based on the duct system inputs. // BAW 120517

2.4 HOW TO CREATE CSE CONDITIONED ZONE INTERNAL MASS INPUTS

BAW Rev 1 120830

2.4.1 Background

2.4.2 Approach

Internal mass objects are completely inside a zone so that they do not participate directly in heat flows to other zones or outside. They are conected to the zone radiantly and convectively and participate in the zone energy balance by passively storing and releasing heat as conditions change. For now only in Conditioned Zones.

The main internal mass objects in the are:

- Interior walls
- Interior floors
- Furniture
- Cair
- Specific masses (for addition later)

CBECC inputs to add:

- Specific masses (for addition later)

2.4.3 Inputs

Floor Area of zone

For each Conditioned Zone

1. Interior Floor Setup. Input for inside the conditioned zone interior floors as mass elements.

   Calculate:

   a. Xflr = sum of the area of floors to ground, crawl space, exterior or other zones
   b. IntFlr = Floor Area-Xflr
2. Interior Wall Setup. Input for inside the conditioned zone interior walls as mass elements.

   Calculate:

   a. IZwall = sum of the area of interior walls to other conditioned zones
   b. Intwall(zone) floor area - .5 * IZwall
3. Write objects to the CSE input

Light stuff

1. znCAir=floor area * 2
2. Interior wall if Intwall(zone) > 0

   SURFACE IntWallC(zone) sfType=Wall sfArea=0.75*Intwall(zone) sfCon=IntwallCav; sfAZM=0 sfExCnd=ADJZN sfAdjZn=(zone)

   SURFACE IntWallF(zone) sfType=Wall sfArea=0.25*Intwall(zone) sfCon=IntwallFrm; sfAZM=0 sfExCnd=ADJZN sfAdjZn=(zone)

3. Furniture

   SURFACE Furniture(zone) sfType=wall sfArea= Floor Area * 2.; sfCon=FurnCon; sfAZM=0 sfExCnd=ADJZN sfAdjZn=Zone

4. Interior Floor if IntFlr(zone) >0

   // floor construction for interior mass. Assumes 2x10 @ 16" OC. Both floor and ceiling are in the conditioned zone

   SURFACE IntFlrFrm sfType=Floor sfCon=IntFFrm2x10 sfArea=0.1 * RaisedFlr; sfExCnd=ADJZN sfAdjZn=(Zone)

   SURFACE IntFlrCav sfType=Floor sfCon=IntFCav2x10 sfArea=0.9 * RaisedFlr; sfExCnd=ADJZN sfAdjZn=(Zone)

4. Constructions

   CONSTRUCTION FurnCon // 2.5" wood Revised Layers BAW 8/4

   Layer lrMat="SoftWood" lrThk=2.5/12

   CONSTRUCTION IntwallCav // 2x4 Revised Layers BAW 8/4

   Layer lrMat="Gypsum Board"

   Layer lrMat="Gypsum Board"

   CONSTRUCTION IntwallFrm // 2x4 Revised Layers BAW 8/4

   Layer lrMat="Gypsum Board"

   Layer lrMat="SoftWood" lrThk=3.5/12.

   Layer lrMat="Gypsum Board"

   CONSTRUCTION IntFFrm2x10 // 9.25" (2x10)

   Layer lrMat="Carpet"

Layer lrMat="Wood layer"

Layer lrMat="SoftWood" lrThk=9.25/12.

Layer lrMat="Gypsum Board"

CONSTRUCTION IntFCav2x10 // 9.25" (2x10) BAW 11/30

Layer lrMat="Carpet"

Layer lrMat="Wood layer"

Layer lrMat="Carpet" // Air space with 1 psf of stuff (cross bracing wiring, plumbing etc) approximated as 1" of carpet

Layer lrMat="Carpet" // Air space with 1 psf of stuff (cross bracing wiring, plumbing etc) approximated as 1" of carpet

Layer lrMat="Gypsum Board"

2.5 APPLIANCES, MISCELLANEOUS ENERGY USE AND INTERNAL GAINS

BAW Rev 6 120831

Revised to match CSEmeters3.doc

Rev 6 fixed a parentheses problem in 1c. Already done this way in CBECCr

Rev 6 fixed a parentheses problem in 2e. Already done this way in CBECCr

2.5.1 Background

This model is derived from the 2008 HTM (California Energy Commission, HERS Technical Manual, California Energy Commission, High Performance Buildings and Standards Development Office. CEC-400-2008-012). This is a major change from the 2008 RACM in that internal gains are built up from models for refrigerator, people, equipment and lights instead of the simple constant plus fixed BTU/ft^2 used there. The HTM derived model has been used in the 2013 Development Software throughout the 2013 revision process.

This model has another significant change beyond the HTM model with the addition of latent gains required as input for the new CSE air conditioning model. There was no information on latent gains in either the 2008 RACM or the HTM. The latent model here was created by applying the best available information on the latent fraction of internal gains to the HTM gains model.

2.5.2 Approach

The approach here is to calculate the Appliances and Miscellaneous Energy Use (AMEU) for the home and use that as the basis for the internal gains. This will facilitate future expansion of the procedure to calculate a HERS Rating.

2.5.2.1 Problems

The procedure here (also used in the 2013 development program) does not work correctly for multifamily buildings unless all of the units are the same (CFA and number of bedrooms). I don't believe this problem was considered in developing the HTM. I believe that the only exactly correct solution involves simulating each unit as a separate zone with a different internal gain. For now we will ignore this problem and assume that average values are OK.

The HTM equations are FUBAR if there is a gas range and electric oven.

The allocation of internal gain to zones is not specified in either the RACM or the HTM. A proposed approach is presented here.

2.5.3 Inputs

Units	Number of dwelling units in the building.
BRperUnit	Bedrooms/DwellingUnits rounded to an integer
CFA	Conditioned Floor Area in the building
CFAperUnit	CFA/DwellingUnits

New CBECC input at the building level: an Appliances Input Screen (for a single conditioned zone, most of these default, we are assuming that MF buildings will be done as one zone):

Refrigerator/Freezer	Efficiency (Choice of Default = 669 kWh/year, no other choices at this time), Location (Choice of zones if multiple conditioned zones). // HTM assumes all Dwelling units have refrigerators. Different for additons and alterations when we get to them.
Dishwasher	Efficiency (Choice of Default, no other choices at this time), Location (Choice of zones if multiple conditioned zones). // HTM assumes all Dwelling units have refrigerators. Different for additons and alterations when we get to them.
Clothes Dryer	Location (Choice of zones if multiple zones, No Dryer space or hookup provided) Dryer power (Choice Electric, Gas or other) //Assuming gas for now
Clothes Washer	Location (Choice of zones if multiple zones), No Washer space or hookup provided)
Range/Oven	Location (Choice of zones if multiple conditioned zones, No Range/Oven space and hookup provided) Range/Oven power (Choice Electric, Gas or other) Assumes gas for now.

Assumes CSE Meters are set up elsewhere:

Mtr_Elec

Mtr_NatGas

Mtr_Othewr //PropaNE

Write Constants to the CSE input:

#redefine Intgain_mo choose1($month, 1.19,1.11,1.02,0.93,0.84,0.8,0.82,0.88,0.98,1.07,1.16,1.21) //The monthly internal gain multiplier (same as 2008 RACM).

#redefine Lights_hr hourval(0.023,0.019,0.015,0.017,0.021,0.031,0.042,0.041,0.034,0.029,0.027,0.025, \

0.021,0.021,0.021,0.026,0.031,0.044,0.084,0.118,0.113,0.096,0.063,0.038) // Changed 0.117 to 0.118 to add to 1

#redefine OutdoorLights_hr hourval(0,0,0,0,0,0,0,0,0,0,0,0,0,0,0,0,0,0,0,0,0.25,0.25,0.25,0.25) //

#redefine People_hr hourval(0.035,0.035,0.035,0.035,0.035,0.059,0.082,0.055,0.027,0.014,0.014,0.014, \

0.014,0.014,0.019,0.027,0.041,0.055,0.068,0.082,0.082,0.070,0.053,0.035)

#redefine Equipment_hr hourval(0.037,0.035,0.034,0.034,0.032,0.036,0.042,0.044,0.037,0.032,0.033,0.033, \

0.032,0.033,0.035,0.037,0.044,0.053,0.058,0.060,0.062,0.060,0.052,0.045)

1. Setup the gains that are distributed across the zones per CFA of the zone and write to CSE input: Calculations are generally more complicated in future for HERS
   a. //Lights Returns Btu/day-CFA - based on ElectricityInteriorLights = (214+ 0.601×CFA)×(FractPortable + (1-FractPortable)×PAMInterior) //HTM Eqn 11, p. 30

      #define FractPortable .22 //fixed for now, variable later for HERS

      #define Paminterior 0.625 //fixed for now, variable later for HERS

      #Redefine LightsGainperCFA (((214. + 0.601 * CFAperUnit) * (FractPortable + (1-FractPortable) * Paminterior) * 3413. / 365) * DwellingUnits /CFA)

   b. People Returns BTU/day-CFA - 100% is internal gain 57.3% sensible, 42.7% latent Based on HTM and BA existing bldgs Sensible 220, Latent 164 BTU

      #redefine PeopleperUnit (1.75 + 0.4 * BRperUnit)

      #Redefine PeopleGainperCFA ((3900/0.573) * PeopleperUnit * DwellingUnits / CFA)

   c. Misc Electricity Returns BTU/day-CFA - 100% is internal gain

      #Redefine MiscGainperCFA ((723. + (0.706 * CFAperUnit))* DwellingUnits * 3413. / 365.)/CFA //Rev 6 120831

2. Setup the gains that are point sources located in a particular zone and write to CSE input. Calculations are generally more complicated in future for HERS
   a. Refrigerator. In the HTM all Standard Design refrigerators use the same amount of electricity (669 kWh/year) regardless of the size of dwelling unit or number of bedrooms. The proposed use is based on the energy label of the actual refrigerator installed or if that is not available the default. For existing home HERS calculations the default is (775

kWh/year). Refrigerators run at a constant power 24 hours per day, regardless of the interior air temperature or number of times the door is opened.

Returns BTU/day - 100% is internal gain. Installed refrigerator rating is input for proposed in HERS later

#Redefine RefrigeratorGain (DwellingUnits * 669. * (3413. / 365.))

b. Dishwasher. 0 based choose returns BTU/day // uses Table based in INTEGER bedrooms per dwelling.

#Redefine DishwasherGain (choose (BRperUnit,90,90,126,126,126,145,145,174,174,174,default 203) * DwellingUnits * 3413. / 365.)

c. Stove and Oven – Assumes both are gas with electonic igniter Returns BTU/day - Full Energy Use, 90% is internal Gain

define CookGain (((31. + (.008 * CFAperUnit))* 0.43* 0.9)* DwellingUnits * 100000. / 365.) //Added the 0.43 for the electronic ignition 12/4 BAW

d. Clothes Washer - // Returns BTU/day

#Redefine WasherGain ((-64 + 0.108 * CFAperUnit) * DwellingUnits * 3413. / 365.)

e. Clothes Dryer - Assumes gas with electonic igniter Returns BTU/day - Full energy Use, 30% is internal gain

define DryerGAin (13. + (.01 * CFAperUnit))* DwellingUnits * 100000. / 365. //Added the 0.43 for the electronic ignition //120831

f. Exterior Lights Returns Btu/day - based on HTM Eqn 14

#define PamExterior 0.49 //fixed for now, variable later for HERS

#Redefine ExtLightGain (-81+ 0.152 × CFA)×PAMExterior * 3413. / 365)

3. For each conditioned zone: //Write GAIN objects inside each conditioned zone

GAIN Lights(zone) gnPower= LightsGainperCFA*CFA(Zone)*Lights_hr*Intgain_mo gnFrRad=0.4 gnEndUse=Lit gnMeter= Mtr_Elec

GAIN People(zone) gnPower= PeopleGainperCFA*CFA(Zone)*People_hr*Intgain_mo gnFrRad=0.3 gnFrLat=0.427 // Free Energy so not metered

GAIN Misc(zone) gnPower= MiscGainperCFA*CFA(Zone)*Equipment_hr*Intgain_mo gnFrRad=0.3 gnFrLat=0.03 gnEndUse=Rcp gnMeter= Mtr_Elec

Write any of the following if the source is located in this zone:

GAIN Refrigerator gnPower= RefrigeratorGain/24 gnFrRad=0 gnEndUse=Refr gnMeter= Mtr_Elec // No *Intgain_mo, change fro 2013 DevProg

GAIN Dishwasher gnPower= DishwasherGain*Equipment_hr*Intgain_mo gnFrRad=0 gnFrLat=0.25 gnEndUse=Dish gnMeter= Mtr_Elec //

GAIN Cooking gnPower= CookGain*Equipment_hr*Intgain_mo gnFrRad=0 gnFrLat=0.67 gnEndUse=Cook gnMeter= Mtr_NatGas gnFrZn=.9 //

GAIN Washer gnPower= WasherGain*Equipment_hr*Intgain_mo gnFrRad=0 gnEndUse=Wash gnMeter= Mtr_Elec //

GAIN Dryer gnPower= DryerGAin*Equipment_hr*Intgain_mo gnFrRad=0 gnFrLat=0.5 gnEndUse=Dry gnMeter= Mtr_NatGas gnFrZn=.3 //

Write the following to the 1st zone only (one gain per building):

GAIN ExtLights gnPower= ExtLightGain*OutdoorLights_hr gnFrZn=.0 gnEndUse=Ext gnMeter= Mtr_Elec // outside lights, no internal gain

4. For each unconditioned zone write the following if the source is located in this zone: //Garage or Basement Maybe 2nd refrigerator in garage later?

GAIN Washer gnPower= WasherGain*Equipment_hr*Intgain_mo gnFrRad=0 gnEndUse=Wash gnMeter= Mtr_Elec //

GAIN Dryer gnPower= DryerGAin*Equipment_hr*Intgain_mo gnFrRad=0 gnFrLat=0.5 gnEndUse=Dry gnMeter= Mtr_NatGas gnFrZn=.3 //

2.6 SEASONAL ALGORITHM

These are constant control rules. You could substitute values for defined terms in some cases like Winter_Vent Winter_Cool Summer_heat and Sumr_Vent_Temp

//Thermostats and associated controls

//Heat Mode

#redefine SZ_Heat_hr
hourval(65,65,65,65,65,65,65,68,68,68,68,68,68,68,68,68,68,68,68,68,68,68,68,65)

#redefine Liv_Heat_hr
hourval(65,65,65,65,65,65,65,68,68,68,68,68,68,68,68,68,68,68,68,68,68,68,68,65)

#redefine Slp_Heat_hr
hourval(65,65,65,65,65,65,65,68,65,65,65,65,65,65,65,65,65,65,65,65,65,68,68,65)

#redefine Winter_Vent 77

#redefine Winter_Cool 78

//Cool Mode

#redefine SZ_Cool_hr
hourval(78,78,78,78,78,78,78,83,83,83,83,83,83,82,81,80,79,78,78,78,78,78,78,78)

#redefine Liv_Cool_hr
hourval(83,83,83,83,83,83,83,83,83,83,83,83,83,82,81,80,79,78,78,78,78,78,78,83)

#redefine Slp_Cool_hr
hourval(78,78,78,78,78,78,78,83,83,83,83,83,83,83,83,83,83,83,83,83,83,78,78,78)

#redefine Summer_Heat 60

#redefine Sumr_Vent_Temp 68 //

// Summer Winter mode switch based on 7 day average temp. Winter<=60>Summer

#redefine Coolmode select(@weather.taDbAvg07 >60., 1,default 0)

#redefine HeatSet select(@weather.taDbAvg07 >60., Summer_Heat, default SZ_Heat_hr)

#redefine CoolSet select(@weather.taDbAvg07 >60., SZ_Cool_hr, default Winter_Cool)

#redefine Tdesired select(@weather.taDbAvg07 >60., Sumr_Vent_Temp, default Winter_Vent)

// Window interior shade closure

#define SCnight 0.8 // when the sun is down. 80%

```
#define SCday 0.5      //  when the sun is up  50%
#define SCcool 0.5     //  when cooling was on previous hour.  50%?
```

Appendix A. Derivation of Duct Loss Equations Using Heat Exchanger Effectiveness and Y-Delta Transformations

This derivation is for one zone only, and the nomenclature is specific to this appendix alone.

Heat transfer through the duct walls can be illustrated in the electrical analogy in Figure A-1. The first node on the left represents the temperature of the air in the duct (T_d) and is connected to the temperate on the surface of the duct (T_s) by the conductance through the duct wall (U_d). The convective heat transfer coefficient (h_c) connects the surface temperature to the duct zone air temperature (T_a). The radiation heat transfer coefficient (h_r) connects the surface temperature to the duct zone radiant temperature (T_r).

Figure A-1: Electrical Analogy of Heat Transfer through a Duct Wall

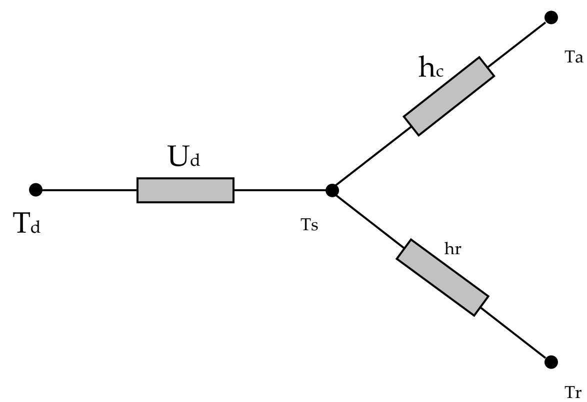

The temperatures of the duct zone are assumed to be constant; the duct surface temperature is not. The duct surface temperature can be removed from the analysis by using a Y-Δ transform. Figure A-2 shows the result of this transformation with direct connections between the duct air temperature, the duct zone radiant and air temperatures through combined coefficients defined in Equation A- 1.

$$U_r = \frac{U_d h_r}{D} \qquad U_c = \frac{U_d h_c}{D} \qquad U_x = \frac{h_c h_r}{D}$$

Equation A- 1

where

$$D = U_d + h_c + h_r$$

Figure A-2: Heat Transfer through a Duct Wall with Surface Temperature Removed

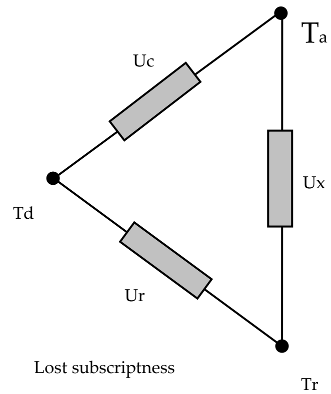

Using an energy balance, the rate of change of heat flow along the length (x) of duct must equal the heat flow through the duct wall, or

$$-mc_p \frac{dT_d(x)}{dx} = U_c P(T_d(x) - T_a) + U_r P(T_d(x) - T_r)$$

Equation A- 2

where

mc_p = capacitance flow rate of the air in the duct

T_d = temperature of air in the duct

U_c = equivalent heat transfer coefficient (see Equation A- 1)

P = perimeter of duct

T_a = temperature of air in duct zone

U_r = equivalent heat transfer coefficient (see Equation A- 1)

T_r = radiant temperature in duct zone

Regrouping by temperature terms

$$mc_p \frac{dT_d(x)}{dx} = -(U_c P + U_r P)T_d(x) + U_c PT_a + U_r PT_r$$

Equation A- 3

and dividing through by the quantity $(U_c P + U_r P)$ gives

$$\frac{mc_p}{(U_cP+U_rP)}\frac{dT_d(x)}{dx}=-T_d(x)+T_{amb}$$

Equation A- 4

where

$$T_{amb}=\frac{U_cP}{(U_cP+U_rP)}T_a+\frac{U_rP}{(U_cP+U_rP)}T_r$$

Equation A- 5

Let $y(x)$ be

$$y(x)=T_{amb}-T_d(x)$$

Equation A- 6

The derivative of which is

$$dy=-dT_d$$

Equation A- 7

Substituting Equation A- 6 and Equation A- 7 into Equation A- 4 gives

$$-\frac{mc_p}{(U_c+U_r)P}\frac{dy}{dx}=y(x)$$

Equation A- 8

Rearranging

$$\frac{1}{y(x)}dy=-\frac{(U_c+U_r)P}{mc_p}dx$$

Equation A- 9

and integrating from entrance ($x=0$) to exit ($x=L$)

$$\int_0^L\frac{1}{y(x)}dy=\int_0^L-\frac{(U_c+U_r)P}{mc_p}dx$$

Equation A- 10

gives

$$\ln y(L)-\ln y(0)=-\frac{(U_c+U_r)PL}{mc_p}$$

Equation A- 11

Recalling the definition in Equation A- 6 and replacing the product of the perimeter and length with the surface area (A) of the duct, and a bit of manipulation yields the following relationships

$$\frac{y(L)}{y(0)} = \frac{T_d(L) - T_{amb}}{T_d(0) - T_{amb}} = \exp\left(- \frac{(U_c + U_r)A}{mc_p} \right)$$

Equation A- 12

Let

$$\beta = \exp\left(- \frac{(U_c + U_r)A}{mc_p} \right)$$

Equation A- 13

Then

$$\frac{T_d(L) - T_{amb}}{T_d(0) - T_{amb}} = \beta$$

Equation A- 14

Solving for the exit temperature gives

$$T_d(L) = \beta(T_d(0) - T_{amb}) + T_{amb}$$

Equation A- 15

The temperature change in length L of duct is

$$T_d(0) - T_d(L) = -\beta(T_d(0) - T_{amb}) - T_{amb} + T_d(0)$$

Equation A- 16

This can be rewritten as

$$T_d(0) - T_d(L) = (1 - \beta)(T_d(0) - T_{amb})$$

Equation A- 17

Let ε be the sensible heat exchanger effectiveness

$$\varepsilon = (1 - \beta)$$

Equation A- 18

Then the conduction loss from the duct to the duct zone can then be written as

$$Q_{loss} = mc_p(T_d(0) - T_d(L)) = \varepsilon mc_p(T_d(0) - T_{amb})$$

Equation A- 19

Appendix B. Screen Pressure Drop

The following algorithms are not currently implemented in the code, but are here for future code use, and in the interim are useful to manually determine the effects of screens on window ventilation flow pressure drop.

The references cited are a few of the papers reviewed to ascertain state of the art regarding screen pressure drop. In one of the more recent papers, Bailey et al. (2003) give the pressure drop through a screen as:

$$\Delta p = K\frac{\rho w^2}{2g_c} = K\frac{m^2}{2g_c\rho A^2}$$

Equation B- 1

where,

$$K = \left(\frac{1}{\beta^2} - 1\right)\left[\frac{18}{Re} + \frac{0.75}{log(Re + 1.25)} + 0.055\,log(Re)\right]$$

Equation B- 2

and,

β = screen porosity = open area/total area perpendicular to flow direction.

$$\beta = \left(1 - \frac{d}{t1}\right)\left(1 - \frac{d}{t2}\right)$$

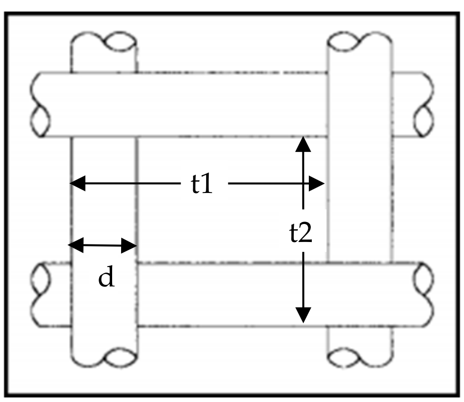

$Re = \frac{wd}{v} = \frac{md}{\rho A v}$ = Renolds number.

w = face velocity = $\frac{m}{\rho A}$, ft/sec.

m = mass flow rate, lb_m/sec.

d = wire diameter, ft.

ν = viscosity ≈ 1.25E-4 + 5.54E-07T(degF); ft²/sec. = 1/6100 ft2/sec at 70-F.

ρ = air density, lb_m/ft^3.

g_c = 32.2 $lb_m ft/lb_f\text{-}sec^2$.

The first term, intended for portraying Re < 1 pressure drops, is the dominate term. The third term, intended for Re > 200, is relatively negligible, and the second term is a bridge between the first and third terms.

The Reynolds number for the screen flow $Re = \frac{wd}{\nu}$ is roughly 5 times the face velocity in ft/sec. For a velocity of 1 ft/sec, Re ~ 5. For the expected range of wind speeds of concern for ventilation (see note #1), and with the motive of making the partial derivatives simple (see below), Equation B- 2 is approximated as

$$K = \left(\frac{1}{\beta^2} - 1\right)\frac{25}{Re}$$

Equation B- 3

[note #1: California CZ12 ave yearly Vmet ≈ 11 ft/sec. Correcting for height and shielding gives Vlocal ≈ 11*0.5*0.32 ≈ 1.8 ft/sec. For max flow case of windows on windward and leeward walls, with typical wall wind pressure coefficients, w ≈ 0.5*Vlocal. Thus, the maximum window velocity expected for the annual average wind velocity of 11 ft/sec is w ≈ 0.5*1.8 = 0.9 ft/sec. In a building with windows in multiple directions, the average w is expected to be much lower, perhaps 0.5 ft/sec. *Stack Effect:* Using old ASHRAE equation, $w(fpm) = 9\sqrt{H[ft](\Delta T[F])} = 9 * \frac{\sqrt{10*10}}{60} = 1.5\ ft/sec$. Together, the wind and stack may be on the order of 1-ft/sec].

The constant 25 in this approximate formula was determined by forcing Equation B- 2 and Equation B- 3 to match when the window air velocity is at the characteristic value $w_c = 21\psi\nu C_d^2$, defined below. As discussed there, at this velocity the pressure drop through the screen is equal to that through the window orifice.

Figure B-1: [Need Caption]

Equation B- 3 can be written as

$$K = \frac{25\psi\nu}{w}\text{, or alternately}\frac{25\psi\rho A\nu}{m}$$

Equation B- 4

where, as a result of the approximation Equation B- 3, the screen inputs can be combined into one characteristic screen parameter ψ (of dimension ft^{-1}):

$$\psi = \frac{1}{d}\left(\frac{1}{\beta^2} - 1\right)$$

Equation B- 5

ψ encapsulates all that needs to be known about the screen for pressure drop purposes. This is only true when K varies in the form assumed byEquation B- 3.

The flow rate through a screenless window is modeled by Airnet as a sharp edged orifice of opening area A.

$$m = C_d A(2\rho g_c \Delta p)^{\frac{1}{2}}$$

Equation B- 6

[Idelchik says this is valid for Re > 10^4].

At the equal pressure point the window orifice Reynolds number is $\mathrm{Re_{wdw}} = (\mathrm{D_h}/\mathrm{d})25\psi\mathrm{d}\mathrm{C_d^2}$.

w_c =1.89 ft/sec for std 14x18x0.011 screen &Cd=0.6; 14&18 are wires/inch.

Re_c = 10.6 for std 14x18x0.011 screen &Cd=0.6

Re_{wdw}= (~1.5*12/0.011)*(10.6)=1,7345 >10^4.

Thus Re is not > 10^4 when w < ~1 ft/sec. But this is when the pressure drop starts to be dominated by the screen, so the orifice drop accuracy is not so important.

Solving for *Δp*,

$$\Delta\mathrm{p} = \frac{1}{C_d^2}\frac{\rho w^2}{2g_c} = \frac{1}{C_d^2}\frac{m^2}{2g_c\rho A^2}$$

Equation B- 7

Adding Equation B- 1 and Equation B- 7 gives the total pressure drop for a window and screen in series:

$$\Delta p = \left(K + \frac{1}{C_d^2}\right)\frac{m^2}{2g_c\rho A^2}$$

Equation B- 8

Solving for mass flow rate,

$$\mathrm{m} = AC_d\left(\frac{1}{1+C_d^2K}\right)^{\frac{1}{2}}(2\rho g_c\Delta p)^{\frac{1}{2}}$$

Equation B- 9

or,

$$m = AC_dS(2\rho g_c\Delta p)^{\frac{1}{2}}$$

Equation B- 10

where S is the ratio of the flow with a screen to the flow rate without a screen, as a function of velocity w, viscosity, and screen and window orifice parameters.

$$S = \left(\frac{1}{1+C_d^2K}\right)^{\frac{1}{2}} = \left(\frac{1}{1+C_d^2\frac{25\psi\nu}{w}}\right)^{\frac{1}{2}}$$

Equation B- 11

Equating Equation B- 1 and Equation B- 7 shows that the velocity when the screen and window pressure drops are equal is given by:

$$w_c = 25\psi\nu C_d^2$$

Equation B- 12

The corresponding Reynolds number is $Re_c = 25\psi d C_d^2$.

Substituting Equation B- 12 into Equation B- 11shows that for this condition,

$$S_c = \frac{1}{\sqrt{2}} = 0.707$$

Equation B- 13

Equation B- 12 and Equation B- 13 show that w_c, which, besides viscosity, only depends on the screen constant ψ and window-orifice coefficient C_d, can be considered a "characteristic" velocity, the velocity at which the flow is reduced by (1 - 0.707) ~ 29.3% by the addition of a screen to the window.

Figure B-2 shows that the typical Δp vs. flow curves for a screen and an orifice separately, not in series. The curves cross at velocity w_c. To the left of w_c, the laminar flow pressure drop dominates the window orifice pressure drop; to the right the orifice pressure drop progressively dominates. Screens give a greater flow reduction at low wind speeds than at high wind speeds.

Figure B-2: Pressure vs. Flow Characteristics

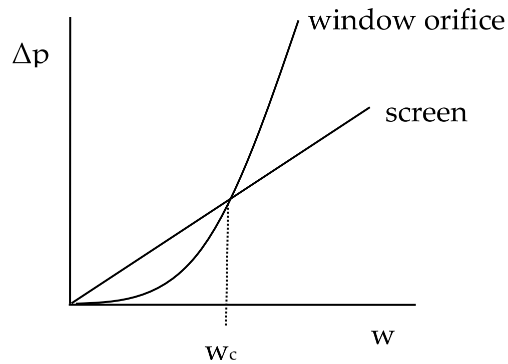

In Figure B-2, to the left of w_c the laminar-flow screen pressure drop is higher, and to the right the orifice pressure drop dominates.

Figure B-3 shows S as a function of air velocity w for two common screen sizes. For the Standard screen, w_c is 1.9-ft/sec. [At w = ~ 1-ft/sec taken as typical according to note #1, S = 0.6, corresponding to a 40% reduction in flow].

Figure B-3: Standard Screen Flow Reduction

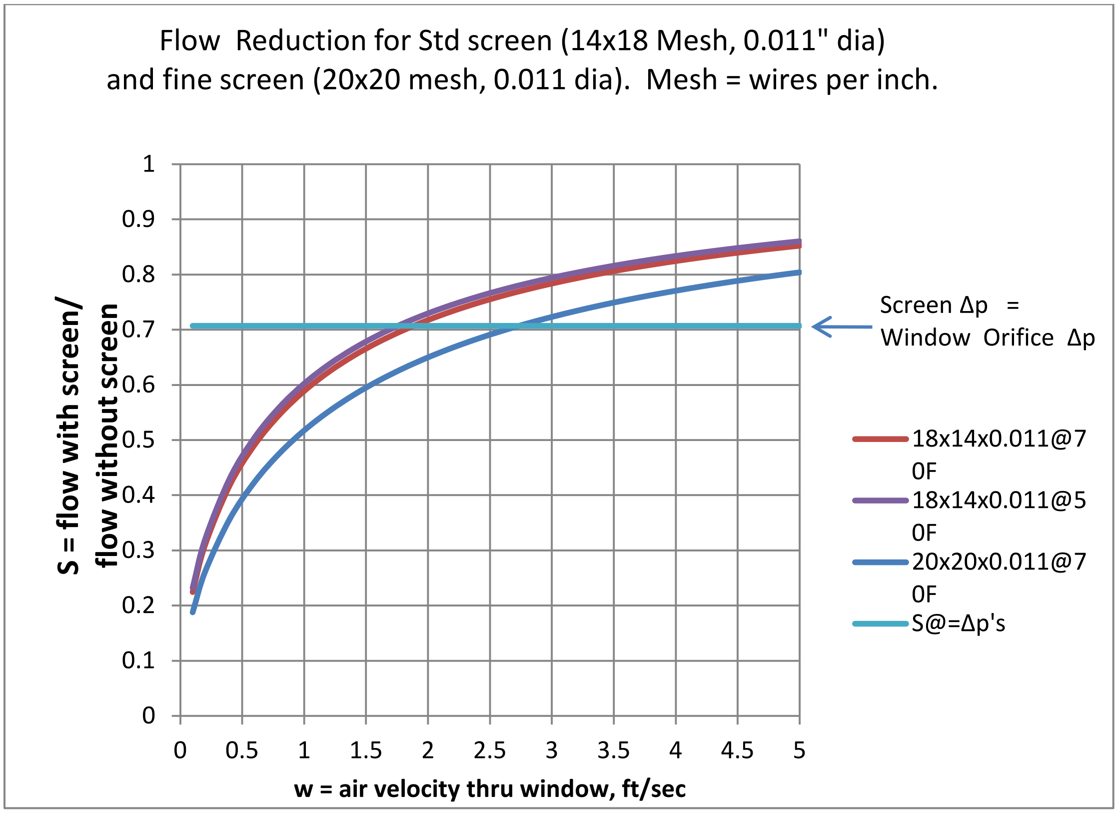

Partial Derivatives for use in Airnet:

From Equation B- 4 and Equation B- 8,

$$\Delta p = \left(\frac{25\psi\rho A v}{m} + \frac{1}{C_d^2}\right)\frac{m^2}{2g_c\rho A^2}$$

Equation B- 14

This can be written in the quadratic form for m:

$$m^2 + bm - a\Delta p = 0$$

Equation B- 15

Where,

$$a = 2g_c\rho C_d^2 A^2$$

$$b = 25\psi\rho v C_d^2 A$$

The single real root of the quadratic Equation B- 15 gives the mass flow rate through a screen in series with a window-orifice as a function of screen and window properties and overall pressure drop:

$$m = \frac{b}{2}\left\{\left(1 + \frac{4a\Delta p}{b^2}\right)^{\frac{1}{2}} - 1\right\}$$

Equation B- 16

If Δp is taken as $\Delta p = P_1 - P_2$, then the partial derivative of m with respect to P_1 is

$$\frac{\partial m}{\partial P_1} = \frac{a}{b\sqrt{1 + \frac{4a\Delta p}{b^2}}}$$

Equation B- 17

$$\frac{\partial m}{\partial P_2} = -\frac{\partial m}{\partial P_1}$$

Equation B- 18

These derivatives are needed in the Newton-Raphson procedure. The derivatives Equation B-17 and Equation B- 18 do not become unbounded when $\Delta p = 0$, as does the orifice Equation B-6, so that no special treatment is needed near $\Delta p = 0$.

But the derivatives do become a little peculiar near zero Δp as shown in Figure B-4 and Figure B-5. The value of $a/b \approx 25$, and $\frac{4a}{b^2} \approx 88$ for thse plots for the standard screen of Figure B-3. It is possible this could cause problems in the N-R method, but testing AirNet with this type of element is the easiest way to find out.

Figure B-4: For Small Δp

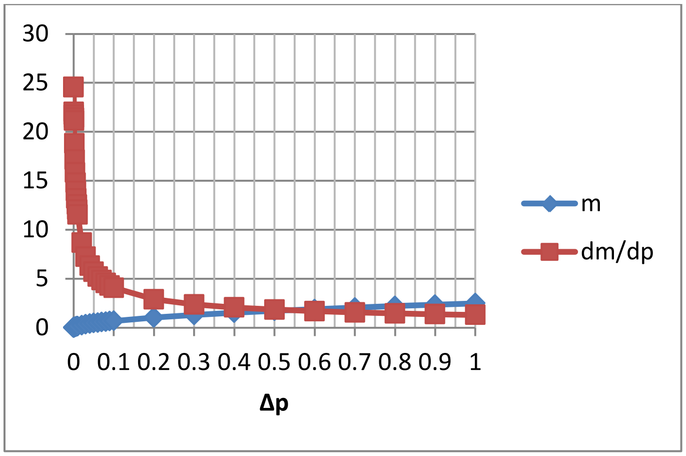

Figure B-5: For Large Δp

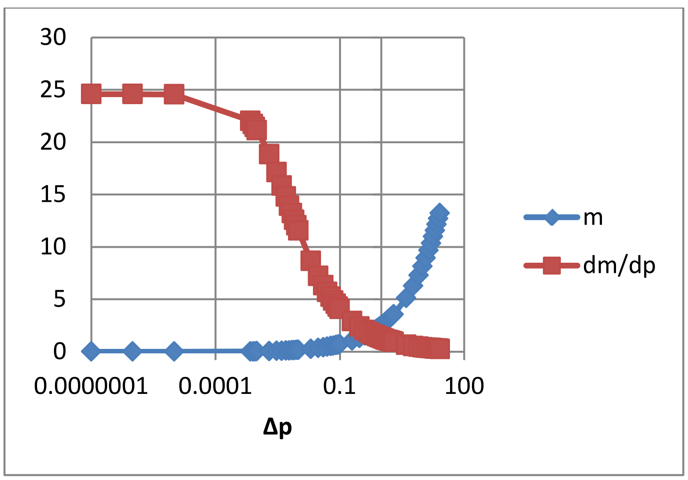

Appendix C. Exact Longwave Radiation Model

Figure C-1 shows the standard Heat Transfer Engineering method of determining the long wavelength radiation exchange between black-body surfaces at uniform temperatures (Oppenheim(1956), Mills(1992)). The areas need not be equal, or symmetrically disposed, but are drawn that way for simplicity. The surfaces are assumed to be isothermal, and each surfaces temperature node is connected to all other surface temperature nodes via conductances $h_b A_i F_{ij}$.

The following methodology is referred to as the "exact" solution in the discussions of Section 1.6. However, it is recognized that it still is an idealization. For instance, surfaces are generally not isothermal. Although the heat transfer q_{ij} [Btu/hr], of Equation C- 2 is accurate if surfaces i and j are isothermal, the *local* surface heat transfer q'_{ij} [Btu/hr-ft²] on the surfaces is nonuniform because the local view factors are different than the integrated value F_{ij}. For example, if the two surfaces are connected along a common edge, then near the edge q'_{ij} will be higher than the average q_{ij}/A_i, which will tend to change the temperatures of each wall near the edge faster than away from the edge. For the same reason, the radiation intensities are also non-uniform over a surface, which affects the accuracy of the treatment of the emissivity effects by the Oppenheim surface conductance term, which assumes uniform irradiation.

From the Stefan-Boltzmann equation, the net heat transfer rate between surfaces i and j is:

$$q_{ij} = h_b A_i F_{ij}(T_i - T_j)$$

Equation C- 1

where,

$h_b = 4\sigma\bar{T}^3 =$ black body radiation coefficient; Btu/(hr-ft²-F).

$\sigma = 0.1714x10^{-8}$ Btu/hr-ft²-R⁴, the Stefan-Boltzmann constant.

$\bar{T}^3 \approx \frac{T_i+T_j}{2}$; degrees R.

The F_{ij} term is the standard view factor, equal to the fraction of radiation leaving surface i that is intercepted by surface *j*. F_{ij} depends on the size, shape, separation, and orientation of the surfaces, and at worst requires a double integration. Reciprocity requires that $A_i F_{ij} = A_j F_{ji}$.

Equation (C-1) is in the linearized form of the Stefan-Boltzmann equation, where for small temperature differences, $\left(T_i^4 - T_j^4\right)$ is approximated by $4\bar{T}^3(T_i - T_j)$.

Figure C-1: View-Factor Method's Radiant Network for Black-Body Surfaces

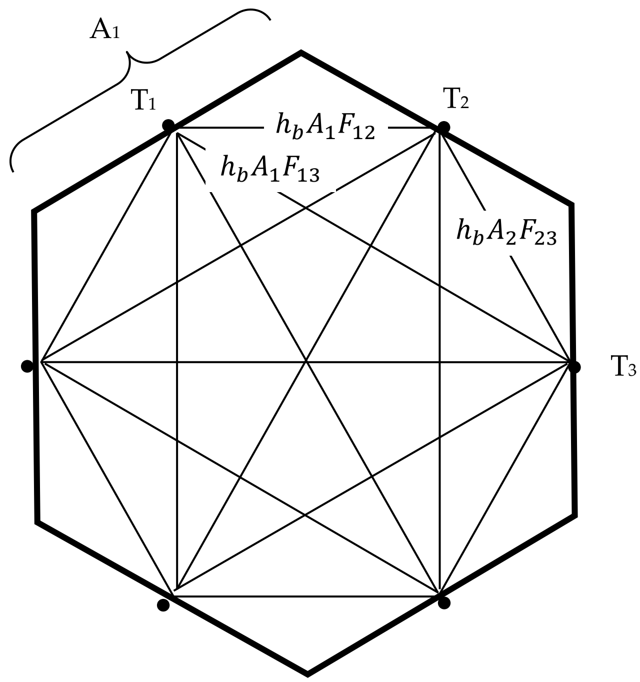

Figure C-2 shows the Figure C-1 black surface case extended to handle diffuse gray surfaces (ε = α = constant over temperature range of interest) with emissivities ε_i, by adding the Oppenheim radiant surface conductances $\frac{A_i \varepsilon_i}{1-\varepsilon_i}$ between the surface temperature nodes and the black body network. (Figure C-2 also represents the un-linearized Stefan-Boltzmann circuit if the surface temperatures are replaced by the emissive power of the surfaces. In this case the surface radiosities are the potentials at the floating nodes.)

Figure C-2: View-Factor Method's Network for Grey Surfaces

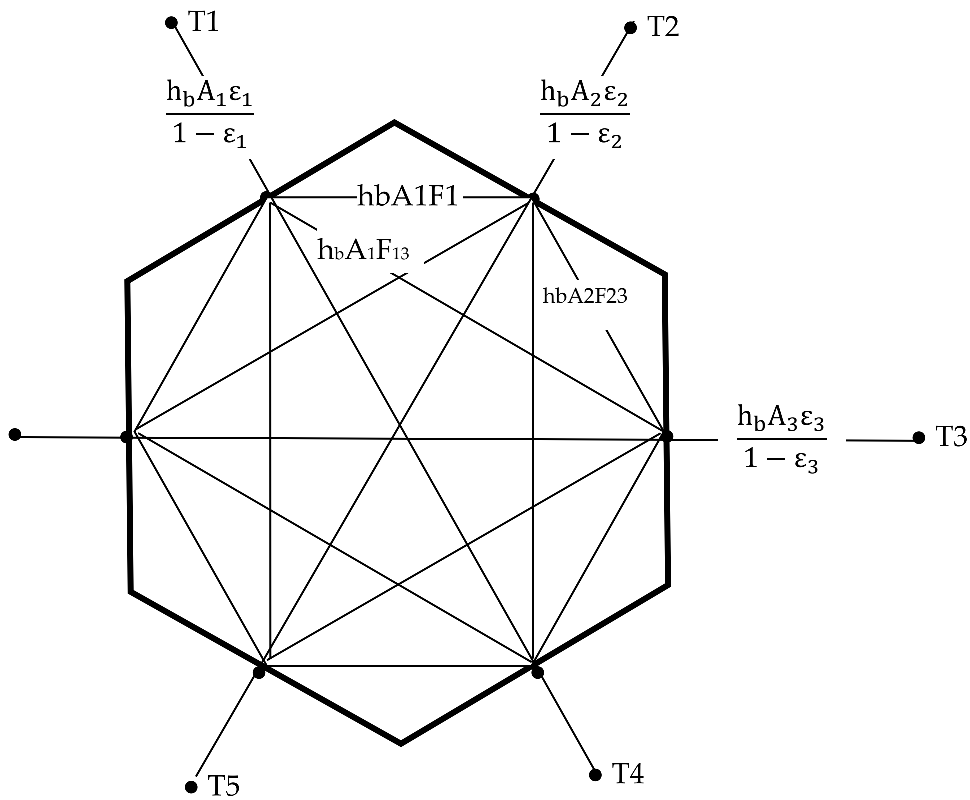

By dissolving the radiosity nodes using Y-delta transformations, Figure C-2 converts into Figure C-3 showing the same circuit form as the black surface circuit of Figure C-1. The transformation provides the conductances $A_iF'_{ij}$ implicit in the conductances of Figure C-2.

Figure C-3: View-Factor Method's Network for Grey Surfaces Reduced to Star Network

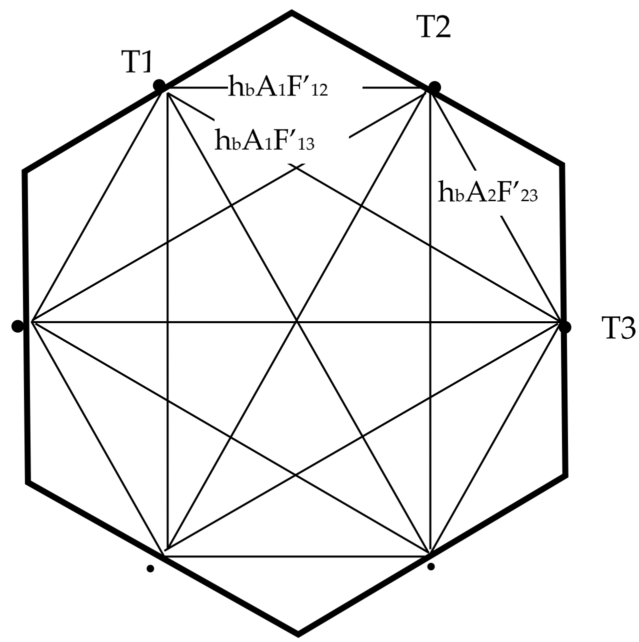

F'_{ij} are the 'radiant interchange factors'. As with the black surfaces view factors, reciprocity holds: $A_iF'_{ij} = A_jF'_{ji}$. The net heat transfer between surface *i* and *j* (both directly and via reflections from other surfaces) is given by:

$$q_{ij} = h_bA_iF'_{ij}(T_i - T_j)$$

Equation C- 2

The total net heat transfer from surface *i* (i.e., the radiosity minus the irradiation for the un-linearized circuit) is given by summing Equation C- 2 for all the surfaces seen by surface *i, j≠i*:

$$q_i = \sum_{j=1}^{n} h_bA_iF'_{ij}(T_i - T_j)$$

Equation C- 3

The above methodology is referred to as the "exact" solution in the discussion of Section 1.6.1. However, as discussed by Carroll, it is recognized that it is still an idealization. For instance, surfaces are generally not isothermal. Although the heat transfer, q_{ij} [Btu/hr], of Equation C- 2 is accurate if surfaces *i* and *j* are isothermal, the *local* surface heat transfer q'_{ij} q'[Btu/hr-ft^2] on the surfaces is nonuniform because the local view factors are different than the integrated value F_{ij}. For example, if the two surfaces are connected along a common edge, then near the edge $q'_{ij}q'$ will be higher than the average q_{ij}/A_i, which will tend to change the temperatures of each wall near the edge faster than away from the edge. For the same reason, the radiation intensities are also non-uniform over a surface, which affects the accuracy of the treatment of the emissivity effects by the Oppenheim surface conductance term, which assumes uniform irradiation.

Appendix D. Determining the Form of the Self-weighting Term F_i

Consider a flat black surface of area $A_1$and temperature T_1viewing the rest of the room of area A_s and surface temperature T_s, with the view factor $F_{1s} = 1$. By Equation C- 1 of Appendix C, the net q from surface A_1 is given by:

$$q_1 = h_b A_1 F_{1s}(T_1 - T_s) = h_b A_1 (T_1 - T_s)$$

Equation D- 1

With Carroll's model applied to this geometry,

$$q_1 = h_b A_1 F_1 (T_1 - T_r)$$

Equation D- 2

where

$$T_r = \frac{A_1 F_1 T_1 + A_s F_s T_s}{A_1 F_1 + A_s F_s}$$

Equation D- 3

Equating Equation D- 1 and Equation D- 2 and solving for F_1 gives:

$$F_1 = \frac{1}{1 - \frac{A_1 F_1}{A_1 F_1 + A_s F_s}}$$

Equation D- 4

The net heat transfer rate from surface 1 is $q_1 = h_b A_1 F_1 (T_1 - T_r)$, with similar expressions for F_s and q_s. This is then generalized to the form of Equation 78 of Section 1.6.1.

References

Anderson, J.V. and K Subbarao, "Spectral Analysis of Ambient Weather Patterns, " Annual System Simulation Conference, Reno, American Society of Mechanical Engineers, 1981.

ASHRAE, American Society of Heating, Refrigeration and Air-Conditioning Engineers. *1993 ASHRAE Handbook, Fundamentals*, pp 22.1.

ASHRAE. 2010. Thermal Environmental Conditions for Human Occupancy. ANSI/ASHRAE Standard 55-2010.

Bailey, B.J., et al, "Airflow Resistance of Greenhouse Ventilators with and without Insect Screens, "Biosystems Engineering (2003) 86 (2),217–229.

Barnaby, Charles S., J.D. Spitler, D. Xiao, "Updating the ASHRAE/ACCA Residential Heating and Cooling Load Calculation Procedures and Data", ASHRAE 1199-RP, Final Report, Aug. 20, 2004.

Bazjanac V., Huang, J., Winkelmann, F.C., "DOE-2 Modeling of Two-dimensional Heat Flow in Underground Surfaces, prepared for the California Energy Commission, February 2000.

Blocken, Defraeye, Derome,Carmeliet, 2009, “High-resolution CFD simulations for forced convective heat transfer coefficients at the facade of a low-rise building”, Building and Environment.

Brundrett E (1993). Prediction of pressure drop for incompressible flow through screens. Journal of Fluid Engineering, Transactions American Society of Mechanical Engineers, 115, 239–242, June 1, 2010.

Burch, J., Casey, R., “ Wind Issues in Solar Thermal Performance Ratings,” Preprint NREL/CP-550-45466, April 2009.

Carroll, J. A., 1980, An ‘MRT Method’ of Computing Radiant Energy Exchange in Rooms, Proceedings of the Second Systems Simulation and Economic Analysis Conference, San Diego, CA.

Carroll, J.A., 1981, A Comparison of Radiant Interchange Algorithms, Proceedings of the ASME Solar Energy Division Third Annual Conference on Systems Simulation, Economic Analysis/Solar Heating and Cooling Operational Results, Reno, Nevada. 132, 133, 165

Carroll, J. A., 1980a, "An MRT method of computing radiant energy exchange in rooms," Proceedings of the 2nd Systems Simulation and Economic Analysis Conference, San Diego, CA.

Carroll J.A., J. R. Clinton, 1980b, "A Thermal Network Model of a Passive Solar House," Proceedings of the 5th National Passive Solar Conference, American Section of ISES.

Carroll J.A., J. R. Clinton, 1982, " Appendix H: A Thermal Network Model of a Passive Solar House," Final Report USDOE Contract DE AC04-79AL10891. July, 1982.

Carroll, J. A., 1981, "A Comparison of Radiant Interchange Algorithms," Proceedings of the 3rd Annual Systems Simulation and Economics Analysis/Solar Heating and Cooling Operational Results Conference, Reno. Solar Engineering, Proceedings of the ASME Solar division.

Carslaw, H.S., J.C. Jaeger, Conduction of Heat in Solids, 2nd Ed., Oxford Press, 1959.

Chirlian, Signals, Systems, and the Computer, Intext Educational Publishers, 1973.

Clarke, J.A., Hensen, J.L.M., "An Approach to the Simulation of Coupled Heat and Mass Flows in Buildings,", 11th AIVC Conference, Belgirate, Italy, Sept. 1990.

Clear, R.D., L. Gartland and F.C. Winkelmann, 2001, "An Empirical Correlation for the Outside Convection Air Film Coefficient for Horizontal Roofs," Lawrence Berkeley National Laboratory, Jan 2001.

Cooper, L.Y., "Calculation of the Flow Through a Horizontal Ceiling/Floor Vent", NISTIR 89-4052, Mar. 1989.

Deru, M., and P. Burns. 2003, "Infiltration and Natural Ventilation Model for Whole Building Energy Simulation of Residential Buildings," NREL/CP-550-33698; ASHRAE preprint, Kansas City, Missouri.

Emmel, Abadie, Mendes, “New external convection heat transfer coefficient correlations for isolated low-rise buildings”, Energy and Buildings 39 (2007).

Energy Plus Engineering Reference, Oct, 2009.

European Convention for Constructional Fieldwork,”Recommendations for the Calculation of Wind Effects on Buildings and Structures”. Technical General Secretary, Brussels, Belgium, September 1978.

Francisco, P.W., and L. Palmiter, 1999, revision 2003, "Improvements to ASHRAE Standard 152P," U.S. DOE Subcontract 324269-AU1.

Goldstein, F. B., Some Analytical Models of Passive Solar Building Performance: A Theoretical Approach to the Design of Energy Conserving Buildings, LBL-7811, Lawrence Berkeley Laboratory, Berkeley, 1978. This was confirmed for winter weather.

Holmes, J. D. , "Wind Loading In Structures," Spon Press, 2003.

Holmes, J.D., " Wind loading and structural response", Lecture 18.

Holmes, J. D. , Wind Loads on low rise buildings - a review. CRISO, Div. of Building Research, Highett, Victoria, Australia, 1993.

Howell, J.R., Radiation Configuration Factors, McGraw-Hill, 1982.

Idelchik, I.E., “Handbook of Hydraulic Resistance”, 3rd Ed, Springer-Verlag, Berlin, 1986.

Kusuda, T., P. R Achenbach, "Earth Temperature and Thermal Diffusivity at Selected Stations in the United States," NBS REPORT 42103-12-4210436 June 22, 1965.

Lorrenzetti, D.M.,"Computational Aspects of Multizone Airflow Systems", Building and Environment 37, (2002) 1083-1090.

Martin, Marlo and Berdahl, Paul, "Characteristics of Infrared Sky Radiation in the United States." Solar Energy Vol. 33, No. ¾, pp 321-336, 1984.

McAdams, Heat Transmission, McGraw-Hill, 3rd Ed., 1954.

McAdams eq. (7-8) for horizontal plates with heat transfer down from a cold plate, or up from a hot plate, for the turbulent case: $\mathrm{Nu} = 0.14\mathrm{Ra}^{1/3} \quad (2 * 10^7 < \mathrm{Ra} < 3 * 10^{10})]$

Mills, A.F. , 1992, "Heat Transfer," Irwin Press, Boston.

Churchill, S. W., and Chu, H. H. S., "Correlating equations for laminar and turbulent free convection from a vertical plate," *Int. J. Heat Mass Transfer*, 18, 1323-1329 (1975).

Niles, P., L. Palmiter, B. Wilcox, and K. Nittler, "Unconditioned Zone Model", PIER Research for the 2008 Residential Building Standards. PIER Contract 500-04-006. See http://www.energy.ca.gov/title24 /2008standards/documents/2006-03-28_workshop/2006-03-27_UZM_MODEL.PDF.

Oppenheim, A.K., "Radiation Analysis by the Network Method," Trans of the ASME, May 1956.

Palmiter, L. and T. Bond. 1992, "Impact of Mechanical Systems on Ventilation and Infiltration in Homes," ACEEE.

Palmiter, L., and T. Bond. 1991a, "Modeled and Measured Infiltration: A Detailed Case Study of Four Electrically Heated Homes, " Electric Power Institute report CU-73227, Palo Alto, California.

Palmiter, L., E. Kruse, and P. Francisco, 2004, "Duct Efficiency Under Full-load or Modulating Conditions: Implications for Heat Pump Performance," ACEEE.

Palmiter, L., and T. Bond. 1991b, "Interaction of Mechanical Systems and Natural Infiltration, " AIVC, Ottawa, Canada.

Palmiter, L., and T. Bond. 1991a, "Modeled and Measured Infiltration: A Detailed Case Study of Four Electrically Heated Homes, " Electric Power Institute report CU-73227, Palo Alto, Calif.

Palmiter, L., and T. Bond. 1991b, "Interaction of Mechanical Systems and Natural Infiltration, " AIVC, Ottawa, Canada.

Palmiter, L. and P.W. Francisco, 1996, "Modeled and Measured Infiltration: Phase III-A detailed Study of Three Homes". TR-106228, EPRI WO3512-12.

Palmiter, L, and E. Kruse, 2003, "Derivation of Duct Efficiency Equations in ASHRAE Standard 152", ASHRAE Seminar, Feb. 2003. Available from author at Ecotope Inc.

Parker, D.S., P. Fairey and L. Gu, 1993. "Simulation of the Effect of Duct Leakage and Heat Transfer on Residential Space Cooling Use," Energy and Buildings, 20, Elsevier Sequoia, Netherlands.

Parker, D., P. Broman, J. Grant, L. Gu, M. Anello, R. Vieira and H. Henderson, 1999, "EnergyGauge USA: A Residential Building Energy Design Tool." Proceedings of Building Simulation '99, Kyoto, Japan. International Building Performance Simulation Association, Texas A&M University, College Station, TX, September 1999.

Press, H. P., B. P. Flannery, S. A. Teukolsky, W. T. Vetterling, Numerical Recipes, Cambridge University Press, 1986.

Residential Alternative Calculation Method (ACM), Approval Manual For Compliance with California's 2005 Energy Efficiency Standards, Publication Number: 400-03-003F, Dated Published: October 2004, Effective Date: October 1, 2005

Sebald, A. V., 1985," Efficient Simulation of Large Controlled Passive Solar Systems: Forward Differencing in Thermal Networks", Solar Energy Vol. 34, No. 3.

Sharples, S., "Eaves and roof ridge pressure coefficients on an isolated low-rise dwelling: Wind tunnel study", Proc. CIBSEA: Building Serv. Eng. Res. Technol. 18(1) 59-61 (1997).

Sherman, M., "The Use of Blower Door Data", LBL #35173, March, 1998. Appendix: Modeling Tools.

Sherman, M.H., Grimsrud, D.T., "Measurement of Infiltration Using Fan Pressurization and Weather Data, Oct 1980, LBL-10852.

Subbarao, K., J. Anderson, "A Frequency-Domain Approach to passive Building Energy Analysis", SERI/TR-254-1544, July 1982.

Teitel, M., A. Shklyar, Pressure Drop Across Insect-Proof Screens, Trans. ASAE, Vol. 41(6), 1998.

Valera, D.L., A.J. Alvarez ad F.D. Molina, "Aerodynamic analysis of several insect-proof screens used in Greenhouses," Spanish Journal of Agricultural Research (2006) 4(4), 273-279.

Walker, Iain, 2005, " REGCAP Model Outline."

Walker. I.S., T.W.Forest, D.J. Wilson,"An attic-interior infiltration and interzone transport model of a house.," Building and Environment 40 (2005) 701-718.

Walker, I.S., T.W. Forest and D.J. Wilson (1995), "A Simple Calculation Method for Attic Ventilation Rates", Proc. 16th AIVC Conference, Vol. 1, pp. 221-232, Air Infiltration and Ventilation Centre, Coventry, UK.

Walker, I.S. and D.J. Wilson. 1994, " Practical Methods for Improving Estimates of Natural Ventilation Rates," Proc. 15th AIVC Conference, Buxton, U.K., 1994: 517-525.

Walker, I.S., and D. J. Wilson, 1990, "The Alberta Air Infiltration Model, AIM-2". The University of Alberta, Dept. of Mechanical Engineering, Tech Report 71.

Wright, J.L., Kotey, N.A., 2006. Solar Absorption by Each Element in a Glazing/Shading Layer Array, ASHRAE Transactions, Vol. 112, Pt. 2. pp. 3-12.

Wright, J.L. 2008. "Calculating Centre-Glass Performance Indices of Glazing Systems with Shading Devices," ASHRAE Transactions, Vol. 114, Pt. 2.

Walton, G.N. , 1983, Thermal Analysis Research Program Reference Manual, NBSSIR 83-2655. National Bureau of Standards.

Walton, G.N., A New Algorithm for Radiant Interchange in Room Loads Calculations, ASHRAE Transactions, 1980, Vol. 86, Pt. 2.

Wallenten, Petter, "Heat transfer coefficients in a full scale room with and without furniture", Lund Institute of Technology, Sweden.

Wallenten, P., 2001. Convective heat transfer coefficients in a full-scale room with and without furniture, Building and Environment 36(6), 743-751.

Woloszyn, M., Rusaouën G., Airflow Through Large Vertical Openings in Multizone Modelling, " Building Simulation '99, vol 6, Kyoto (Japan): IBPSA, 1999 p. 465-471.

Xu, Y.L., G.F. Reardon, "Variations of wind pressure on hip roof with roof pitch", Journal of Wind Engineering and Industrial Aerodynamics, 73 (1998) 267-284)